

**This dissertation has been  
microfilmed exactly as received**

69-8020

CRESSWELL, George Robert, 1937-  
FAST TEMPORAL AND SPATIAL CHANGES IN  
AURORAS.

University of Alaska, Ph.D., 1968  
Geophysics

University Microfilms, Inc., Ann Arbor, Michigan

FAST TEMPORAL AND SPATIAL CHANGES IN AURORAS

A

DISSERTATION

Presented to the Faculty of the  
University of Alaska in Partial Fulfillment  
of the Requirements  
for the Degree of  
DOCTOR OF PHILOSOPHY

by

George Robert Cresswell, B.Sc. (Hons.)

College, Alaska

May 1968

FAST TEMPORAL AND SPATIAL CHANGES IN AURORAS

APPROVED:

\_\_\_\_\_  
\_\_\_\_\_  
*Albert E. Belov*  
*Lyudmila Mearf*  
*J. Neil Davis*  
Chairman

*Roger Sheridan*  
Department Head

APPROVED: *C. Bilke* DATE: *Feb. 27, 1968*  
\_\_\_\_\_  
Dean of the College of Mathematics, Physical  
Sciences and Engineering

*A. Cas*  
\_\_\_\_\_  
Vice President for Research and Advanced Study

## ABSTRACT

Several types of pulsing and fast-moving auroras were examined with photometers and television systems. Pulsating auroras were seen to be restricted primarily to the equatorward boundary of the auroral display in the midnight and morning sectors following substorm onsets. At such times the local horizontal magnetic component is strongly negative or recovering from a negative bay. The pulsating auroras appear to fall into two main classes: pulsating patches and pulsating arcs, and these can be further characterized by: rapid motions (if any) during their growth and decay, approximate period, direction of-drift motion, and amount of modulation. The patches, apart from gradual changes, maintain their shapes during successive quasi-periodic appearances, while they drift steadily. This behavior suggested that each patch is related to a flux tube that is being steadily convected in the magnetosphere and disturbed at intervals causing it to lose part of its electron population. Flaming auroras appear to occur under the same conditions as pulsating auroras and, in fact, pulsating auroras have sometimes been observed to flame. A synthetic flaming aurora was considered by assuming multi-energy electrons to be released simultaneously from a point on the local field line, and by allowing for velocity dispersion and differential atmospheric penetration. The results showed that the observed flaming velocity, which ranged from  $60 \pm 8$  to  $90 \pm 9$  km/sec for a range of assumed initial lower border heights of 90-110 km, corresponded to release points ranging from the

equatorial plane to  $2.5 R_e$  from the ionosphere. Flickering auroras were occasionally observed as part of bright discrete features seen before midnight on active days. They were made up of numerous small patches, 1-2 km across, each of which underwent rapid ( $\sim 10$  cps) changes of size, shape, and intensity. Fast auroral waves are east-west aligned, arc-like features that were seen to propagate southward at 50-300 km/sec and at about once per second in the College vicinity after midnight. They occurred only when the preceding daylight hours, and often the evening hours, were magnetically undisturbed, and always after a short-lived (1-2 hour) substorm. It is suggested that the waves are due to hydromagnetic processes occurring near the equatorial plane that provide electrons in the loss cone. The hydromagnetic velocity across the field lines there projects down to the atmosphere to give velocities in the observed fast auroral wave velocity range.

## ACKNOWLEDGEMENTS

I have been extremely fortunate in having Dr. T. N. Davis, Professor A. E. Belon, and Dr. S.-I. Akasofu as my advisory committee. The study was initiated by Professor Belon and he was joined by Dr. Davis in overseeing it. All provided numerous invaluable suggestions and relevant criticisms during the work and in the preparation of this manuscript.

I was greatly encouraged by the continued interest shown by Professor K. B. Mather, the Geophysical Institute Director.

The strongly research-oriented atmosphere of the Geophysical Institute contributed much to the work, as did the smoothly operated facilities, of which the drafting office directed by the late Mr. Dan Wilder rated highly. The majority of the typing work was handled by Miss Peggy Snodgrass. My office companion, Mr. F. T. Berkey, I thank for many discussions. The acquisition of most of the auroral television data was due to the electronic skill of Mr. T. J. Hallinan.

The work, in general, was aided inestimably by the way in which my wife, Diana Crosswell, adapted to the Alaskan environment.

I gratefully acknowledge the financial support of this work by the United States Air Force under Contracts AF 49(638)-1100 and AF 33(657)-13703 and the National Science Foundation under Grants GP-5246 and GP-5540.

## TABLE OF CONTENTS

	Page
ABSTRACT	iii
ACKNOWLEDGEMENTS	v
TABLE OF CONTENTS	vi
LIST OF ILLUSTRATIONS	viii
LIST OF TABLES	xvii
CHAPTER 1 INTRODUCTION	1
CHAPTER 2 INSTRUMENTATION	8
2.1 The photometers	8
2.2 The television system	12
CHAPTER 3 PULSING AURORAS	18
3.1 Pulsating auroras	19
3.2 Flaming auroras	54
3.3 Flickering auroras	64
CHAPTER 4 FAST AURORAL WAVES: OBSERVATIONS	74
4.1 March 14, 1964	79
4.2 November 1, 1964	88
4.3 January 28, 1965	97
4.4 December 22, 1965	101
4.5 January 26, 1966	107
4.6 March 16, 1966	118
4.7 Nights when waves did not occur	126
4.8 Observational summary	133

	Page
CHAPTER 5 FAST AURORAL WAVES: DISCUSSION	142
5.1 Electron precipitation patterns	142
5.2 Electron sources	146
CHAPTER 6 CONCLUSIONS AND RECOMMENDATIONS	154
6.1 Conclusions	154
6.2 Recommendations	160
APPENDIX 1 MOTIONS OF ENERGETIC ELECTRONS IN THE GEOMAGNETIC FIELD	163
BIBLIOGRAPHY	166

## LIST OF ILLUSTRATIONS

		Page
Figure 1.1	Schematic diagram to show the development of both the auroral and polar magnetic substorms, from (a) a quiet situation, (b) an early epoch of the expansive phase, (c) the maximum epoch of the substorm to (d) an early epoch of the recovery phase. The region where a negative bay is observed is indicated by the lined shade, and the region of a positive bay by the dotted shade (from Akasofu et al, 1966).	7
Figure 2.1	A schematic view, looking west, of the wave photometer (Type III). The chart shows the type of record obtained when a wave passes overhead from north to south.	11
Figure 2.2	The geometry required for determining the field aligned (flaming) velocities of forms off the TV camera's meridian. The flaming takes place on the line with ends marked $(\theta_1, \phi_1)$ and $(\theta_2, \phi_2)$ . The parabola is the intersection of the plane containing this line together with the $\theta_2$ cone.	17
Figure 3.1	The eastward progression of a pulsating patch that pulsated on and off 6 times within the field of view. The 6 frames are from the middle of each 'on' period. Arrows on the frames indicate points used for drift velocity measurements. The dark lower edges on these negative prints are instrumental. The prominent stars are Ursa Major $\gamma$ , $\delta$ , $\epsilon$ , and $\zeta$ .	24
Figure 3.2	Drift velocity in m/sec versus time between pulsations for the pulsating aurora of Fig. 3.1. The smooth curve shows the drift velocity (left-hand scale) and electron energy (right-hand scale) versus time of oscillation, $T_o$ , for electrons having an equatorial pitch angle of $3^\circ 20'$ and mirroring at 100 km on the $L = 5.5$ field line.	25

Figure 3.3a	Tracings from the TV films showing the initial shape of the patch and the successive positions of its leading edge during cycle 5. The time increments are 1/6 sec. A and B are the positions of the eastern edge of the patch for cycles 1 and 20 respectively, corresponding to a westward drift velocity of 180 m/sec. Elevation angles above the southern horizon appear on the right side of the frame. Also shown are distances subtended by the field of view at the 100 km level; the 116 km refers only to the centerline of the frame.	29
Figure 3.3b	The motion of the trailing edge of the patch during cycle 5. The patch faded between time intervals 13 and 14 (2 1/6 and 2 1/3 sec).	29
Figure 3.4a	Cycle 3 in which the growth stage involved two apparently related patches.	30
Figure 3.4b	Cycle 9 in which a small patch appeared and then grew to become part of the basic form.	30
Figure 3.5	Schematic pictures showing the cross sections of the precipitating electron bunches required to produce the behavior in Figs. 3 and 4a respectively. Luminosity is taken to be produced at the 100 km altitude level. The slopes of the leading and trailing edges are greatly underexaggerated (see text).	31
Figure 3.6	The growth phase at several epochs during the second pulsating cycle. The numbers under each diagram give the frame number from an arbitrary zero (24 frames/sec). 'X' marks the position of the magnetic zenith. Elevations above the southern horizon are given to the left of the first frame. Azimuths measured from south appear across the center of frame one. Distances subtended at the 100 km level appear in frame two.	34

Figure 3.7	The positions of the western edges of the patch when fully developed in the first and tenth cycles. The corresponding drift velocity is 180 m/sec.	35
Figure 3.8	An example of a pulsating aurora in which adjacent regions pulsate alternately: the appearance of the wedge in the frames on the left is followed by the appearance of its "ghost" in the frames on the right. The third pair is the best. The prints are negative.	37
Figure 3.9	Six photocell traces of intensity from six different regions of the $14^{\circ} \times 13^{\circ}$ television field of view during a pulsating display (0123-0128.5, March 17, 1964).	39
Figure 3.10	Successive ground plots at 2 min. intervals from 0341-0349 on December 4, 1965, of 2 patches in the northern and southern sky at College. The 2 selected patches show the drift trend of many others. The northern patch drifted westward at 770 m/sec while, at the same time, the southern patch drifted eastward at 170 m/sec.	41
Figure 3.11	Photocell tracings made from projected television film with photocells placed on the images of an arc southwest (upper trace) and northeast (middle trace) of the magnetic zenith, respectively. The lower trace results from monitoring the full field of view with a photocell. The insert at lower right shows the field of view with its area at 100 km altitude and the placement of photocells on the images of the pulsating forms.	43
Figure 3.12	Ground projections of eastward drifting patches made from the Ft. Yukon all-sky camera film of December 1, 1964. 'N' shows where the College northern photometer was directed to get the power spectrum of Fig. 3.13.	46
Figure 3.13	Power spectra of two four-minute samples of auroral pulsations taken at the College zenith and from $42^{\circ}$ north of the zenith, respectively. Both samples are from the same time interval, 0355-0359, December 1, 1964.	47

Figure 3.14	The results of a "sonagraph" spectral analysis of simultaneous pulsating aurora records from a $165^\circ$ field and a $1\ 1/2^\circ$ field centered on the zenith. After 0526 the $1\ 1/2^\circ$ field photometer was directed $49^\circ\text{N}$ of the zenith.	48
Figure 3.15	The last four of five consecutive frames covering the flaming aurora example of February 16, 1967. The filming rate was 30 frames/sec. The bottom of the ray that appeared and then moved upwards from elevation $56.8^\circ\text{S}$ to $58.5^\circ\text{S}$ is marked by an arrow in each of the frames. For an assumed initial lower border height of 100 km the flaming velocity was $70 \pm 9$ km/sec.	57
Figure 3.16	Plots of the apparent upward velocities of synthetic flaming auroras due to electrons being released with zero pitch angle at several points on the $L = 5.5$ field line. The distances are in units of earth radii and are measured from the earth's surface.	60
Figure 3.17	$165^\circ$ field of view of the sky at 2207, February 22, 1966. The flickering was observed in the broad diffuse feature near the zenith.	66
Figure 3.18	Photocell traces made from the television films at 2207 showing the rapidity of the flickering and the dissimilarity between the light output from different points. The photocells were randomly placed in the $22 \times 16$ km field intersected at the 100 km altitude level.	67
Figure 3.19	Tracings made at 2207 from corresponding parts of 16 consecutive TV frames centered on the magnetic zenith. The flickering can be seen to be due to rapid changes in size and shape of individual patches. The field shown intersects an area roughly $12 \times 10$ km at the 100 km altitude level.	68

Figure 3.20	Plots of the flickering index and the narrow beam riometer absorption (shaded).	72
Figure 4.1	The College magnetograph H component traces for the nights on which wave displays occurred. The times that waves were seen or recorded are marked by bars. Subtract 10 hours for Alaska Standard Time.	77
Figure 4.2	The College $\lambda 4278$ zenith photometer traces for the last five nights on which wave displays occurred. The times that waves were seen or recorded are marked by bars.	78
Figure 4.3	A tracing of the photometer records of three fields of view showing luminous waves having velocities of 60-70 km/sec and widths 30, 45, and 100 km respectively. The three $1\ 1/2^\circ$ fields of view intersect the 100 km altitude level at $\sim 5$ km intervals.	84
Figure 4.4	A series of all-sky camera photographs at 30 minute intervals taken before and during the period when the waves were seen.	85
Figure 4.5	The Huet zenith spectrum for the night of March 13/14, 1964.	86
Figure 4.6	The distribution of auroras over Alaska at several epochs during the March 14, 1964, display. Arrows near a feature show it to be moving; wavy arrows show fast auroral waves; dots show diffuseness.	87
Figure 4.7	College all-sky camera frames at 30 minute intervals before and during the wave display of November 1, 1964.	91
Figure 4.8	Ft. Yukon all-sky camera frames at 30 minute intervals before and during the wave display of November 1, 1964.	92
Figure 4.9	(A, B, C,) photometer traces starting at 0334 of fast auroral waves from $1\ 1/2^\circ$ fields of view $30^\circ\text{N}$ and $23^\circ\text{S}$ of the College zenith. Traces (B) and (C) are fast-run samples selected from the slow-run trace (A). The velocities of the waves shown were commonly 60 km/sec.	93

Figure 4.10	Photometer traces at 0341 showing the waves to travel to the zenith from the north, but to lose intensity farther south.	94
Figure 4.11	A "sonagram" showing the frequency spectrum of the fast auroral waves of November 1, 1964. The photometer was directed at a number of places during the display.	95
Figure 4.12	The distribution of auroras over Alaska at several epochs during the November 1, 1964 display. Arrows near a feature indicate it to be moving; wavy arrows indicate fast auroral waves; dots indicate diffuseness.	96
Figure 4.13	The distribution of auroras over Alaska at two epochs during the January 28, 1965 display. Arrows near a feature indicate it to be moving; wavy arrows indicate fast auroral waves; dots indicate diffuseness.	100
Figure 4.14	A series of all-sky camera pictures covering part of the December 22, 1965, auroral display. The quality of the wave photometer traces was best around 0240. The evidence for patches before and after this time is quite clear.	104
Figure 4.15	Wave photometer records for December 22, 1965. 'NS' and 'DC' respectively refer to night sky and dark current deflections (A) 0225, wave motions were seen visually but the waves must have traveled less than 50 km. (B) 0234, waves can be seen to cross the 3 southernmost fields. The slow variations on channel 1 are probably due to pulsating patches. Waves A-D traveled at 50-60 km/sec. (C) 0245, channel 3 and 4 only were traversed by waves. Channel 1 indicates a steady signal 10 times the night sky value while channel 2 is greatly disturbed, possibly the result of pulsating auroras.	105

- Figure 4.16 The distribution of auroras over Alaska at several epochs during the December 22, 1965, display. Arrows near a feature indicate it to be moving; wavy arrows indicate fast auroral waves; dots indicate diffuseness. 106
- Figure 4.17 Wave photometer records for January 26, 1966. 'NS' and 'DC' respectively refer to night sky and dark current deflections. (A) 0303, fields 1-3 show various types of pulsations while 4 shows steady low intensity except for some 2 cps tape recorder noise. (B) 0324, fields 1 and 2 show convincing evidence for waves but these did not reach fields 3 and 4. Example A had a velocity of 150 km/sec. (C) 0330, the wave path reached south to include field 3 with 1 and 2. There were no gain changes between 0324 and 0330. 114
- Figure 4.18 Wave photometer records for January 26, 1966. 'NS' and 'DC' respectively refer to night sky and dark current deflections. (A) 0340, the wave path had continued to spread south and included all fields of view. Wave A's velocities between the fields were 150, 150, and 100 km/sec respectively. Wave B had velocity 140 km/sec. (B) 0356, wave A had two components and shows how consecutive waves can have different velocities. (C) 0413, wave A traveled at 140 km/sec between fields 2 and 3 and 100 km/sec between 3 and 4. 115
- Figure 4.19 Wave photometer records for January 26, 1966. 'NS' and 'DC' respectively refer to night sky and dark current deflections. (A) 0420, the waves were less frequent than before. (B) 0500, infrequent waves crossed fields 1 and 2. The three southernmost fields are down to or below night sky levels (determined on another night). 116
- Figure 4.20 The distribution of auroras over Alaska at several epochs during the January 26, 1966 display. Arrows near a feature indicate it to be moving; wavy arrows indicate fast auroral waves; dots indicate diffuseness. 117

- Figure 4.21 Wave photometer records for March 16, 1966. 'NS' and 'DC' respectively refer to night sky and dark current deflections. (A) 0219, channel 1 was inoperative. Waves crossing fields 2 and 3 seem to have lost intensity and fine structure by the time they reached 4. Waves A and B traveled at 40-45 km/sec. (B) 0223, the fine structure carry-over between fields 3 and 4 had improved. Wave A traveled at 60 km/sec and B at 60 km/sec between 2 and 3 and 75 km/sec between 3 and 4. (C) 0228, the signal from field 2 had deteriorated, possibly because the wave path had migrated southward. The waves shown had velocities around 50 km/sec. 122
- Figure 4.22 Wave photometer records for March 16, 1966. 'NS' and 'DC' respectively refer to night sky and dark current deflections. (A) 0230, the fine structure carry-over between fields 3 and 4 had improved. The waves marked had velocities of 60-70 km/sec. (B) 0238, only field 4 recorded wave-like variations. Field 2 may have recorded in situ pulsations. (C) 0310, there may have been a slow (25-50 km/sec) wave-like motion. 123
- Figure 4.23 Pairs of all-sky camera frames from College and Ft. Yukon during and after the wave display. The "homogeneous" arc seen from College was, in fact, multiple arcs over Ft. Yukon. 124
- Figure 4.24 The distribution of auroras over Alaska at several epochs during the March 16, 1966 display. Arrows near a feature indicate it to be moving; wavy arrows indicate fast auroral waves; dots indicate diffuseness. 125
- Figure 4.25 The College magnetograph H component traces for the nights discussed in Sec. 4.7. Note that the two bottom traces are from the insensitive (storm) magnetograph. Subtract 10 hours for Alaska Standard Time. 127

- Figure 4.26      A model distribution of the auroras over part of Alaska during a fast auroral wave display. The length of the wave path within which all waves propagate is variable, as is its position within the sub-visual glow. The sub-visual glow may contain weak pulsating patches as well as waves. Its intensity is commonly  $I_{4278} \approx 1 \text{ kR}$  while that of the waves is  $I_{4278} < 1 \text{ kR}$ . 141
- Figure 5.1      Schematic pictures showing the orientation of precipitating electron slabs required to produce some of the fast auroral wave properties: (A) Wave velocity and width. (B) Overtaking. (C) Speeding up. (D) Wave Path. The horizontal dimension of the diagram is greatly exaggerated because  $\alpha$  is almost  $90^\circ$ . 143

LIST OF TABLES

Table		Page
1	Properties of the photomultipliers.	10
2	Temporal and spatial characteristics of the patch of 0124 March 17, 1964.	22
3	Temporal information about the pulsations of 0221 February 23, 1966.	27
4	Temporal information about the pulsating patch of 0348 February 23, 1966.	36
5	Temporal information about the pulsations of 0110 March 17, 1964.	38
6	A comparison of the magnetic and auroral conditions for the nights with and without waves.	134
7	Fast auroral wave display summary.	137

## Chapter 1

### INTRODUCTION

"The metropolis was surprised on Tuesday night by a brilliant display of Northern Lights...(which) loosened the tongues of a hundred prophets." London newspaper, 1827 (Kendall, 1827).

The aurora is at present believed to be analogous to the image produced in a cathode-ray tube (Akasofu, 1965). Its behavior is directly related to the source of charged particles and the deflecting electric and magnetic fields in the magnetosphere. Therefore it would seem that the position and properties of the source and the fields can be conjectured by carefully observing the aurora.

A major step toward giving an understandable ordering to the bewildering behavior of the aurora, as seen from College, Alaska, was made by Heppner (1954). He determined two patterns relating auroral activity and magnetic disturbance. The simpler pattern can roughly be represented as:

Homogeneous arcs in early evening; small positive disturbance	→	Rayed arcs and bands in later evening; positive disturbance	→	Breakup into active forms near midnight; large negative disturbance	→	Diffuse-appearing pulsating patches or arcs until twilight; recovery of negative disturbance
---	---	---	---	---	---	--

This thesis deals primarily with the auroral types of the last category for several reasons. Foremost is that these auroral types stand out from the others in an auroral display because of their quasi-periodic behavior in time and space. It was felt that an

understanding of auroral types with such definite physical characteristics would ultimately aid in understanding more complex types.

Secondly, post-breakup auroras warrant attention because of the energy output: Murcray (1959) collected light energy from the whole sky and averaged and plotted hourly values for nine months. A plateau maximum resulted that lasted from 0100 until dawn, that is, the time of the post-breakup auroras. More recently this time interval has been found to be characterized by the precipitation of large fluxes of high as well as low (auroral) energy electrons (cf. Brown, 1966), and there is evidence to show that these are precipitated simultaneously (Rosenberg et al, 1967). The morphology of the low energy electron precipitation patterns can be readily determined by optical television methods, whereas the best that can be done for the higher energies is to use balloon-borne, collimated, detectors with separated fields of view (Parks, 1967); rocket and satellite studies suffer from the inability to distinguish between temporal and spatial variations. It would seem then, that an initial understanding of the low energy electron precipitation morphology, followed by coordinated low and high energy observations, would represent a logical approach to understanding the morphology of high energy electron precipitation associated with post-breakup auroras.

Finally, Heppner's study indicated that the quasi-periodic auroras are primarily restricted to relatively low geomagnetic latitudes: below  $67^{\circ}$ . Therefore this particular class of auroras very likely occurs on closed geomagnetic field lines, that is, those which intersect the equatorial plane perpendicularly. The same statement cannot at this time be generalized to include all types of auroras. Thus by restricting this study to the class of auroras occurring only on the equatorward side of the normal auroral display, one uncertainty is removed regarding the phenomenon, namely that of the geometry of the associated geomagnetic field lines.

Since 1954 when Heppner used visual observations to produce the two patterns of auroral activity referred to earlier, Akasofu and co-workers (Akasofu 1966, and references therein) have used all-sky camera networks to establish a world-wide pattern of auroral activity. This pattern is called the auroral substorm, and in this study it was found convenient to use it as a framework to organize the observations. Consequently, a brief summary of the substorm concept is given here, together with some additional comments pointing out where and when the quasi-periodic auroras are observed. To some extent these comments make use of the results of the present study.

In the substorm model, undisturbed conditions are characterized by faint, diffuse, quiet arcs extending along the whole of the auroral zone that is in darkness (Fig. 1.1). With the onset of a substorm

arcs near the midnight meridian brighten and a rapid expansive motion of auroral activity and negative bay influence takes place. Generally the substorm tends to develop most extensively when the equatorward most arc is first activated. The poleward expansion is one of the most spectacular features of a substorm; its speed is most commonly about 500 m/sec but can exceed 1300 m/sec.

In the evening sector, equatorward of the pre-existing arcs, a positive bay is observed at the time of substorm onset. During the westward expansion of the substorm a westward traveling surge propagates along the arcs with a velocity on the order of 1 km/sec. As the surge reaches a station, the positive bay changes to a negative bay. The magnitude of this bay, and also the ionospheric effects associated with the surge, are much less than those caused by active auroras in the morning sector during the same substorm, even though the surge is often brighter than the morning auroras. This has been attributed to harder electrons precipitating into the morning sector than the evening sector (Ansari, 1964).

The equatorward expansion associated with the substorm is not systematic like the poleward expansion but comes about by irregular bands and patches apparently spreading equatorwards.

In the morning sector the region of negative bay influence spreads eastwards with a speed of order 10 km/sec; it is mainly confined to the equatorward side of the pre-existing arcs. Also the arcs develop irregular folds and patches, but the eastward

velocity of the development is 3 km/sec. Once formed, the patches, which lie equatorward of the position of the undisturbed arc, drift eastward with a much lower velocity of 100-500 m/sec.

During the recovery phase of a substorm arcs and bands in the midnight sector undergo a slow equatorward return with a speed of order 200 m/sec or less. At the same time the westward surge becomes attenuated and its speed is reduced. In its wake are left westward drifting loops traveling at about 200-500 m/sec. In the morning sector the originally undisturbed arc reforms. The recovery phase may take several hours.

A factor that can influence the substorm model is the overall storm condition prevailing in the magnetosphere; disturbed conditions cause the auroral oval to expand equatorward, while quiet conditions cause it to contract. If the oval is not used as a frame of reference, then confusion can arise. For instance, unusually disturbed or unusually quiet conditions can put College either inside or outside the auroral oval and, as a result, two similar substorms could be observed to be entirely different.

The quasi-periodic auroras that are the subject of this study can be listed as follows:

1. Those auroras left in the wake of the poleward expansion that signals a substorm onset.
2. The patches that form equatorward of the arcs in the morning sector following substorm onsets.

3. The fast waves that occur in a weak envelope that migrates equatorward in the morning sector after some substorm onsets.
4. The flickering auroras that occur sometimes in bright features on active nights in the evening sector.

A summary of the remaining chapters is as follows: Chapter 2 discusses the instrumentation and observational technique.

Pulsing auroras, namely pulsating, flaming, and flickering auroras, are reviewed in Chapter 3 and examples are treated at length.

In Chapter 4 fast auroral waves are reviewed and the observations of this study are discussed. Chapter 5 follows with a discussion of these observations along with possible interpretations of them.

Finally the findings of the thesis are summarized and recommendations are made for further work in Chapter 6.

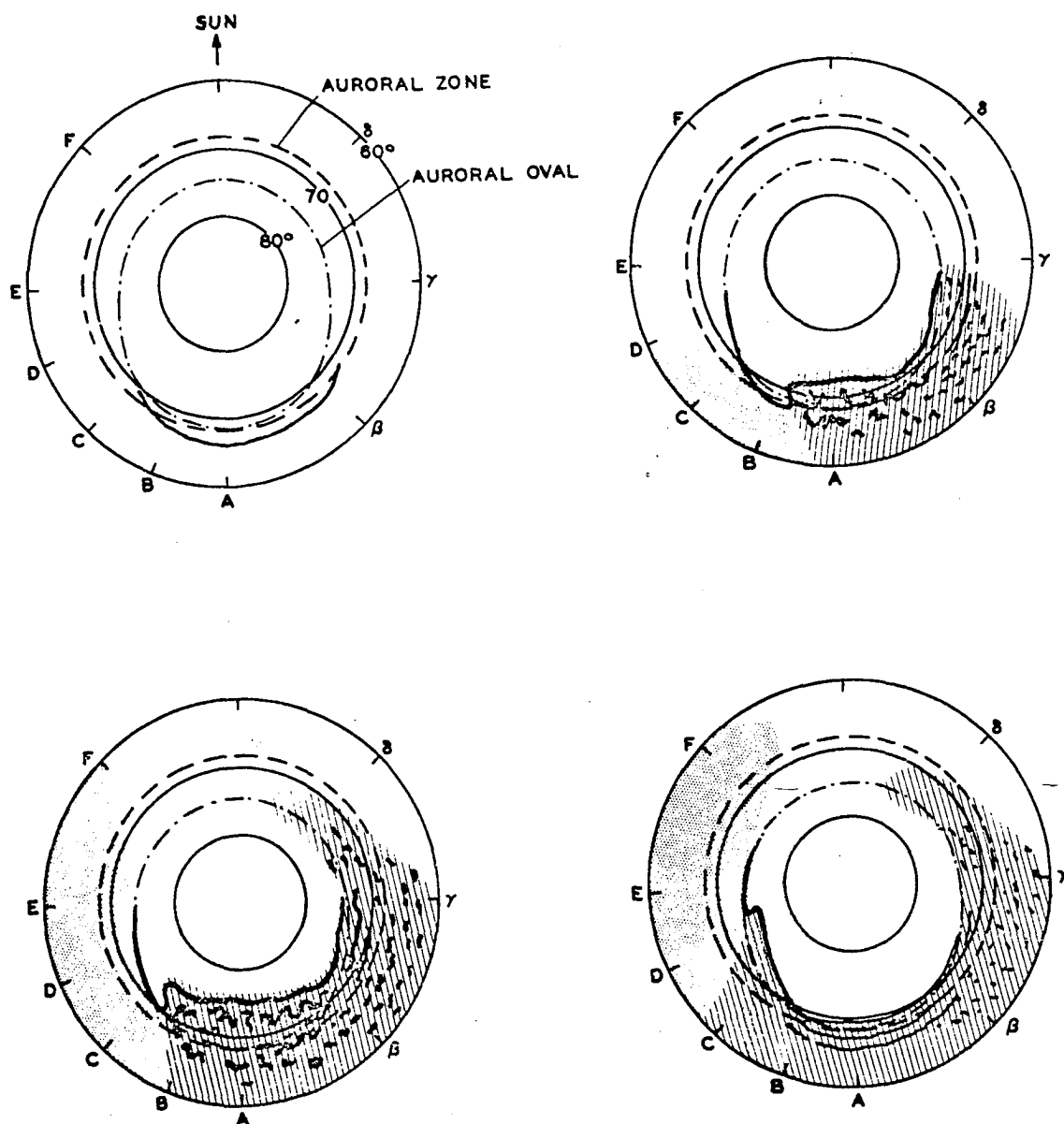


Figure 1.1 Schematic diagram to show the development of both the auroral and polar magnetic substorms, from (a) a quiet situation, (b) an early epoch of the expansive phase, (c) the maximum epoch of the substorm to (d) an early epoch of the recovery phase. The region where a negative bay is observed is indicated by the lined shade, and the region of a positive bay by the dotted shade (from Akasofu et al, 1966).

## Chapter 2

### INSTRUMENTATION

The aurora is a complex phenomenon that can involve apparent velocities of the order of 100 km/sec parallel to the earth's surface or along the magnetic field direction. In addition, it involves in situ intensity fluctuations at least up to 10 cps. To accurately describe it and relate it to processes occurring in the magnetosphere, therefore, requires instrumentation sensitive to rapid temporal and three-dimensional spatial variations. Since the development of photomultipliers the observational task has fallen mainly on photometers. Recently, however, the advance of image orthicon television techniques has lead to the introduction of television systems to auroral research. At the present time a combination of photometers and television systems appears to be the most flexible and fruitful arrangement.

#### 2.1 The Photometers

The original photometer, Type I below, was designed by Professors Belon and Romick for separating motions and in situ variations in pulsating auroras. It was used to collect the first quantitative facts about fast auroral waves (Cresswell and Belon, 1966). The separation of its fields of view, however, was too small for accurately measuring fast auroral wave velocities and it lead to confusion when fast auroral waves and pulsating auroras occurred together. This resulted in the wave photometer, Type III, being built.

Type I (used for the 14 March, 1964 and  
1 November, 1964 wave displays)

This photometer consisted of a single 9.23" focal length, f/3.1, telescope equipped with a broad-band filter (Corning No. 5-60) which transmitted the spectral range covered by the prominent bands of the first negative systems of  $N_2^+$ . A set of four field stops placed in the focal plane of the objective isolated four fields of view ( $1\ 1/2^\circ$  fields on a  $6^\circ$  circle) and directed them respectively to four RCA 7265 photomultipliers. The anode currents were amplified by Keithley "610" electrometers and were recorded on a multi-channel Ampex "SP300" tape recorder. Data on tape were transcribed to paper chart on a multi-channel Honeywell "Visicorder". A photograph of the instrument and a schematic diagram of the optical system is given by Belon et al (1964).

Type II (used for the 25 January, 1965 wave display)

In January of 1965, some cooperative work was done with Dr. T. Neil Davis, then of NASA. A smaller four-field photometer was constructed to fit on the same mount as his image orthicon television system. This was achieved by replacing the rather bulky 7265 tubes and bases by 1P21 tubes.

Type III (used for the 22 December, 1965, 26 January, 1966,  
and 16 March, 1966 wave displays)

In November of 1965, a new four-field photometer was constructed solely for studying fast auroral waves. It was designed such that its fields would intersect the 100 km altitude level at 50 km intervals

along a N-S line. In this way, changes in velocity of particular waves as they progressed southward could be examined. Four 190 mm focal length, f/3, single element lens telescopes having field stops of 20 x 5.5 mm corresponding to fields  $6^\circ \times 1^\circ 40'$  were used. Behind the field stops were RCA 1P21 photomultipliers; the same broad-band filters were used as before. One telescope was directed at the magnetic zenith; another was directed 50 km south of it; two others were directed 50 and 100 km respectively north of it (Figure 2.1). Otherwise, the recording techniques were the same as with earlier photometers.

As measured at 0218 on 23 December, 1965, when the only aurora was in the low northern sky, the night sky anode currents and the dark currents for the four photomultipliers were the following:

Table 1  
Properties of the Photomultipliers

	NIGHT SKY	DARK CURRENT
1 (North)	$2.8 \times 10^{-7}$ amp.	$2.8 \times 10^{-9}$ amp.
2 (N. Zenith)	$1.4 \times 10^{-7}$ amp.	$1.6 \times 10^{-9}$ amp.
3 (S. Zenith)	$1.3 \times 10^{-7}$ amp.	$3.0 \times 10^{-9}$ amp.
4 (South)	$4.6 \times 10^{-7}$ amp.	$2.5 \times 10^{-10}$ amp.

The  $\lambda 4278$  zenith photometer for the entire night was quite undisturbed, showing intensities too small ( $< 150R$ ) to be measured.

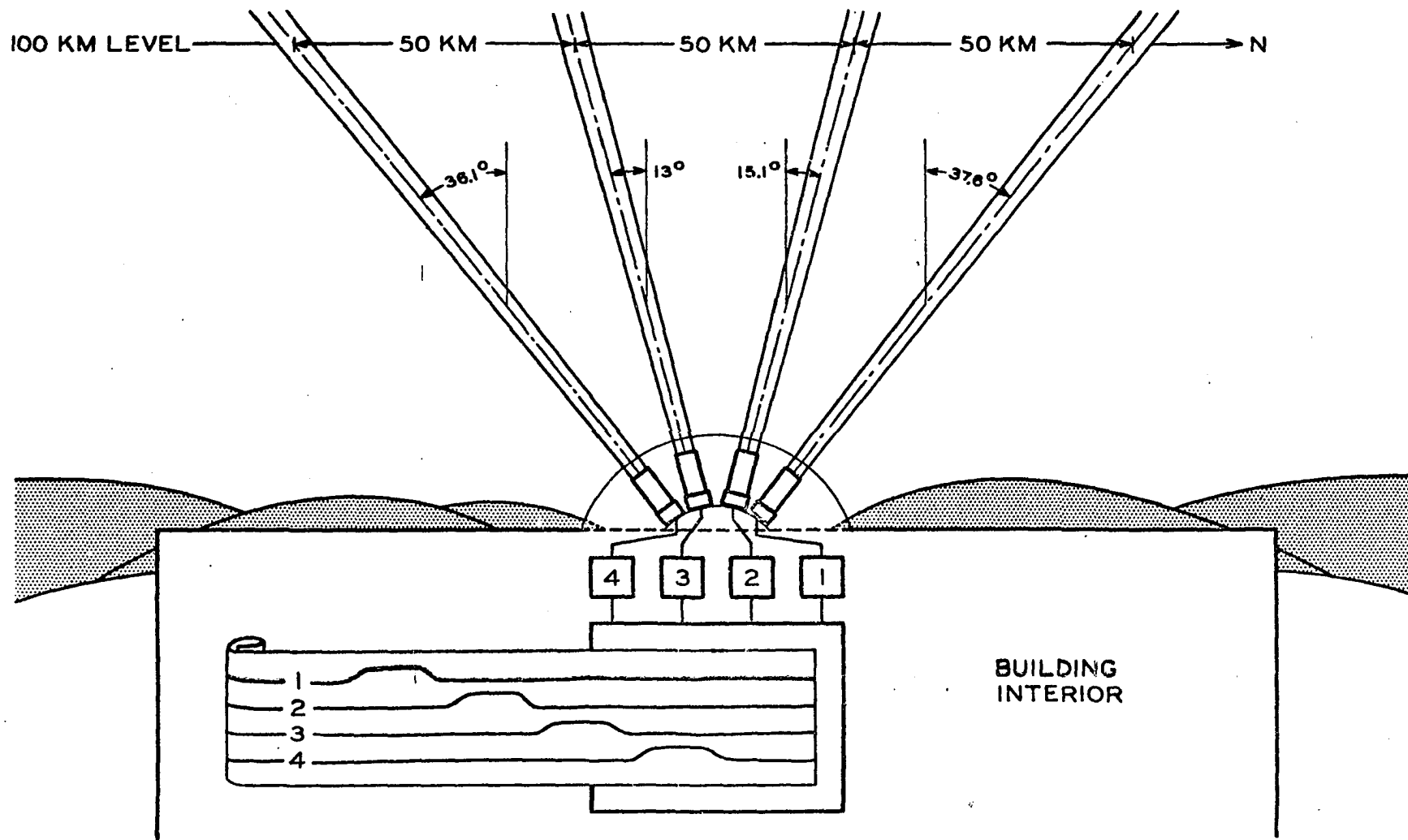


Figure 2.1 A schematic view, looking west, of the wave photometer (Type III). The chart shows the type of record obtained when a wave passes overhead from north to south.

### Photometric observational procedure

On clear, moonless nights when there was mid-evening auroral activity the writer went to the Ester Dome observatory. Photometers for studying fast fluctuations were turned on when pulsating auroras or fast auroral waves were sighted. In the event of fast auroral waves an arbitrary amount of the DC component was removed by driving the amplifier zero level negative; the remainder was amplified. This had the advantage of making the time lags between separated fields of view easier to measure. Unfortunately, intensity information was sacrificed when doing this so one of the channels was left untouched. At the start and finish of a run step voltages from the amplifiers were fed into the tape recorder. A chronometer was used and adequate (once per 15 or 30 minutes) time marks were added by simply closing and opening the shutter on one channel several times.

Visual observations were taken from a plastic dome every five minutes.

Later when the tape was to be analyzed it was played and the recorded data transcribed to paper chart on a Honeywell "Visicorder". The chart was examined for time lags, evidence for migration of the wave propagation path, and other features. Suitable samples were selected, re-transcribed in darkness, and permanized (the visicorder paper is light sensitive).

### 2.2 The Television System

Photometer records of pulsing auroras are generally difficult

to interpret because of the uncertainty in knowing just what the aurora was doing: Was it moving? Did two overlap? Did it move and pulsate? The television system neatly sidesteps these difficulties: temporal and spatial variations can be distinguished. Projecting the film essentially recreates the aurora, at least as a two dimensional matrix of binary (on or off) grains that are characteristic of the system. Examples free from ambiguity can be selected for measurement; actual behavior can be determined by projecting the film many times over.

A description of the system and a history of its use for auroral observations was given by Davis (1966). Here it will suffice to discuss some of the analysis techniques.

#### Application to motions parallel to the earth's surface.

These are the type of motions that are involved in the drift of a pulsating patch. To examine them it was necessary to be able to construct an angular grid for the screen.

At the start of each roll of film, during recording, an angular calibration was performed by moving the television camera in elevation and azimuth across a distant light on the horizon. During analysis the sequence was projected and then stopped at short intervals. At each stop the position of the light and the elevation and azimuth values from the encoder around each frame were marked on a sheet of paper attached to the screen. This enabled an angular grid to be drawn up. It was then a matter of simple trigonometry to determine, for instance, how far a patch had drifted for an assumed height,  $h$ .

### Application to Field-aligned motions

These motions are commonly referred to as 'flaming'. In the simplest case measurements were made on forms that were on the center line of the screen, which was the geomagnetic meridian. The co-elevations ( $\theta_1, \theta_2$ ) of the start and finish of the upward flaming were measured using the grid described in the previous section. For an assumed starting height,  $h$ , the distance along the ground from the station to the point under the form,  $D = h \tan \theta_1$ , was calculated. The distance traveled during the flaming was determined from  $(\frac{D}{\tan \theta_2} - h)$  corrected by the factor  $\sin(180 - \theta_2)/\sin(\theta_2 - 13)$  to allow for the  $13^\circ$  tilt of the field line.

When the flaming form was not on the meridian a slightly more involved technique was necessary. To use it required that the television camera, already calibrated for elevation as described in the previous section, be swept in azimuth across a star background. This had to be done at the camera elevation used during the flaming sequence. An elevation and azimuth grid for this elevation resulted.

Using the grid, the elevations and azimuths of the start and finish points for the flaming can be measured. However, since azimuth cannot be measured with as much accuracy as elevation, some uncertainty in the calculations can be removed by requiring the technique to employ the azimuth of only one of the points, in this case the start point.

The line path of the flaming will lie in its own north-south plane. If the vector from the observer to the finish point of the flaming is rotated in azimuth it will trace out a cone, and the intersection of this with the plane will be a parabola (Figure 2.2).

The measured azimuth and elevation of the start point of the flaming give all that is required about it; it is then denoted the origin of an x-y coordinate system in the meridian plane. The coordinate of the finish point comes from finding the intersection of the line path ( $y = -4.33 x$ ) with the parabola ( $y = ax^2 + bx + c$ ). The various points on the plane are given by

$$x_o = -b/2a, y_1 = c$$

$$y_o = y_1 - b^2/4a = y_1 - ax_o^2$$

$$\text{Thus } a = \frac{y_1 - y_o}{x_o^2}, b = \frac{-2(y_1 - y_o)}{x_o}.$$

The parabola can then be written

$$y = \frac{(y_1 - y_o)}{x_o^2} x^2 - \frac{2(y_1 - y_o)}{x_o} x + y_1$$

and its intersection with the line is given by

$$\frac{(y_1 - y_o)}{x_o^2} x^2 + (4.33 - \frac{2(y_1 - y_o)}{x_o})x + y_1 = 0 \quad (1)$$

The  $x_o$ ,  $y_o$ , and  $y_1$  values come from measurements of azimuth and co-elevation on the television picture.

$$y_1 = h \left( \frac{\tan \theta_1}{\tan \theta_2} - 1 \right)$$

$$y_o = h \left( \frac{\tan \theta_1 \sin \phi}{\tan \theta_2} - 1 \right)$$

$$x_o = h \tan \theta_1 \cos \phi$$

Substituting these into (1) gives the x coordinate of the intersection; the y coordinate follows. The path length of the flaming is then

$$\sqrt{x^2 + y^2}.$$

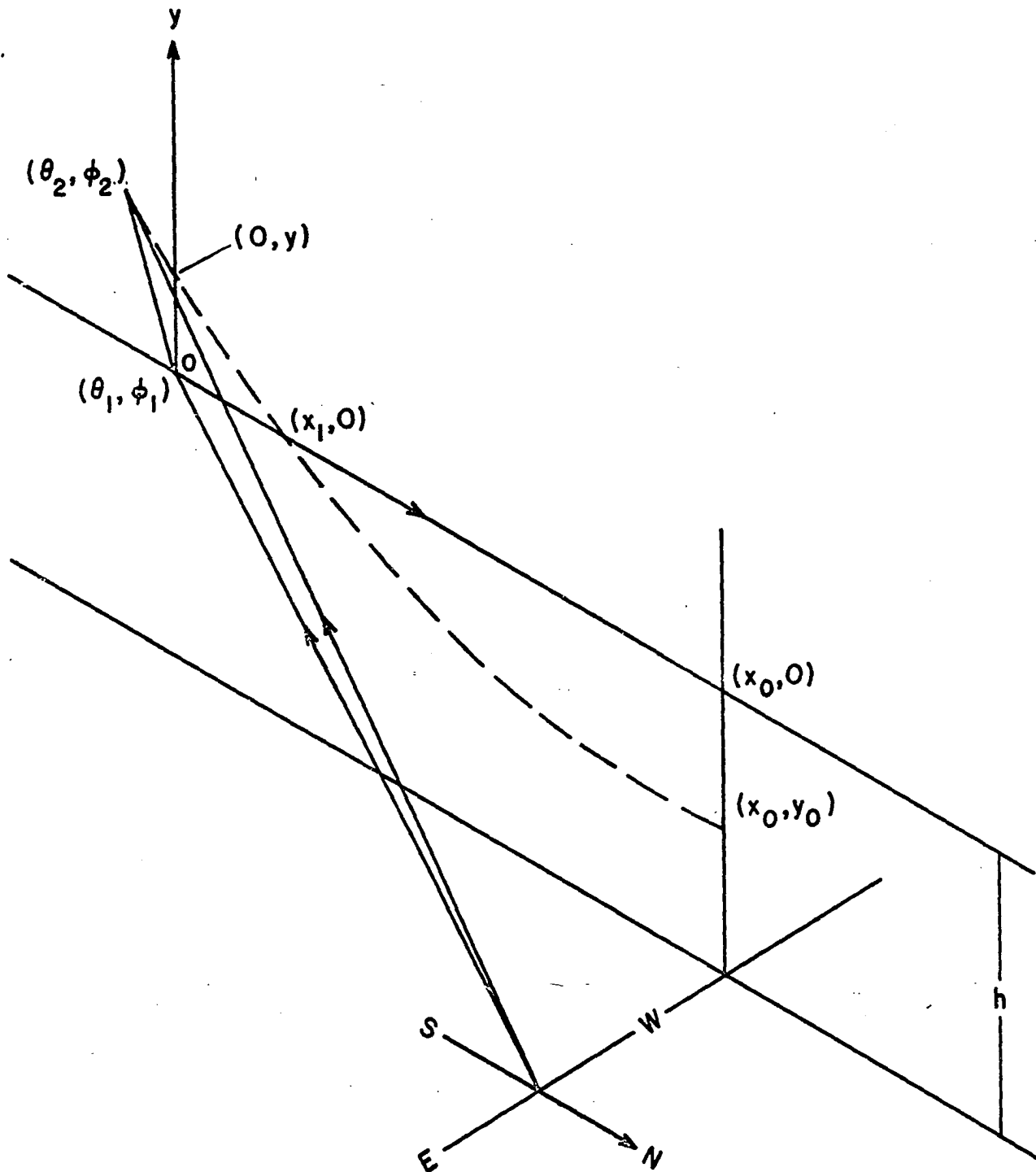


Figure 2.2 The geometry required for determining the field aligned (flaming) velocities of forms off the TV camera's meridian. The flaming takes place on the line with ends marked  $(\theta_1, \phi_1)$  and  $(\theta_2, \phi_2)$ . The parabola is the intersection of the plane<sup>1</sup> containing this line together with the  $\theta_2$  cone.

Chapter 3  
PULSING AURORAS

"Here is one! lo, it is gone! Scarcely has it vanished before it appears again in another place." Observation by Weyprecht, 1872-73, (Chapman and Bartels, 1940).

The terms pulsating and flaming were used in the auroral classification presented in the Photographic Atlas of Auroral Forms (1930). The most recent atlas (International Auroral Atlas, 1963) introduces a new term, pulsing, which embraces pulsating and flaming, together with flickering and streaming. It describes a condition of fairly rapid, often rhythmical fluctuation of brightness. The period of the fluctuation ranges from a fraction of a second to the order of minutes. Three types of pulsing, namely, pulsating, flaming, and flickering, are treated in this chapter.

Pulsing auroras have been studied with photometers over the last few years and the data lent themselves to a statistical study of frequency behavior (cf. Johansen and Omholt, 1966). The recent application of image orthicon television systems to auroral research made it possible in the present study to shift the emphasis from statistical analyses alone. Discrete pulsing sequences have been selected and then the growth and decay characteristics, drift velocities, and field-aligned velocities (if any) have been examined in conjunction with frequency behavior. Attempts were made to interpret this information in terms of present knowledge of auroral processes.

### 3.1 Pulsating Auroras

Accounts of early observations on pulsating auroras were given by Lovering (1868) and Angot (1896). More recently Störmer (1942, 1955) reported on an extensive visual and photographic study of pulsating auroras. His height determinations showed pulsating arcs to occur from 105-115 km and pulsating patches to occur from 80-85 km. Vestine (1943) observed the magnetic elements to vary in an oscillatory manner during a pulsating aurora. Both Vestine and Störmer measured the periods during which the auroras were emitting and found values from a few seconds to more than a minute. Parsons and Fenton (1953) at Macquarie Island found that pulsating auroras were most frequent during the equinoctial months and that "they usually took the form of diffuse surfaces or scattered remnants of previously brighter draperies or coronas." They observed the pulsating auroras to be of strength rarely more than 2 on the 0-4 intensity scale and noted that the emitting times of various pulsating patches were not synchronized. Heppner (1954) found that pulsating auroras at College occurred with almost equal probability between 0100 and 0700 150° WMT, and most often at geomagnetic latitude  $\lambda_m = 64^\circ$  rather than farther north in the auroral zone.

Photometric observations have now been made by a number of investigators. Ashburn (1955) was handicapped by the response time of his recorders, but was able to see small oscillations of period 1-2 seconds superimposed upon major pulsations. Omholt (1957) found that the H $\beta$  emission at 4861Å was "always absent or extremely

weak in the rays and in pulsating forms". Georgio (1959) monitored as many as three different well-separated patches to determine the phase relations between them. Sometimes they were in phase; later the phase relationship would change. He was unable to draw any firm conclusions. In a later paper Georgio (1962) reported the green line intensity of pulsating auroral forms not to exceed 2-3 kR, ie. between IBC I(1kR) and IBC II (10kR). From the spectroscopic results he found the emission spectrum of pulsating auroras to be the same as the ordinary emission spectrum characteristic of diffuse surfaces and homogeneous arcs and bands.

Other investigators have examined auroral coruscations and telluric currents: Campbell and Rees (1961) found day to day coruscation amplitude variation to be similar to those of magnetic micropulsations: the correlation coefficient was 0.6. The terminology 'coruscation' was used in the nineteenth century by Burritt and was re-introduced by Campbell and Rees. As used by them it referred to any short period changes in auroral luminosity seen by their 90° field of view photometer. Flock et al (1962) compared the records of a 1° x 4°  $\lambda$ 3914 zenith photometer with telluric current micropulsations and found the correlation to be better under cloudy conditions. Clouds would effectively increase the field of view of the photometer. Good correlation under clear sky conditions was obtained only when the recordings were very cyclic.

Attempts have been made to classify pulsating auroras by the character of their photometer traces. Nadubovich (1961) used a

180° field of view photometer and for his type A he had groups of pulsating patches that created on the photometer record "a pattern of chaotic change of light flux". His type B referred to pulsations on the record having a "one-sided character", i.e. either positive or negative spikes on an otherwise slowly changing trace. Visual observations showed that type B was associated with pulsating arcs or isolated patches.

The most recent such attempt is that of Johansen and Omholt (1966). They used a 0.6 x 1° field of view photometer and recorded quasi-periodic pulsations that often appeared only as a slight modulation of the total luminosity. As well as classifying pulsating auroras by their photometer traces, they classified them according to the character of their power spectra. Because the pulsations generally did not show decreasing amplitude it was reasoned that they could not be due to groups of semi-trapped electrons that were depleted by each encounter with a mirror point.

The examples of pulsating auroras chosen in the present study appear in the following sections.

### 3.1.1 A relatively simple pulsating patch (eastward drifting)

At 0124 on March 17, 1964, the television system, directed at the College zenith, recorded the passage of a pulsating patch that pulsed six times as it drifted eastward through the field of view. The complete event, which lasted only 25 sec, is represented by Fig. 3.1. which shows negative prints of frames judged

to be near the middle of the "on" periods for the patch; additional information is contained in Table 2. There was a tendency on two appearances, the third and fourth, for the eastern side of the patch to brighten before the western side, the time difference being about one sec.

Table 2

Temporal and Spatial Characteristics of the Patches  
of 0124 March 17, 1964.

Frame No.	Time Difference Seconds	Number of Frames "on"	Drift Distance, km	Drift Velocity, m/sec
1		90		
	2.75		1.5 ± 1.0	550 ± 370
67		50		
	4.9		2.5 ± 1.0	510 ± 200
185		55		
	4.67		2.5 ± 1.0	540 ± 220
297		85		
	5.25		2.0 ± 1.0	380 ± 190
423		50		
	4.95		2.0 ± 1.0	400 ± 200
542		40		

By measuring the time between pulsations and the apparent distance traveled (assumed height 100 km) it was possible to plot drift velocity in meters per second versus time between pulsations in seconds (Fig. 3.2). The uncertainty in velocity is quite large; it is caused

by the feature having both a diffuse edge and a progressive shape change. Also plotted in Fig. 3.2 is a curve of drift velocity versus time of oscillation,  $T_o$ , for electrons having an equatorial pitch angle of  $3^\circ 20'$  and mirroring at 100 km on the  $L = 5.5$  field line (see Appendix I).

From the graph it can be seen that most of the data points are far removed from the electron drift velocity versus  $T_o$  curve. This indicates that the patch could not be due to a particular group of electrons adiabatically oscillating to and fro along the earth's field with some of their number being dumped as each extremity is reached.

If however, the electrons were influenced by equatorward-directed electric fields near their mirror points then their drift velocities would be increased. The electrons spend most of their bounce periods traversing flattened spirals near the mirror points and so are vulnerable to electric fields there. The drift is given by (Spitzer, 1962):

$$v_d = \frac{E_{\perp}}{B} = \frac{10^8 E_{\perp} (\text{volts/cm})}{B(\text{gauss})}$$

The electric field that would cause the electrons to drift 300 m/sec faster than the adiabatic drift would be

$$E_{\perp} = \frac{300 \times 10^2 \times 0.6}{10^8} \text{ volts/cm} = 18 \text{ volts/km}$$

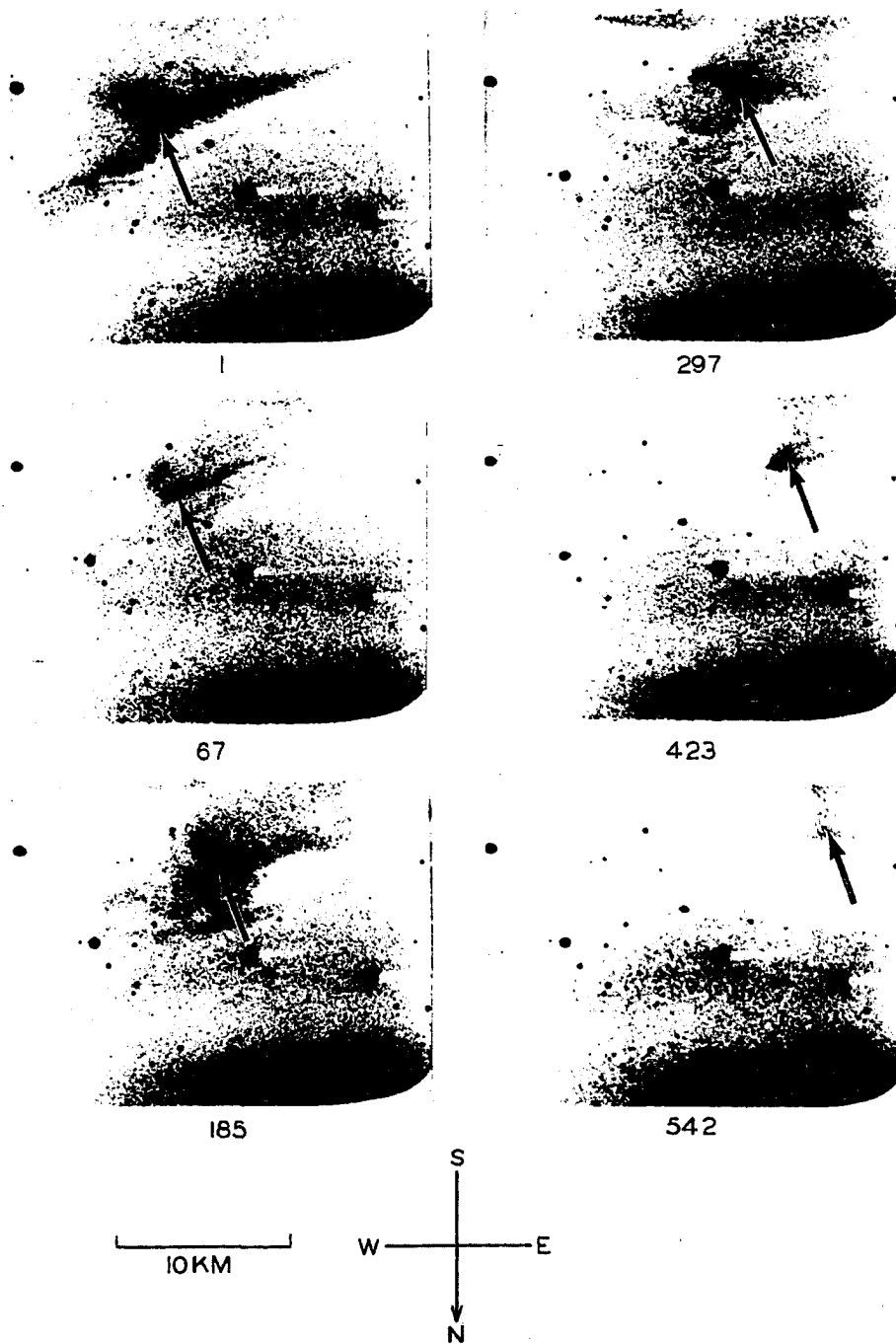


Figure 3.1 The eastward progression of a pulsating patch that pulsated on and off 6 times within the field of view. The 6 frames are from the middle of each 'on' period. Arrows on the frames indicate points used for drift velocity measurements. The dark lower edges on these negative prints are instrumental. The prominent stars are Ursa Major  $\gamma$ ,  $\delta$ ,  $\epsilon$ , and  $\zeta$ .

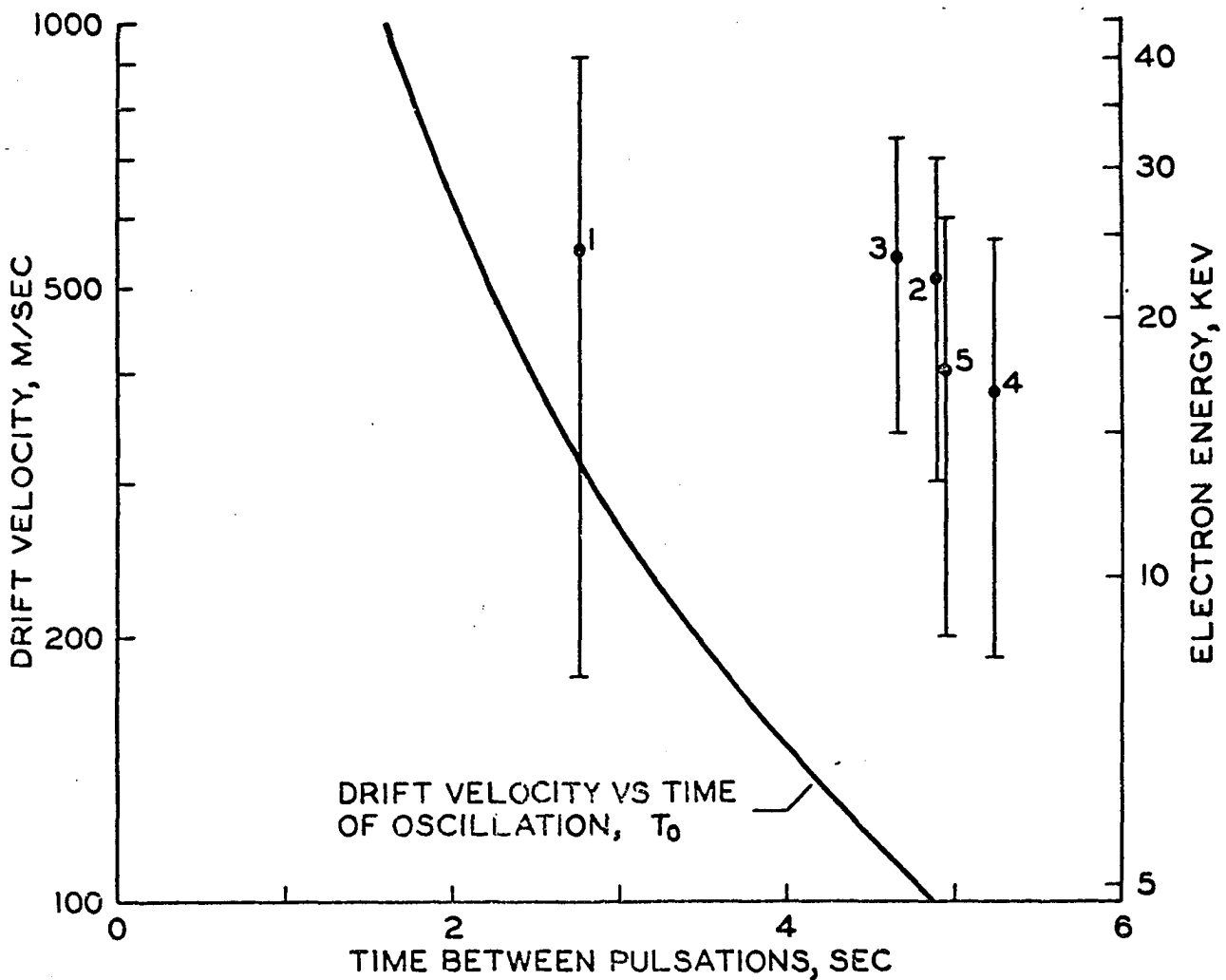


Figure 3.2 Drift velocity in m/sec versus time between pulsations for the pulsating aurora of Fig. 3.1. The smooth curve shows the drift velocity (left-hand scale) and electron energy (right-hand scale) versus time of oscillation,  $T_0$ , for electrons having an equatorial pitch angle of  $3^{\circ}20'$  and mirroring at 100 km on the  $L = 5.5$  field line.

The polar ionosphere magnetic field has been taken to be 0.6 gauss.

An alternative interpretation, since the drift velocity is essentially constant, is that a tube of force is drifting eastward with its feet moving at 400-500 m/sec. Quasi-periodically it is disturbed causing it to lose part of its population of trapped electrons to the atmosphere, thus making the patch visible. The progressive shape change of the patch can be attributed to a change of the tube cross-section.

### 3.1.2 A complicated pulsating patch (westward drifting)

Commencing at 0221 on February 23, 1966, the television system recorded a pulsating patch that had complicated growth and decay phases. On this occasion an unusually large field of view (for the television system) of  $40^\circ \times 26^\circ$  was used. The pulsating sequence lasted five minutes and in this time the patch pulsed on and off 20 times (Table 3). When the patch came on it always had roughly the same shape and then, assuming a height of 100 km, it grew about 50 km to the NW, commonly in one sec (Fig. 3.3a). When the growth phase ceased, the S-SE side that had remained stationary moved in the same direction, but at a reduced speed of 20 km/sec (Fig. 3.3b). The latter motion ceased after about one sec and then the patch rapidly faded. The process was repeated until the patch had drifted to the western side of the field of view; its overall drift velocity was 180 m/sec.

Table 3  
Temporal Information About the Pulsations  
of 0221 February 23, 1966

The times refer to the first appearance of the patch on each cycle. Cycle 1 started at 0221 hrs 20 sec.

Cycle	Time	Delay	Cycle	Time	Delay
1	0	-	11	189.5	11.7
2	24.6	24.6	12	223.5	34.0
3	52.3	27.7	13	239.0	15.5
4	68.8	16.5	14	245.5	6.5
5	95.5	26.7	15	258.2	12.7
6	106.7	11.2	16	270.0	11.8
7	123.7	17.0	17	276.5	6.5
8	143.0	19.3	18	288.0	11.5
9	168.1	25.1	19	293.5	5.5
10	177.8	9.7	20	300.2	6.7

An alternate interpretation of the apparent motion is that, while the westward component of the patch velocity must be horizontal, the northward component could well be due to flaming (upward field-aligned motion). This interpretation was ruled out because the patch appeared to be just part of a large display and, when the camera was directed westward to elevation  $30^\circ$ , motions could be

seen that were predominantly northward; there was no evidence for flaming. Later, at 0336, motions through the magnetic zenith were recorded.

One cycle of the pulsing (Fig. 3.4a) was slightly more complicated than the others. In addition to the patch being considered there was another to the NW. Both brightened at the same time and then grew to bridge the gap. While separated, their adjacent outlines were roughly parallel and contact appeared to be simultaneous along their leading edges (dotted line in Fig. 3.4a). The decay phase was the same as for the other cycles (e.g., Fig. 3.3b).

Another cycle (Fig. 3.4b) included the sudden appearance of a small patch which subsequently grew to become part of the basic form. By making angular measurements on the small patch, and selecting the south side to delineate the lower border (assumed to be 100 km), its maximum possible vertical extension was estimated to be 20 km. This, if applicable to the entire pulsating form, tends to confirm visual impressions that some of the pulsating patches that rapidly grow horizontally do not have much vertical extension. This does not apply to the relatively stable eastward drifting patches which sometimes resemble drifting rayed structure (section 3.1.9). The small vertical extension in the present case, together with the 2dB ionospheric absorption measured by Berkey (1968), imply a hard electron spectrum and a relatively low altitude aurora.

Figure 3.3a Tracings from the TV films showing the initial shape of the patch and the successive positions of its leading edge during cycle 5. The time increments are  $1/6$  sec. A and B are the positions of the eastern edge of the patch for cycles 1 and 20 respectively, corresponding to a westward drift velocity of 180 m/sec. Elevation angles above the southern horizon appear on the right side of the frame. Also shown are distances subtended by the field of view at the 100 km level; the 116 km refers only to the centerline of the frame.

Figure 3.3b The motion of the trailing edge of the patch during cycle 5. The patch faded between time intervals 13 and 14 ( $2 \frac{1}{6}$  and  $2 \frac{1}{3}$  sec).

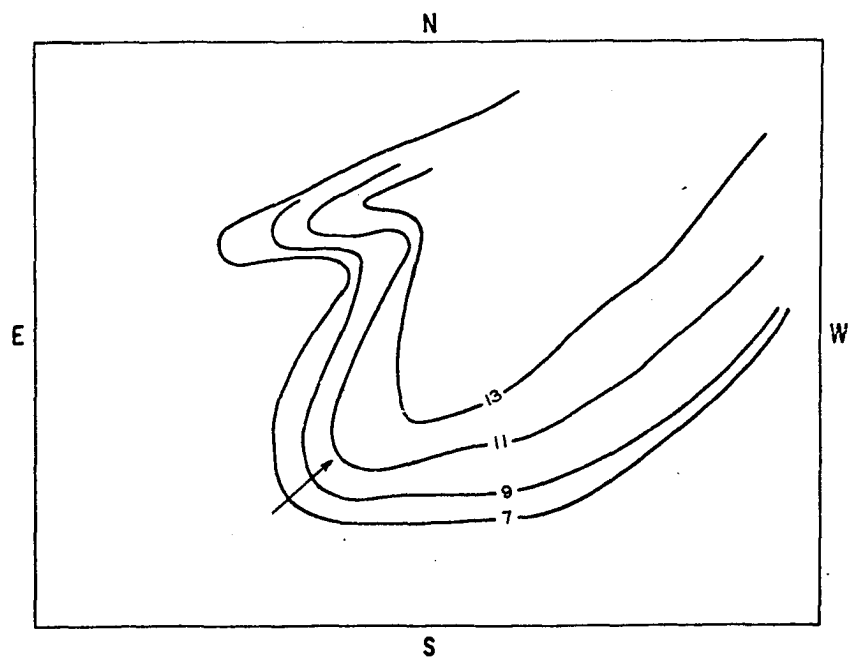
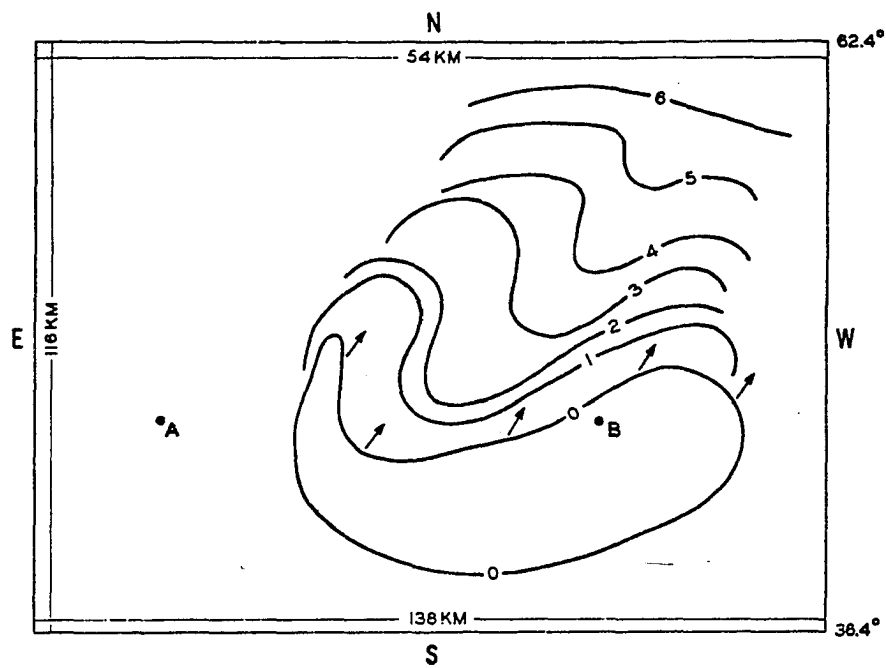


Figure 3.4a Cycle 3 in which the growth stage involved two apparently related patches.

Figure 3.4b Cycle 9 in which a small patch appeared and then grew to become part of the basic form.



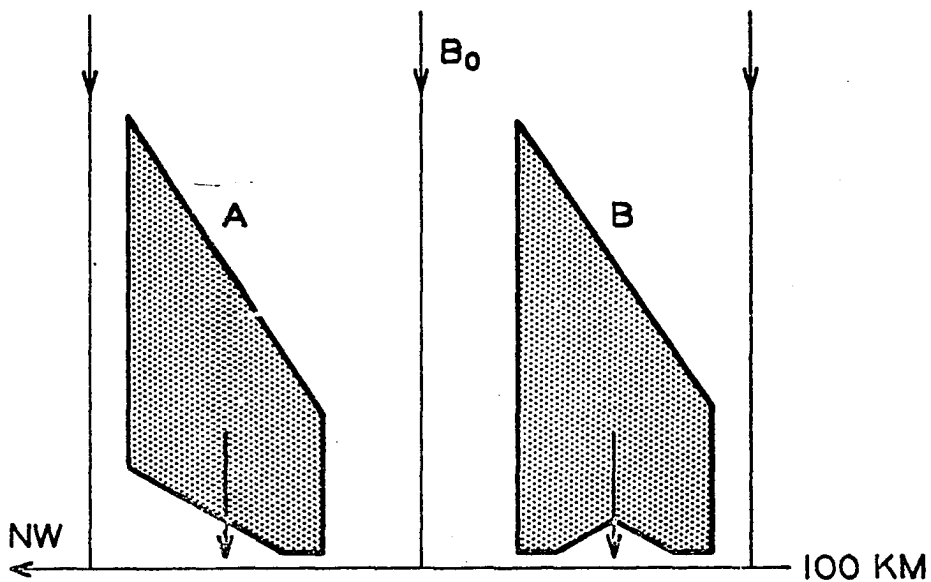


Figure 3.5 Schematic pictures showing the cross sections of the precipitating electron bunches required to produce the behavior in Figs. 3 and 4a respectively. Luminosity is taken to be produced at the 100 km altitude level. The slopes of the leading and trailing edges are greatly underexaggerated (see text).

Assuming electron excitation, the patch could be due to the recurring entry into the atmosphere of electron bunches of particular shapes. The cross-section of the bunch would be as in Fig. 3.5a to give the behavior in Figs. 3.3 a,b, because the apparent velocities would be the result of the sloped faces intersecting with the 100 km altitude level. The behavior in cycle 3 (Fig. 3.4a) could result from the bunch cross-section shown in Fig. 3.5b.

As an approximation, if 5 keV electrons entering the atmosphere with zero pitch angle are assumed, then it can be shown that the sloped faces of the cross-sections are  $89^{\circ}56'$  and  $89^{\circ}58'$  to produce apparent velocities of 50 and 20 km/sec respectively.

The steady drift of the patch superimposed on its more vigorous motions is probably related to the drift of a flux tube. At irregular intervals (see Table 3) electrons are lost from the tube into the atmosphere. These electrons could perhaps have been introduced into the tube at corresponding intervals. Alternatively, they are trapped electrons that are precipitated from the tube.

### 3.1.3 A complicated pulsating patch (eastward drifting)

Examination of the all-sky camera film for February 22/23, 1966 revealed that at  $\sim 0340$  the patches, which had previously drifted westward, started to drift eastward and were apparently more stable than before. The television film, however, showed that, while the drift was eastward, the pulsations were quite complicated.

A pulsating patch showing a complicated growth phase and an overall eastward drift of 180 m/sec over ten cycles of pulsating

was recorded in the vicinity of the magnetic zenith at 0348. It grew in two ways: either it would start at one place and grow south, or it would start at two places and the growths would bridge the gap. The latter can be seen in Fig. 3.6 which shows the growth phase at several epochs during the second cycle. The interval between epochs is either 10 or 20 frames, i.e. 10/24 or 20/24 sec.

The pulsation cycles were often complicated by either moving or in situ intensity variations during the growth and decay phases. The apparent motions are suggested to be related to the shape of the incoming electron bunch (see also the discussion of the previous example) while the intensity variations are related to electron density inhomogeneities in it.

The amount of drift over the ten cycles, together with the remarkable way in which the patch outline was maintained over this period, is shown in Fig. 3.7. Both outlines were drawn at epochs of the respective cycles when the patch was fully developed.

The television film unfortunately ran out before the end of the pulsating sequence. The wave photometer recorded the sequence and showed that it may have lasted for about 25 cycles. The modulation of the 4kR signal above the 4kR diffuse background was essentially 100%; in other words the recorded signal fluctuated between 4 and 8 kR (in  $\lambda 4278$ ).

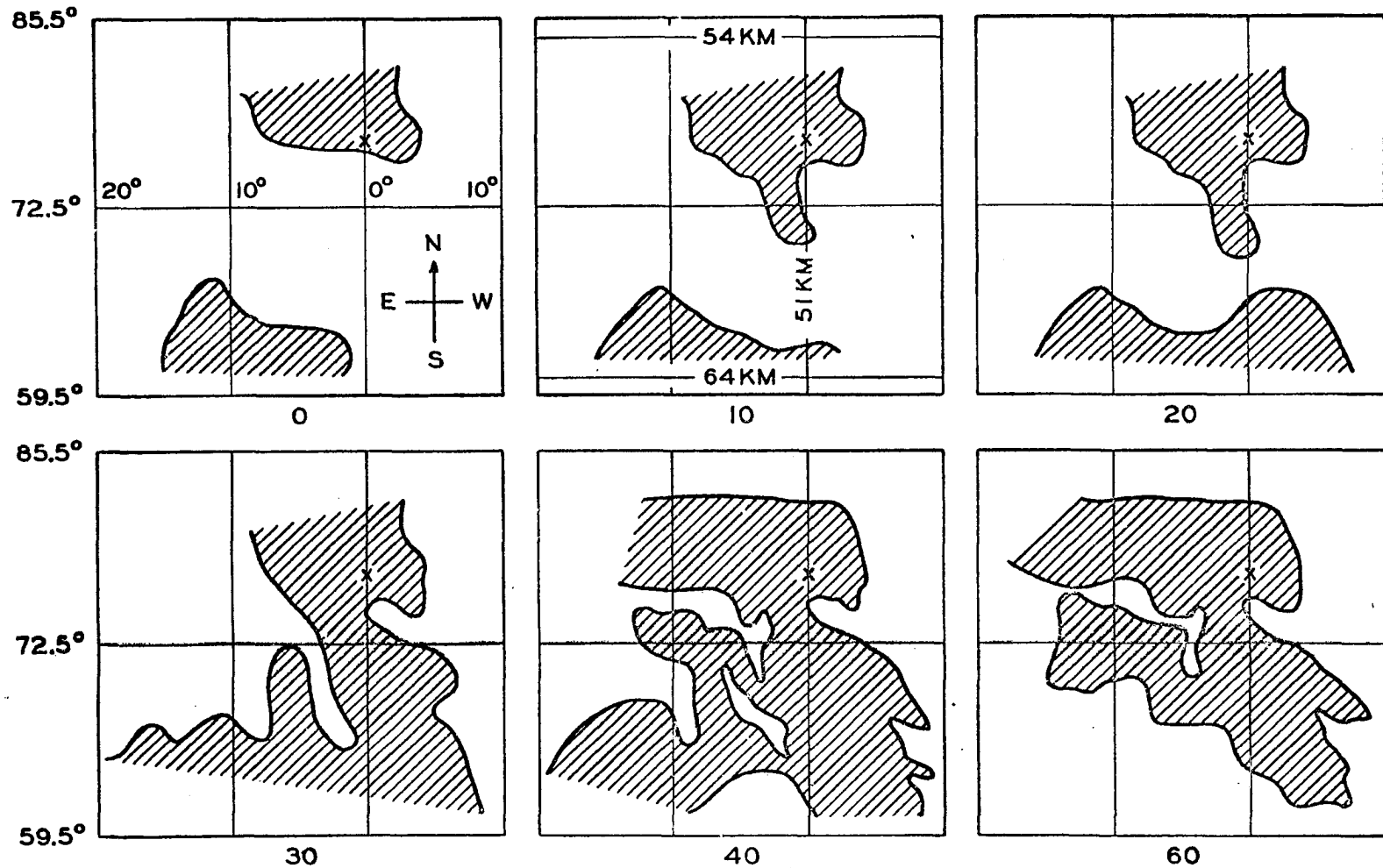


Figure 3.6 The growth phase at several epochs during the second pulsating cycle. The numbers under each diagram give the frame number from an arbitrary zero (24 frames/sec). 'X' marks the position of the magnetic zenith. Elevations above the southern horizon are given to the left of the first frame. Azimuths measured from south appear across the center of frame zero. Distances subtended at the 100 ft

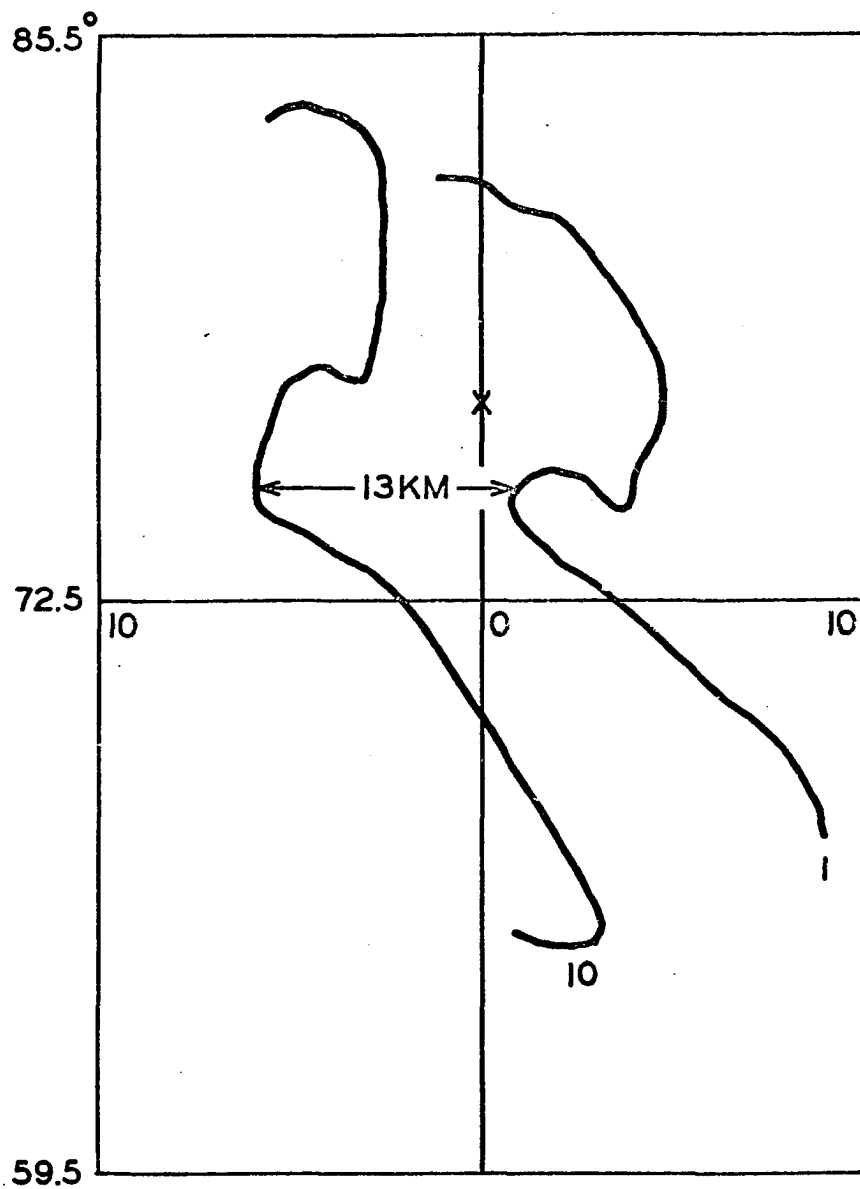


Figure 3.7 The positions of the western edges of the patch when fully developed in the first and tenth cycles. The corresponding drift velocity is 180 m/sec.

Table 4

Temporal information about the pulsating patch of 0348 February 23, 1966.

Cycle	Time	Delay	Approx. Time on
1	0 sec	0 sec	1 sec
2	6.2	6.2	2
3	13.3	7.1	2
4	20.4	7.1	3
5	28.4	8.0	3
6	33.8	5.4	2
7	47.0	13.2	2
8	51.5	4.5	3
9	56.5	5.0	2
10	71.5	5.0	2

#### 3.1.4 Regions that pulsated alternately

At 0110 March 17, 1964 the television system recorded a wedge-like feature aligned SW-NE through the zenith and drifting eastward at  $500 \pm 200$  m/sec. It disappeared and reappeared and then after this a definite trend was observed (see Fig. 3.8): Frame 1 shows the wedge; 1.4 seconds later it disappeared and the surrounding sky was enhanced (frame 34). This gave the impression that the original wedge had been replaced by a "ghost". Several seconds

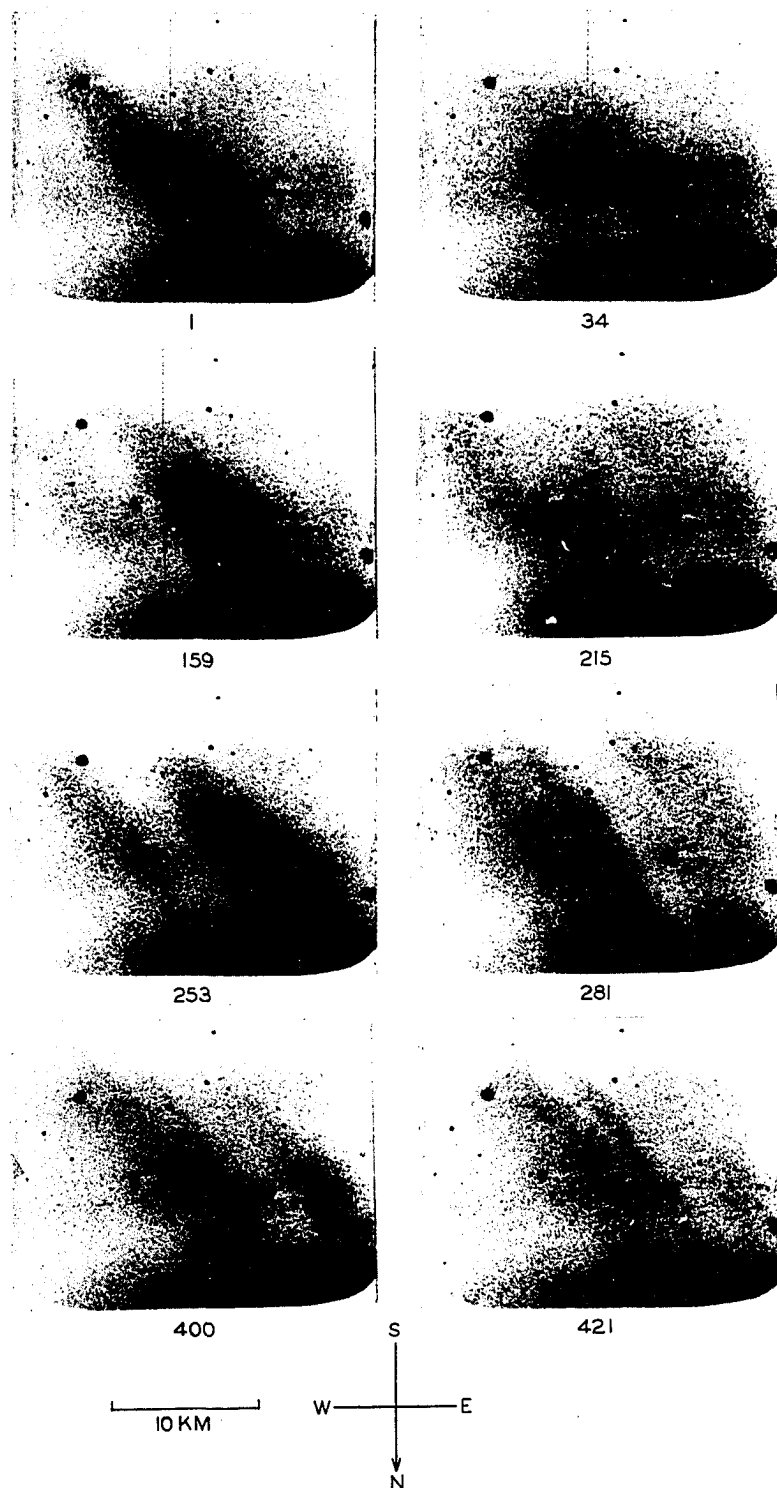


Figure 3.8 An example of a pulsating aurora in which adjacent regions pulsate alternately: the appearance of the wedge in the frames on the left is followed by the appearance of its "ghost" in the frames on the right. The third pair is the best. The prints are negative.

later the wedge reappeared and then the behavior was repeated. In all, this occurred four times before the wedge drifted out of the field of view. The third 'cycle' was the least ambiguous while the fourth was somewhat confused. Details of the complete event are given in Table 5.

Table 5  
Temporal information about the pulsations  
of 0110 March 17, 1964

Time, sec	Frame Number	Number of frames wedge enhanced	Number of frames ghost enhanced	Delay between appearances of wedge & ghost, sec
0	1	12		1.4
1.4	34		10	
6.6	159	11		2.4
9.0	215		9	
10.5	253	8		1.2
11.7	281		30	
16.7	400	?		0.9
17.6	421		?	

### 3.1.5 Asynchronous intensity pulsations of different patches

The visual observer of pulsating auroras rapidly becomes aware that, almost invariably, different patches appear to pulsate asynchronously. An example supporting this finding was obtained from the television

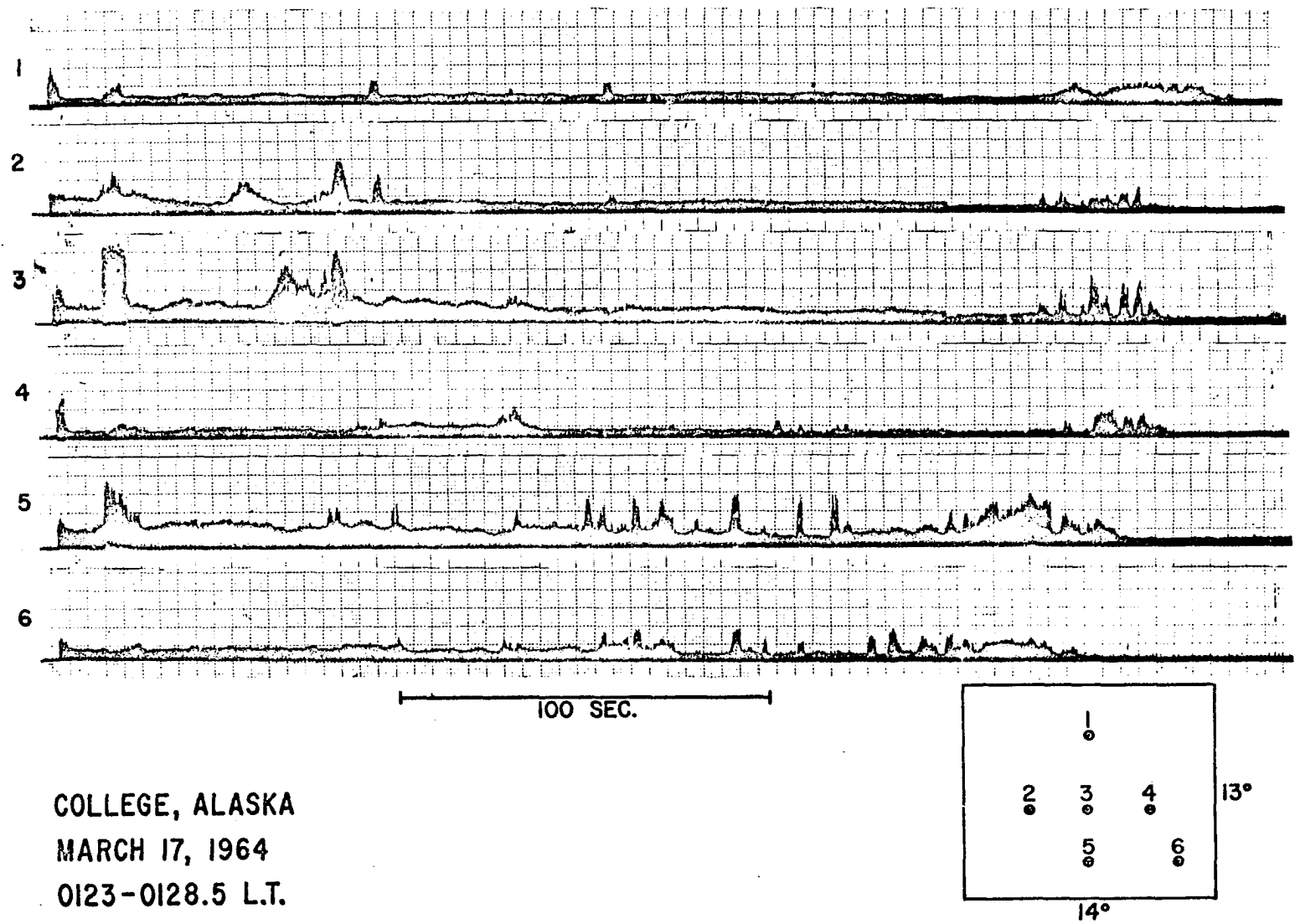


Figure 3.9 Six photocoell traces of intensity from six different regions of the 14° x 13° television field of view during a pulsating display (0123-0128.5 March 17, 1964).

films of a pulsating display on March 17, 1964. The television field of view contained both the magnetic and geographic zeniths. The projection of the film revealed the pulsating display to be made up of numerous small forms that pulsed asynchronously. When photocells were attached to various places on the projection screen the traces in Fig. 3.9 resulted.

As would then be expected, when the sampling is from more scattered areas in the sky the result is the same: no evidence of synchronism. This can be seen from the wave photometer records during a pulsating auroral display (e.g. Fig. 4.17 a).

#### 3.1.6 Eastward and westward drifting patches that occurred simultaneously

At ~0100 December 4, 1965, following a substorm onset north of College, eastward drifting patches developed. Careful examination of the College all-sky camera film revealed that from 0320-0420 the patches in the southern half of the sky drifted eastward, while those in the northern half drifted westward (Fig. 3.10). When projected at cine speed the eastward drifting patches appeared more stable than the westward drifting ones. As determined from photometer records, the intensity above the accompanying diffuse background of the eastward drifting patch in Fig. 3.10, was modulated at 1 cps by up to 40%; in other words, it was always visible. On the other hand, the westward drifting patch had a corresponding modulation at 0.25 cps of up to 95% and thus could essentially disappear between pulsations. This difference in modulation appears to be the explanation of why the eastward drifting auroras appeared more stable when viewed on the all-sky camera film.

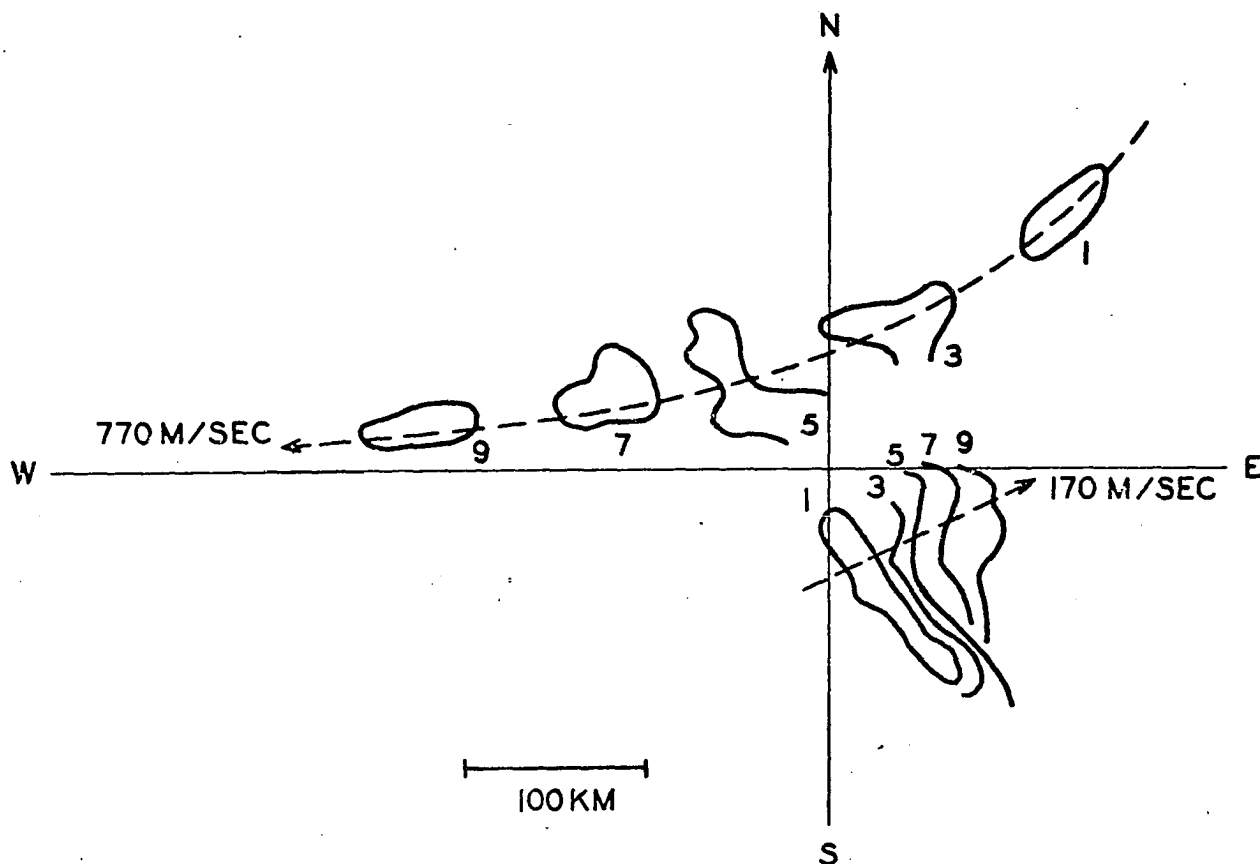


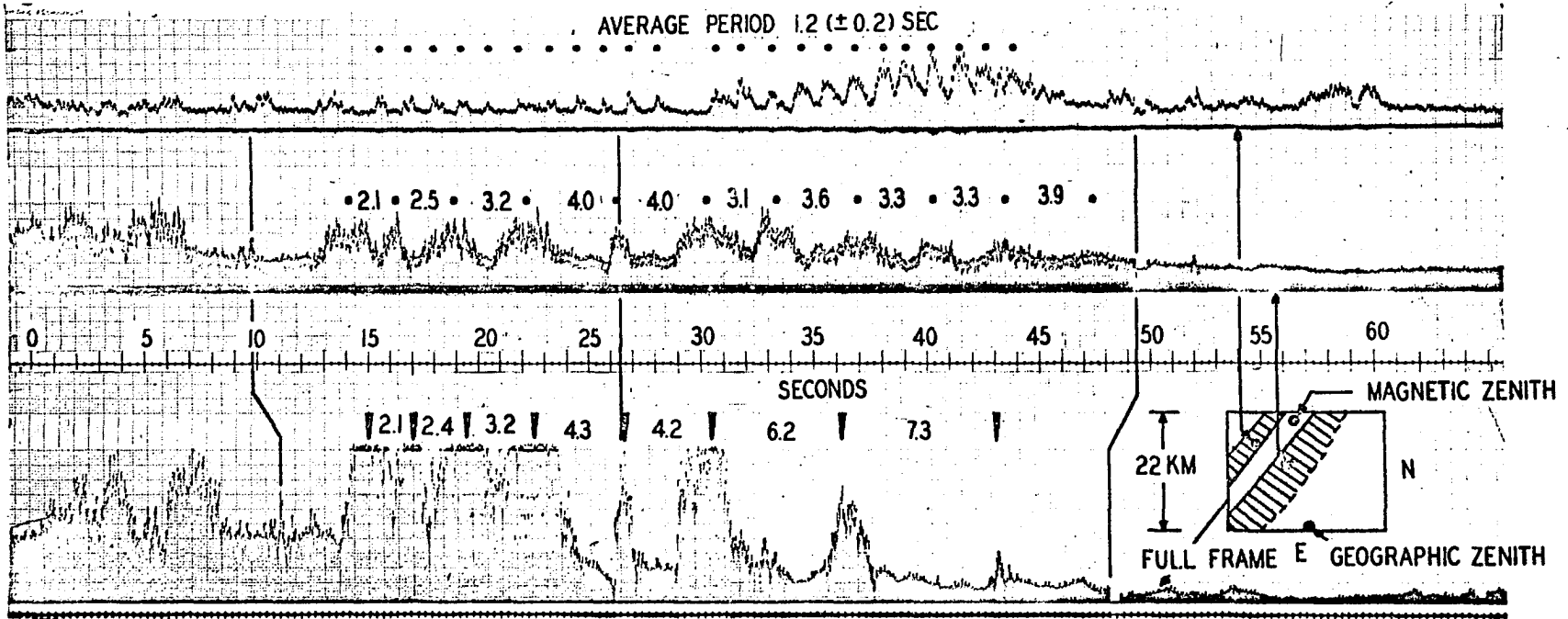
Figure 3.10 Successive ground plots at 2 min. intervals from 0341-0349 on December 4, 1965, of 2 patches in the northern and southern sky at College. The 2 selected patches show the drift trend of many others. The northern patch drifted westward at 770 m/sec while, at the same time, the southern patch drifted eastward at 170 m/sec.

It is interesting to project these motions from the ionosphere along the geomagnetic field to 0400 LT at the equatorial plane; it at once suggests a large scale shear motion. The eastward motion becomes motion within  $5.5 R_e$  in the direction of the sun. The westward motion becomes motion beyond  $5.5 R_e$  away from the sun. It is suggested that, in this case,  $5.5 R_e$  defines the boundary of stable trapping and that the fast (770 m/sec) westward motion is related to convection of flux tubes outside the boundary. The convection could be induced by viscous interaction with the solar wind (cf. Axford and Hines, 1961).

#### 3.1.7 Pulsating arcs

Often pulsating arcs, usually aligned E-W, will occur as part of a pulsating aurora display. An example of adjacent pulsating arc-like forms appears in Fig. 3.11. It was observed with the TV system at 0105 on March 17, 1964. By placing photocells on the projected TV film image it was found that, while the pulsations of each arc were coherent along its entire length (in the TV field of view), the pulsations of the two arcs were quite different. In fact, by monitoring the entire field of view, as would a large field photometer, the high frequency information of the smaller arc was lost (trace 3).

One feature that was visually apparent from cine projection of the TV films was that the light signals from the arcs had components that were  $180^\circ$  out-of-phase. The photocell traces of the arcs are



COLLEGE - MARCH 17, 1964 - 0105 L.T.

Figure 3.11 Photocell tracings made from projected television film with photocells placed on the images of an arc southwest (upper trace) and northeast (middle trace) of the magnetic zenith, respectively. The lower trace results from monitoring the full field of view with a photocell. The insert at lower right shows the field of view with its area at 100 km altitude and the placement of photocells on the images of the pulsating forms.

not too convincing in this respect but do show supporting evidence between the 32 and 40 sec marks. There the peaks of the upper trace match the dips of the lower trace and vice-versa. This places a restriction on the pulsating arc mechanism: somehow electrons are channeled into one arc at the expense of the other.

### 3.1.8 Frequency spectra of pulsating auroras

(a) A power spectrum analysis has been obtained using a sample of photometer data from a display of 1 December, 1964. The pulsating aurora display commenced when a diffuse envelope containing patches spread SSE to 50 km S of College at  $\sim 200$  m/sec between 0342 and 0351. The patches were 200-300 km long and  $\sim 20$  km wide (as seen by the all-sky camera) and were aligned NW-SE. They drifted eastward at  $\sim 300$  m/sec and elongated as the diffuse envelope spread southward.

Examples of the drift behavior of patches at subsequent times are shown in Fig. 3.12. From 0355-0359 simultaneous records were obtained from the College zenith and  $42^\circ\text{N}$  of that vicinity with narrow field photometers ( $1.5^\circ$ ). The power spectra resulting from a fine mesh analysis (1/25 sec scaling interval) of the two samples are shown in Fig. 3.13 and show a number of differences: the relative power spectral density in the 0.1-to-1 sec range is much higher in the zenith region than in the region near zenith distance  $42^\circ$ . Both spectra have appreciable spectral density in the 1-20 sec period range with the peaks lying near 8 sec, but the zenith spectral

density plot shows the greater complexity. These spectra are not necessarily typical of these particular regions of the sky since occasions when the northern field of view contained a stronger short-period component than the zenith field of view can be found.

(b) Another method of spectral analysis is to use a "Sonagraph". It has some advantages: no scaling is necessary because it accepts the tape recorder signal. Long time intervals can be analyzed, although this is a function of the spectral resolution desired. The change of spectral character with time can be studied.

Photometer signals from  $1\ 1/2^\circ$  and  $165^\circ$  field of view photometers run on the night of November 1/2, 1964, were analyzed by means of a "Sonagraph". The small field of view showed a broad spectrum while the large field showed a narrow one (Fig. 3.14). The explanation may be that the larger ( $165^\circ$ ) field integrates the signals from many small asynchronously pulsating patches, tending to smear their frequency information into noise. This effect was noticed when a wide field was used for the two arcs in section 3.1.7. The influence of several large patches could be significant since these would have less tendency to cancel one another. Visually one has the impression that large patches pulsate more slowly ( $\sim 10$  sec) than small ones. The reason for the small field having apparently more long period ( $> 20$  sec) components than the large field may be due to drifting patches. For instance, taking a representative drift velocity of  $\sim 300$  m/sec then structures about 3 km across

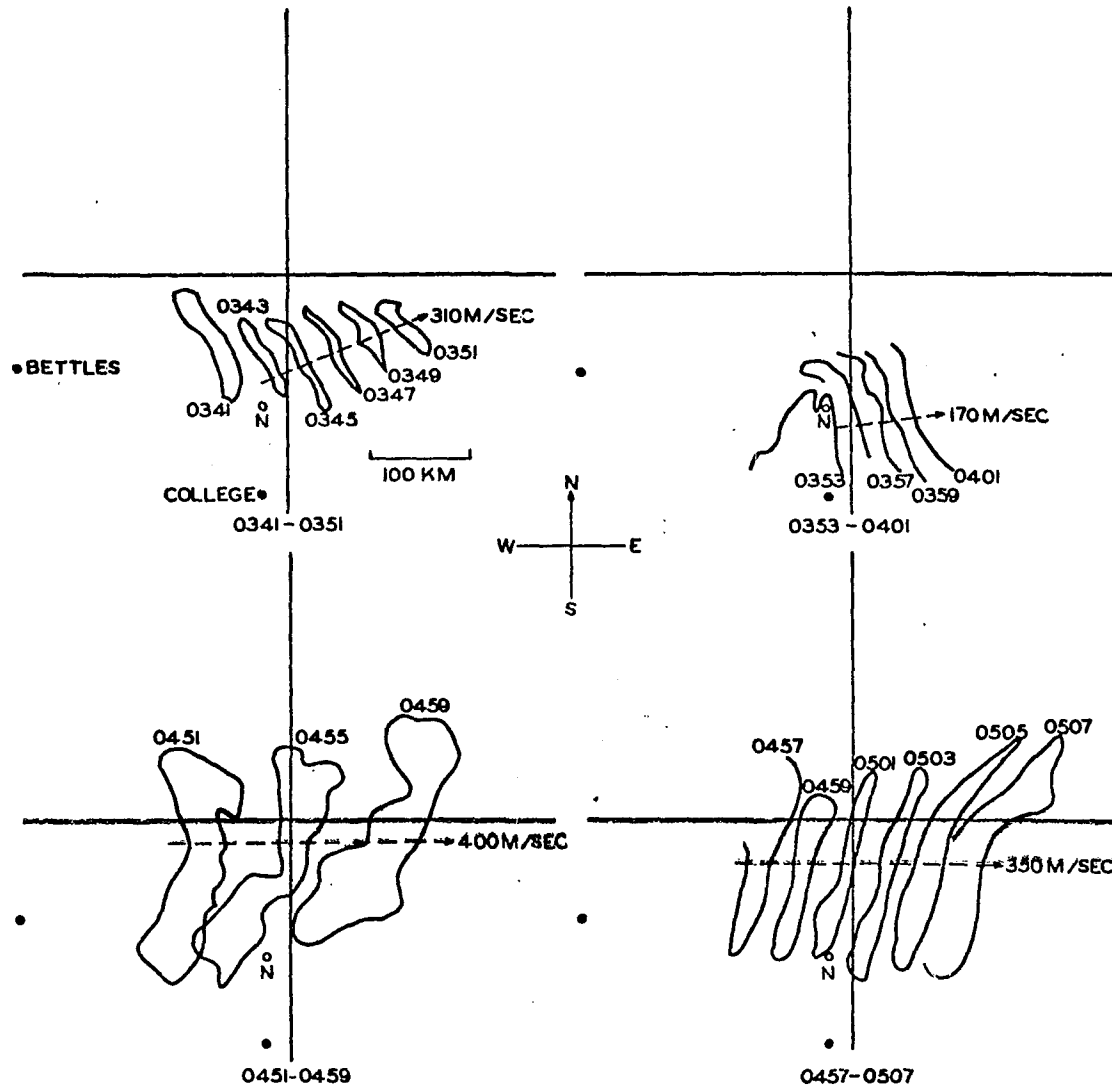


Figure 3.12 Ground projections of eastward drifting patches made from the Ft. Yukon all-sky camera film of December 1, 1964. 'N' shows where the College northern photometer was directed to get the power spectrum of Fig. 3.13.

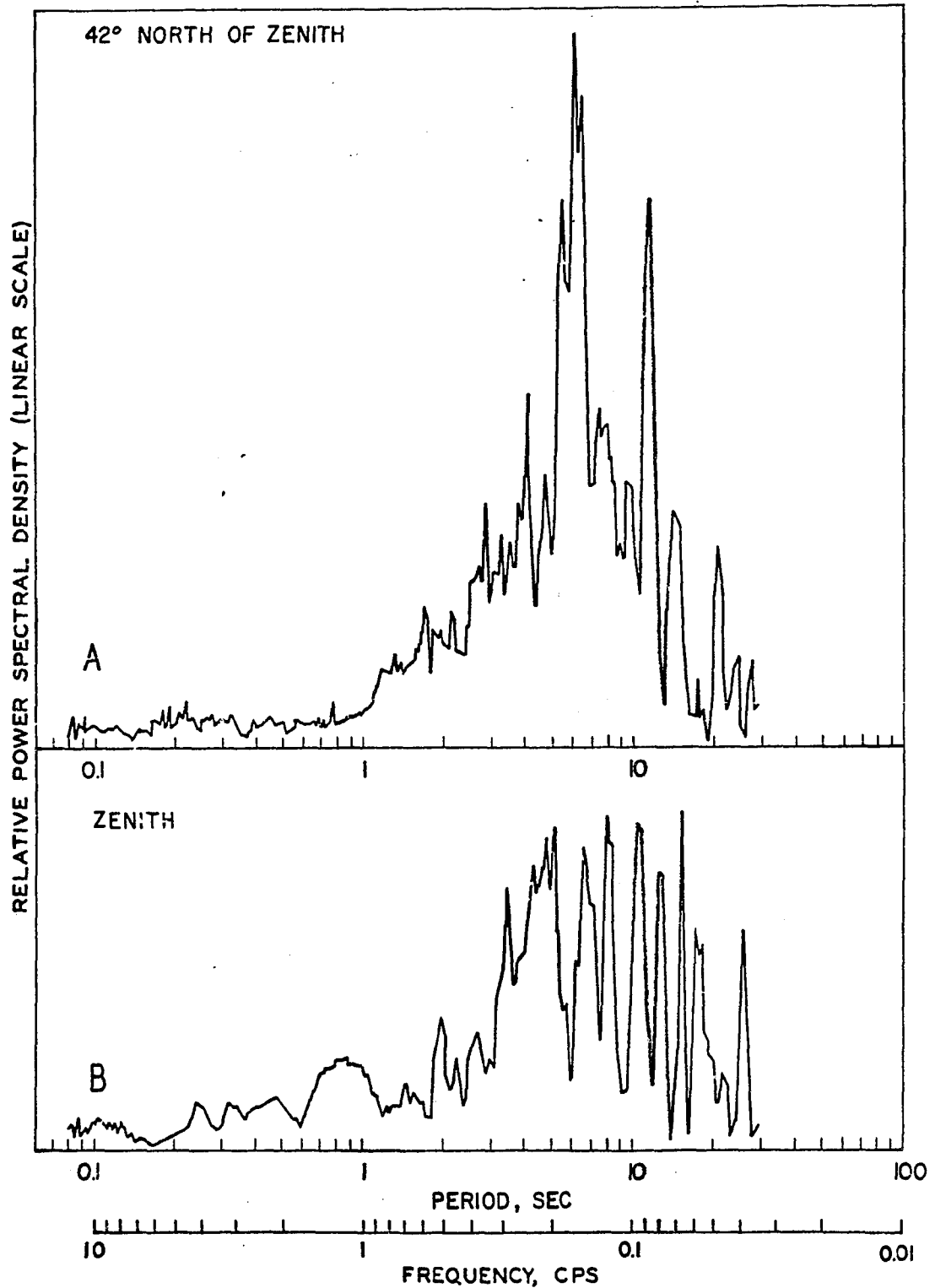


Figure 3.13 Power spectra of two four-minute samples of auroral pulsations taken at College zenith and from  $42^\circ$  north of the zenith, respectively. Both samples are from the same time interval, 0355-0359, December 1, 1964.

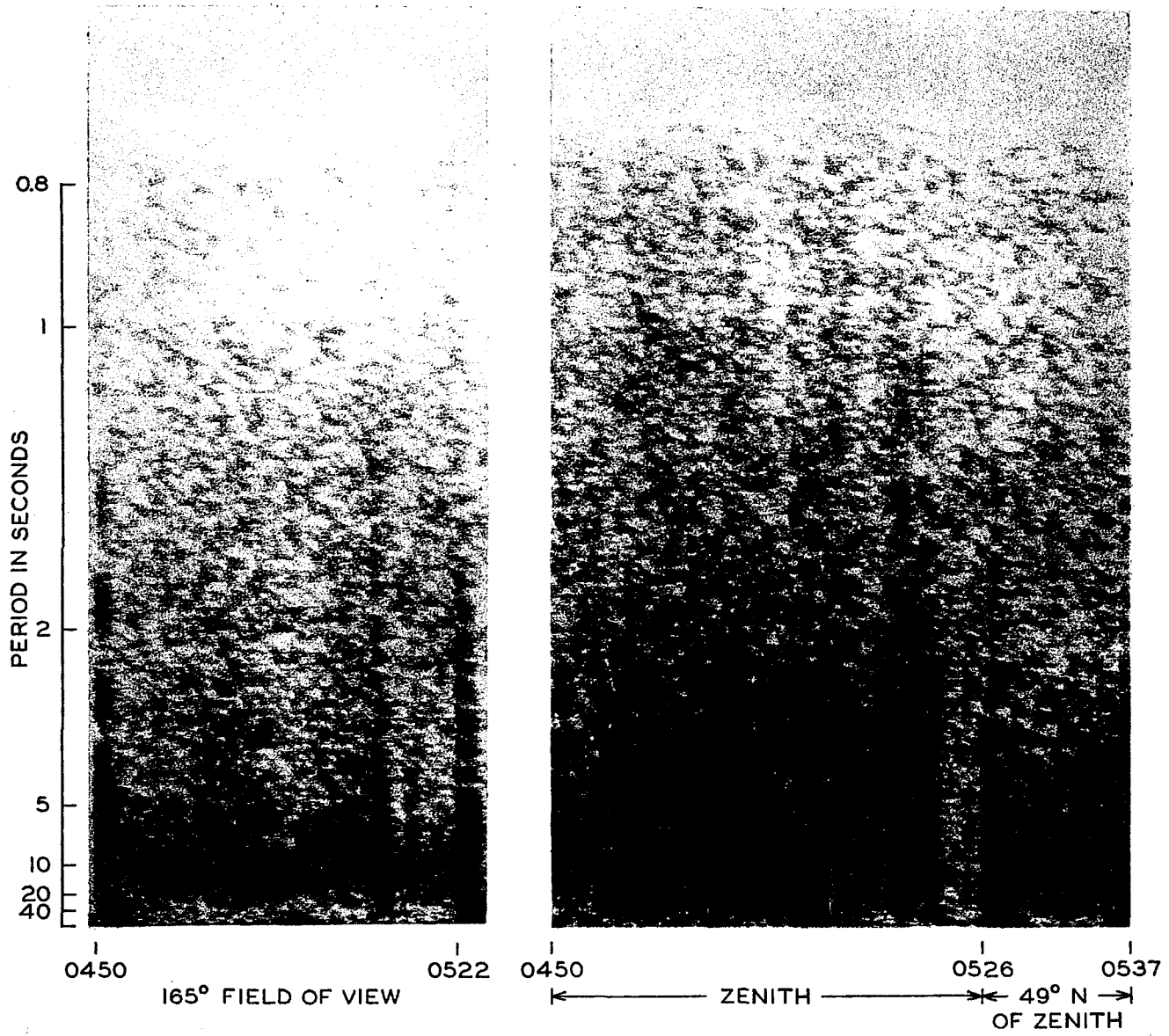


Figure 3.14 The results of a "sonagraph" spectral analysis of simultaneous pulsating aurora records from a 165° field and a 1 1/2° field centered on the zenith. After 0526 the 1 1/2° field photometer was directed 49°N of the zenith.

and separated by 3 km would give rise to a 20 sec period variation in the small field photometer signal; longer periods would result from larger patches. This would not show up in the signal from the 165° photometer.

### 3.1.9 The eye as a pulsation detector

The night of December 3/4, 1965, has been briefly summarized elsewhere (section 4.7). On two occasions, 0250 and 0307, large patches, almost 200 km across and drifting eastward at  $\sim 200$  m/sec, entered the magnetic zenith and were recorded by channel 3 of the wave photometer. Very little, if any, ionospheric absorption was associated with the passage of the patches through the zenith.

Visual observations failed to detect pulsations and, in fact, described the patches as being composed of rayed structure. The photometer, however, showed  $\sim 1$  cps pulsations, but these represented only small modulations on the main pulses which corresponded to the drift times of the patches through the field. In the first case, the modulation amounted to 1.5 kR maximum on a 9 kR maximum signal above a 3 kR diffuse background. In the second case it amounted to 3 kR maximum on a 5 kR maximum signal above a 2 kR diffuse background.

In comparison, the pulsating sequence of 0348 February 23, 1966, (section 3.1.3), has associated modulation of about 100%: the recorded signal was either the maximum value of 8 kR, or it was the diffuse background of 4 kR. These pulsations were readily seen.

One can conclude that the eye may sometimes miss pulsations for normal pulsating aurora intensities ( $\lesssim 10$  kR), when the modulation of the signal above the background is less than about 50%.

#### 3.1.10 Summary

Pulsating auroras are restricted primarily to the equatorward boundary of auroral displays in the midnight and morning sectors following substorm onsets. At such times the local horizontal magnetic field component is strongly negative or recovering from a negative bay. There seem to be at least four ways in which pulsating auroras can appear over a station: they can be left in the wake of a poleward expansion accompanying a substorm onset; they can be seen as patches that drift eastward through the zenith from the western horizon; they can occur in the diffuse glow produced as an arc in the north expands southward; or they can simply materialize up to 100 km south of such an arc and then commence drifting eastward.

Pulsating auroras can drift either east or west, but most commonly to the east. In this regard, the February 23, 1966, display is interesting because at 0340 the drift changed from west to east (section 4.7). Also it has been seen that it is possible to have eastward drifting patches in the southern sky accompanied by westward drifting patches in the northern sky.

A diffuse background of several kR in  $\lambda 4278$  invariably accompanies pulsating aurora displays. The pulsating auroras are superimposed on this and are most readily recognized if their intensity fluctuates

- -

from this level to a maximum and down again. Their intensity above the background commonly ranges up to 10 kR in  $\lambda 4278$ ; the brightest ever seen were 11 kR above a 11 kR background (section 4.7). Often patches can be observed that do not appear to pulsate. This is because their intensity does not vary enough for the eye to register it: even a 3 kR lops fluctuation on a 5 kR maximum signal above a 2 kR diffuse background can be missed.

Pulsating patches appear to take many forms but seem to fall into two main categories:

- (a) Those in which the growth and decay phases are simultaneous, or very nearly so, over the entire form.
- (b) Those in which the growth and decay phases are not simultaneous over the entire form. This results in apparent motion and changes in size and shape and is seen more frequently in large patches ( $\gtrsim 50$  km across) than in small ones.

Also, during the time that a patch is visible it sometimes has moving and in situ intensity variations within it. Photometer records of patches reveal quasi-periodic pulsations. Different patches commonly pulsate asynchronously.

The power spectrums for pulsating aurora displays peak roughly at 10 sec. Visually one has the impression that large patches ( $\gtrsim 50$  km across) pulsate more slowly ( $\sim 10$  sec) than smaller ones. A narrow field of view photometer reveals relatively more of the

shorter period components ( $\lesssim 1$  sec) than does a broad field. This is probably because the broad field would integrate many small patches pulsating rapidly while the narrow field would not. Also, small weak patches on the steady background of several kR that accompanies pulsating auroras would give a better signal to noise ratio with the small field of view.

#### 3.1.11 Discussion

The most significant finding has been that patches can, except for gradual changes, maintain their shapes and drift velocities for long periods while they pulsate quasi-periodically. This means that something associated with the patch also maintains its shape and drift velocity. It could be a drifting flux tube (cf. Atkinson, 1966) having the patch at its feet in the ionosphere, and containing the quasi-periodic modulation mechanism for the intensity fluctuations of the patch.

The possible relevance of adiabatic particle drifts to pulsating auroras was considered in section 3.1.1. Now it seems that adiabatic drifts are of secondary importance because pulsating auroras have been observed to 1) drift westward, and 2) drift westward in the northern half of the sky and eastward in the southern half of the sky simultaneously; this suggesting a shearing motion in the equatorial plane (cf. Axford and Hines, 1961). Also suggesting adiabatic drifts to be of secondary importance are the simultaneous balloon observations of X-rays and  $\lambda 5577$  during pulsating auroras by Rosenberg

et. al. (1967). These revealed the X-rays and visible emission to pulsate together, thus showing that both high and low energy electrons are precipitated together. If the pulsations were due to particular groups of electrons adiabatically oscillating to and fro along the earth's field with some of their number being dumped as each extremity was reached, then the lower energy electrons would soon be left behind in the drift to the east and coherence would be lost.

At present, then, the most likely explanation seems to be that pulsating patches are associated with flux tubes drifting in the magnetosphere. Quasi-periodically the trapped electron population of the tube is disturbed, causing some of it to precipitate and lead to patch brightening. Possibly the tube could have been filled with electrons early in the substorm. Alternatively, as pointed out by Rosenberg (private communication), fresh electrons may be continuously injected into the tube to remain trapped until influenced by the modulation mechanism.

It is suggested that the shape of the leading and trailing edges of the precipitating-electron bunches can give rise to the observed apparent velocities during the growth and decay phases. These shapes would result from the modulation mechanism starting and finishing at one side or another of the tube. Electron density inhomogeneities in the bunch would then produce the observed intensity fluctuations while the patch is visible.

### 3.2 Flaming Auroras

Flaming auroras are termed by the International Auroral Atlas (1963) to be type  $p_2$  pulsing auroras. Large areas of the sky are lit by surges of luminosity which move upwards along the field direction and thus appear to converge on the magnetic zenith. Downward flaming has been reported.

No quantitative information has been published on flaming auroras. Photometer measurements made by Carleton (private communication) revealed flaming velocities of  $\sim 1000$  km/sec, while television measurements, to be reported here, gave velocities at least an order of magnitude smaller.

The cause of flaming auroras is not known. However, if electrons of various energies start simultaneously from a point on a magnetic field line and travel to the atmosphere, then a flaming effect could result. The higher-energy members would arrive before, and would produce luminosity lower in the atmosphere than, the lower-energy ones. Measuring the resulting velocity of flaming then gives a way of fixing the position of the electron release point. This concept is applied in section 3.2.2 in synthesizing flaming auroras.

#### 3.2.1 Observations

Very few measureable examples of flaming auroras have been collected by the television system. One reason is that over the past few years they have been infrequent. The other is that during post-breakup auroras the camera has often been directed at the

magnetic zenith to simplify the geometry when recording pulsating forms. However, this is one of the worst vicinities for getting usable flaming aurora data.

The first example of a flaming aurora recorded by the television system was obtained at about 0100 on March 17, 1964, during a pulsating aurora display. A form was observed to show four cycles of flaming before it drifted from the field of view. The drift velocity was  $550 \pm 100$  m/sec eastward and the upward velocity of flaming was calculated to be 70 km/sec, but this value was very uncertain. The intervals between the flaming were 9, 10, and 5.5 sec.

The second example, from 0304, March 23, 1966, was taken with a  $16^\circ \times 6^\circ$  field that viewed several flaming forms. The chosen event was short-lived, lasting 3 frames, which corresponded to a lapsed time of  $1/12$  sec. The form, having a vertical extent of  $\sim 10$  km and the appearance of a short ray bundle, moved up only  $6.7 \pm 2.7$  km at  $80 \pm 30$  km/sec. The center of luminosity in the first frame was taken to be 100 km. This center, two frames later, and  $1/2^\circ$  higher up, turned out to be  $106.7 \pm 2.7$  km. Had it not been for the telescopic  $6^\circ$  vertical dimension of the television field of view, the  $1/2^\circ$  motion from  $8^\circ$  to  $8.5^\circ$ S (uncertainty:  $0.1^\circ$ ) would not have been noticed. Without a doubt it would have been missed by a visual observer. Possibly it indicates that a small amount of "flaming" takes place in most pulsating auroras, since an observer beneath this display would have described it as pulsating.

The third example is from 0133 on February 16, 1967. The flaming was in the form of luminosity traveling up bright ray-like structures (Fig. 3.15) and lasted from about 0130 to 0215. This period was accompanied by a negative bay of the H component that had a value of  $\sim 2000\gamma$ :  $K_p$  at this time was 8.

To the eye the flaming showed coherence over large sections of the display; this could not be detected in the television films and, in fact, selecting measureable examples was difficult. The chosen example consisted of a ray that suddenly appeared. During the next four frames (at 30/sec) the bottom of the ray apparently moved up from  $56.8^\circ\text{S}$  to  $58.5^\circ\text{S}$  and then the ray either disappeared or was confused with other rays. Assuming initial lower border heights of 90, 100, and 110 km respectively and allowing for an instrumental accuracy of  $\pm 0.1^\circ$  resulted in the lower border moving up to  $100 \pm 1.5$ ,  $111.5 \pm 1.5$ , and  $123 \pm 1.5$  km respectively. These corresponded to velocities of flaming of  $60 \pm 8$ ,  $70 \pm 9$ , and  $80 \pm 9$  km/sec.

### 3.2.2 Synthetic flaming auroras

The introductory part of section 3.2 contained a description of how a flaming effect in auroras could be produced by electrons of various energies simultaneously leaving a point in the magnetosphere; this has also been considered by Carleton (private communication). There is doubt, of course, as to whether the electrons of different energies will leave the release point simultaneously. For instance,

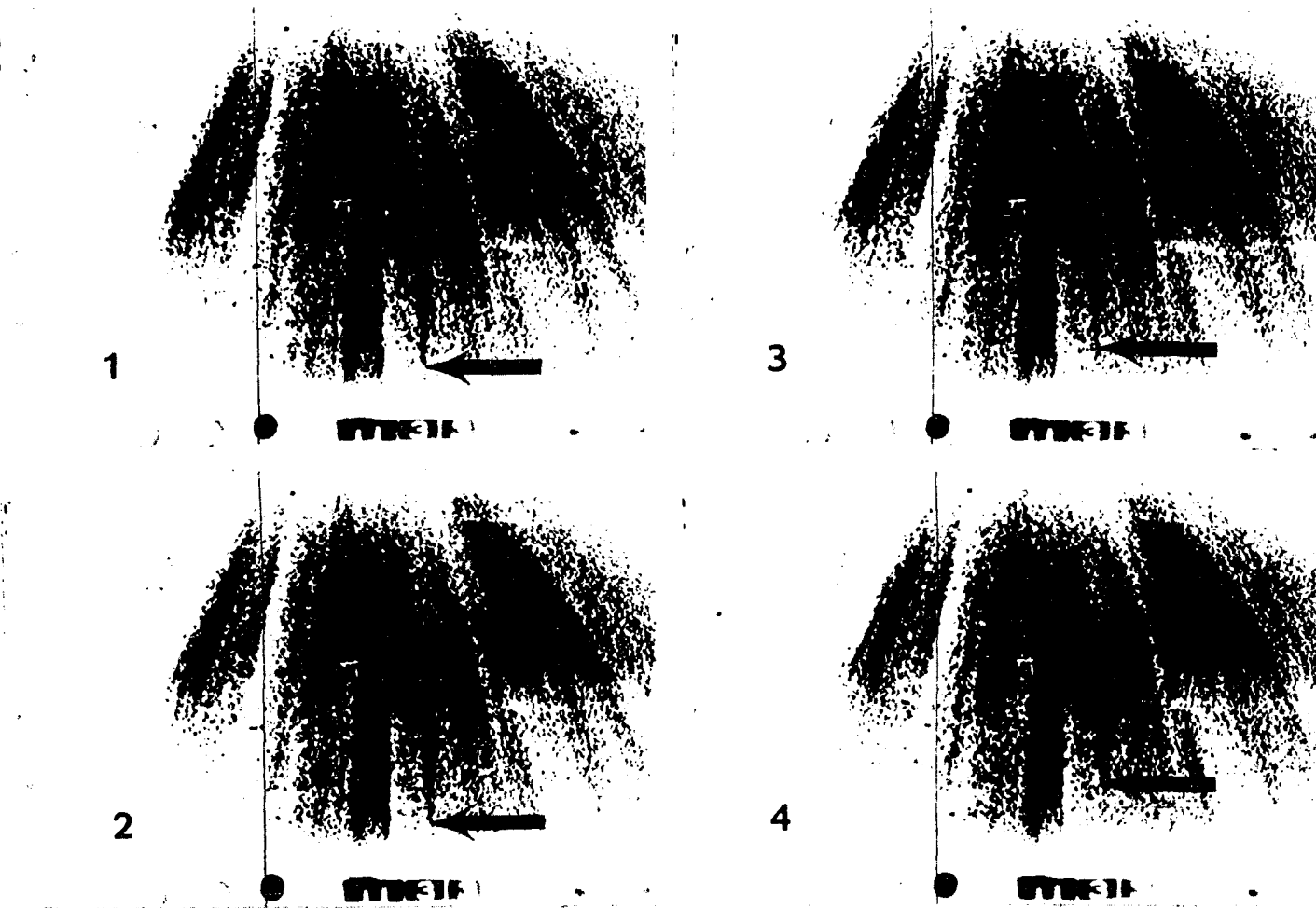


Figure 3.15 The last four of five consecutive frames covering the flaming aurora example of February 16, 1967. The filming rate was 30 frames/sec. The bottom of the ray that appeared and then moved upwards from elevation  $56.8^{\circ}\text{S}$  to  $58.5^{\circ}\text{S}$  is marked by an arrow in each of the frames. For an assumed initial lower border height of 100 km the flaming velocity was  $70 \pm 9$  km/sec.

there may be an acceleration process acting that takes longer to produce the higher energy electrons and so they would leave later than the lower energy electrons. This could, in fact, reverse the direction of flaming.

For the simplest case of electrons being released simultaneously with zero pitch angles on the  $L = 5.5$  field line, the apparent flaming velocity was determined; a number of release points were chosen. Fourteen electron energy values\*,  $E_n$ , in the range 0.1 to 100 kev were taken and, allowing for relativistic effects, the corresponding velocities,  $V_n$ , were calculated.

The heights at which the different energy electrons produced their maximum luminosity,  $h_n$ , were obtained from Rees (1964), Table 2 for  $\lambda_m = 67^\circ$ . The distances,  $D_n(N)$ , traveled from the release points to these heights, and the corresponding transit times,  $T_n(N)$  were determined from

$$D_n(N) = N(6370) + (282 - h_n) \quad \text{km}$$

and,

$$T_n(N) = \frac{N(6370) + (282 - h_n)}{V_n} \quad \text{sec}$$

---

\*  $E_n = 0.1, 0.2, 0.3, 0.5, 0.7, 1.0, 1.5, 2, 3, 5, 10, 17, 50, 100$  kev.

where  $N$  ranged 1, 2, ..., 7, 8, and where 282 km, the height associated with the 0.1 keV electrons, was taken as an origin. The value  $N = 6.5$  takes the release point out to the equatorial plane. The apparent upward flaming velocity at a height  $h_n$  was taken to be

$$v_n(N) = \frac{h_{n-1} - h_{n+1}}{T_{n-1}(N) - T_{n+1}(N)} \text{ km/sec.}$$

The results for  $N = 1, 2, 3, 4, 6,$  and  $8$  appear in Fig. 3.16. It can be seen that there are two places where the slope changes markedly. The first, at 170 km, is due to relativistic effects: the velocity versus energy curve for electrons starts to flatten off, while the penetration versus energy curve remains essentially linear. The result is a decrease of the flaming velocity. The second, at 125 km, is related to atmospheric penetration: following the flattening off the velocity versus energy curve for the electrons for penetrations to 170 km, the penetration versus energy curve starts to flatten near 125 km. The result is an increase of flaming velocity.

The examples in the previous section showed a velocity of flaming of 70-80 km/sec between 100 and 110 km. Figure 3.16 shows this to correspond to a release point 4 earth radii along the field line; this is about two thirds of the way between the ionosphere and equatorial plane. However, this method of determining the release point is greatly subject to the assumed starting height of the flaming: taking the best (third) example of flaming, one finds that starting heights

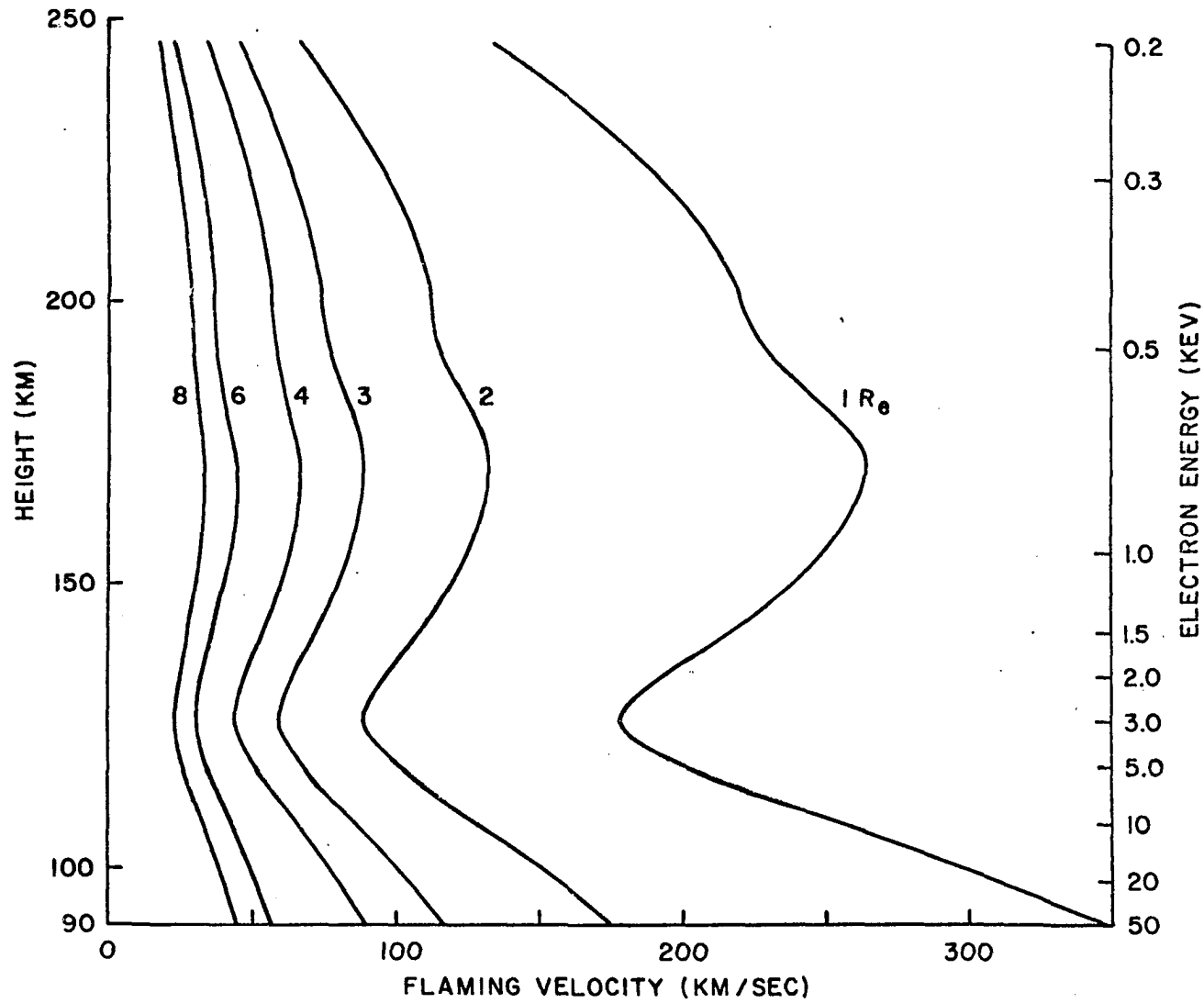


Figure 3.16 Plots of the apparent upward velocities of synthetic flaming auroras due to electrons being released with zero pitch angle at several points on the  $L = 5.5$  field line. The distances are in units of earth radii and are measured from the earth's surface.

in the range 90-110 km give release points ranging from the equatorial plane to 2.5 Re along the field line from the ionosphere.

Assuming that the method just described is the one which does produce flaming, then we can examine some of the consequences. If the release of electrons lasts only a very short time, then luminosity will first be seen at low elevations, due to high energy electrons, and then it will apparently move upwards. More likely the release will last longer; then the auroral feature will appear first at low elevations, due to high energy electrons, and then grow up to higher elevations with the arrival of the lower-energy electrons. The feature will remain unchanged for a duration equal to that of untrapping. Then as the supply of freshly untrapped electrons is depleted the effect will be first seen with the highest energies and finally with the lowest. An observer will see the lower border move upward until the feature eventually disappears (see Fig. 3.15).

In a display made up of numerous, flaming, ray-like forms having little horizontal separation the flaming, although no doubt readily apparent to the eye, could be difficult to measure from TV films. This would arise because the form considered would be confused with luminosity both in front and behind it. That in front would cover the upper portion by an amount related to the observer's elevation angle.

It is believed that this was the state of affairs during the flaming display of February 16, 1967, and lead to the difficulty in finding measureable examples.

### 3.2.3 Discussion

From the limited observations, flaming auroras appear to occur under the same conditions as pulsating auroras, namely near the equatorward boundary of auroral displays during their postbreak-up phase. Of the three examples treated here, one was seen during a pulsating aurora display; one was the flaming seen by viewing a pulsating aurora side on; the other was selected from a massive flaming display of numerous ray-like forms. For an assumed starting height of 100 km, all had velocities in the vicinity of 70-80 km/sec which, from electron velocity dispersion considerations, could be due to electron release points two thirds of the way between the ionosphere and equatorial plane. However, allowing the assumed starting height to range from 90-110 km resulted in the release point ranging from the equatorial plane to 2.5  $R_e$  from the ionosphere. The photometric determinations of flaming aurora velocities by Carleton (private communication) gave values of  $\sim 1000$  km/sec which placed the electron release point at  $\sim R_e/2$  from the ionosphere.

Other determinations of the release points of electrons during postbreakup auroras have been made in different ways: Omholt and Pettersen (1967) found that the power spectrum of photometric pulsations consistently showed an exponential fall off with increasing frequency above 1-2 cps. This was shown to be consistent with the existence of a modulation mechanism near the equatorial plane with energy dispersion smearing out the higher frequencies. Bryant et al (1967) flew 10 kev and 4 kev detectors aboard a rocket into

a postbreakup aurora and found that pulsations in 10 keV electrons preceded those in the 4 keV electrons by 0.55 sec. Assuming simultaneous modulation and subsequent adiabatic motion of the electrons, the source was found to be in the vicinity of the equatorial plane on the  $L = 6$  magnetic shell. This calculation does not suffer from the uncertainty introduced in assuming a lower border for the flaming aurora. In terms of flaming aurora the 10 keV and 4 keV electrons would produce maximum luminosity at 108 km and 121 km (from Rees (1964)); the observed flaming velocity would be 24 km/sec. Balloon measurements of X-rays and the  $\lambda 5577$  emission were made by Rosenberg (1967, private communication). Pulsations in the  $\lambda 5577$  emission, due to relatively low energy electrons, lagged only 0.5 sec behind pulsations in the X-ray flux, produced by higher energy electrons. The lag was ascribed to the lifetime of the atomic oxygen metastable state and the shape of the excitation function. It was concluded that the electron modulation mechanism lay quite close to the ionosphere ( $< 1 R_e$ ).

Concerning other auroras, Evans (1967) flew detectors sensitive to various energies aboard a rocket into a breakup at Ft. Churchill. He found a 10 cps periodicity in the flux of electrons of energy 1-120 keV. The results indicated the source of the periodicity to be within 1500 km of the earth. The source was such that it provided 8 keV electrons 0.015 sec before 60 keV ones. This time lead is of interest because it would produce downward flaming of the order of 1600 km/sec.

The electron source location of daytime microburst activity has been calculated from data obtained at Ft. Churchill using rockets equipped with 60-90, 90-150, and 150-300 kev electron detectors. In one case the source was found to be within  $1.5 R_e$  of the northern auroral zone, and in the other, at a distance of  $22 \pm 5 R_e$ , or roughly at the southern hemisphere end of the  $L = 8$  magnetic field line (Lampton, 1967). This suggested that daytime energetic electron precipitation is associated with the ionosphere.

### 3.3 Flickering Auroras

Flickering auroras are termed by the International Auroral Atlas to be type p3 pulsing auroras. A large part of a display undergoes rapid, more or less irregular changes in brightness as if lit by flickering flames.

Auroras of this type were not observed by the writer during the solar minimum period and were only observed twice over the last year (1966-67). On both occasions the flickering, being both vigorous and bright, occurred before midnight in discrete forms: a westward surge and an arc respectively.

#### 3.3.1 First example

The night of 22/23 February 1966 was magnetically very disturbed with the College magnetogram showing bays in H with magnitudes up to  $1000 \gamma$  (Fig. 4.25). At 2200 150° WMT there occurred a westward traveling surge; its attitude at 2207 is shown in Fig. 3.17. During the surge the College  $\lambda 4278$  zenith photometer was off scale

(full scale deflection = 10 kR). For the 10 minute period around 2200 narrow beam riometers showed 1 dB of absorption (Berkey, 1968).

At the time that the surge became noticeable one of the observers was inside the observatory operating the auroral television system while another was outside taking still photographs. Both noticed that in the bright broad part of the surge were numerous small patches superposed on a bright diffuse background. These were rapidly pulsating and the visual observer estimated their frequency to be about 5 cps. It was difficult to see any phase coherence between different patches. Patches as they brightened overlapped those being extinguished.

With very fast pulsations the television system may be misleading because, (1) it produces 30 scans (or pictures) per second while the 16 mm recording camera exposes 24 frames per second and (2) the phosphor on the monitor has a decay characteristic of 33 ms to 10%. Nevertheless it was possible to obtain reasonable frequency information by attaching photocells to the screen on which the TV films are projected during analysis. In Fig. 3.18 frequency components up to 10 cps can be discerned (note that a 120 ms time constant was used to prevent the pens from faithfully reproducing the projector shutter). The four traces are quite dissimilar, which indicates the small spatial scale of the pulsations.

#### Microscopic Character of the Flickering

When the TV films of flickering auroras were examined in real time it was difficult to determine just what was happening, even though



Figure 3.17  $165^\circ$  field of view of the sky at 2207, February 22, 1966. The flickering was observed in the broad diffuse feature near the zenith.

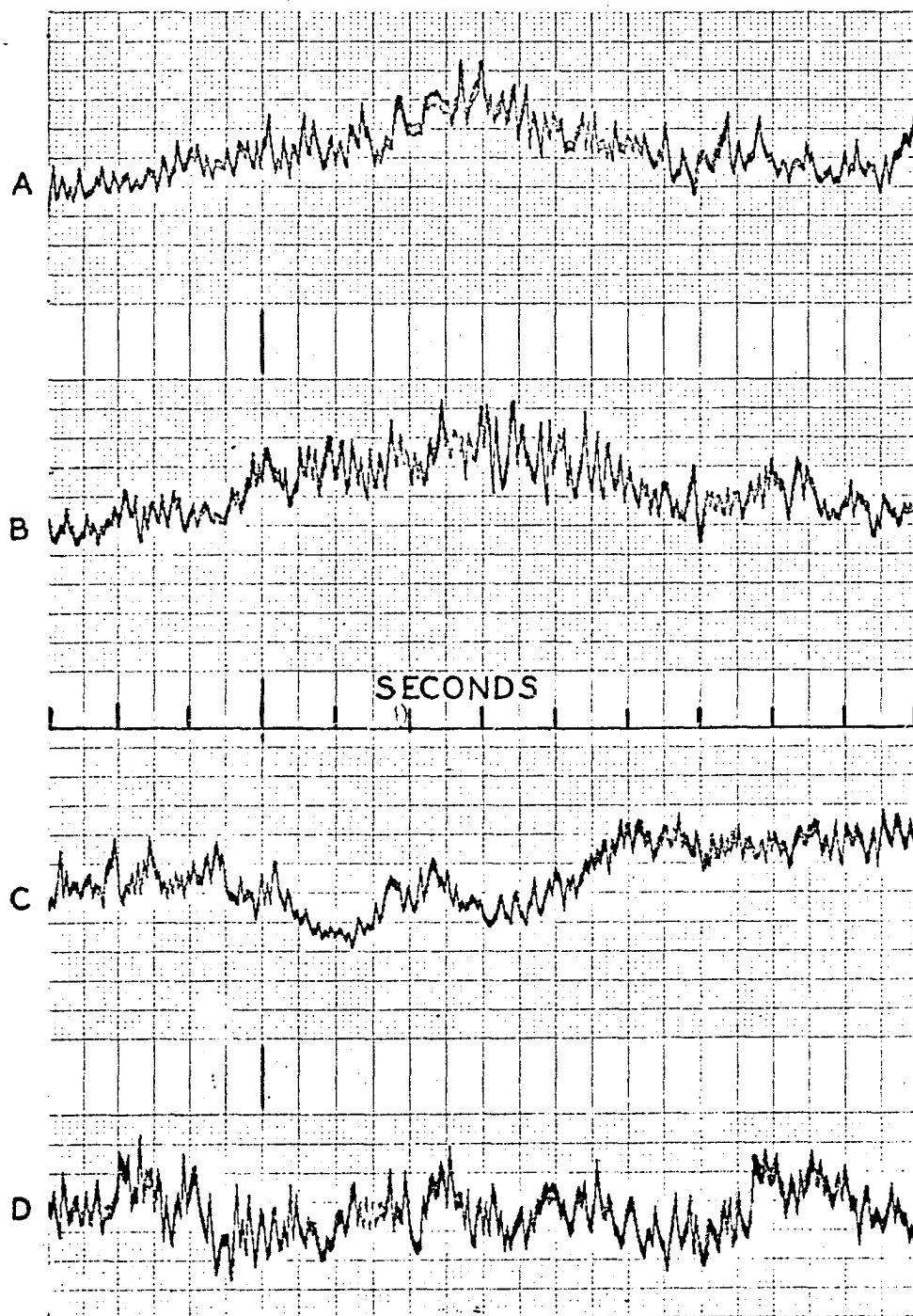


Figure 3.18 Photocell traces made from the television films at 2207 showing the rapidity of the flickering and the dissimilarity between the light output from different points. The photocells were randomly placed in the 22 x 16 km field intersected at the 100 km altitude level.

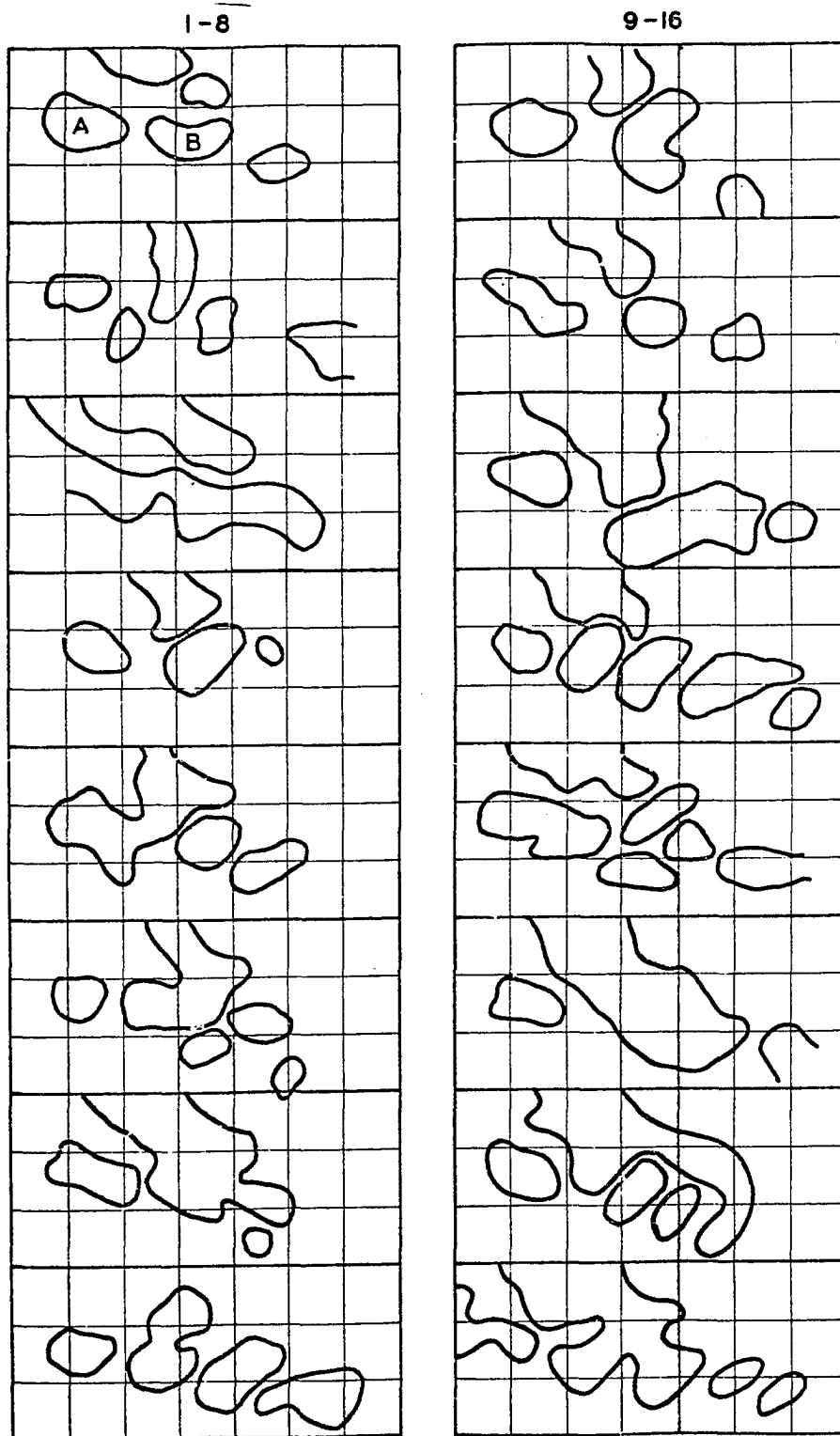


Figure 3.19 Tracings made at 2207 from corresponding parts of 16 consecutive TV frames centered on the magnetic zenith. The flickering can be seen to be due to rapid changes in size and shape of individual patches. The field shown intersects an area roughly 12 x 10 km at the 100 km altitude level.

the flickering was very obvious. In Fig. 3.19, tracings made at 2207 from corresponding parts of 16 consecutive frames centered on the magnetic zenith are shown. The technique used was simply to project each frame onto a sheet of white card and draw around the brightest areas. Examining, as an example, spot A in frame 1, and following it through the entire sequence, one can see changes in size and shape from one frame to the next. This, then, is what constitutes the flickering in its simplest form: rapid changes of size and shape of particular patches.

Following spot B through the sequence is not quite as clear cut: possibly at times it splits into two, or, alternatively, it disappears and others take its place.

Slight evidence for periodic behavior across an extended area is shown by frames 8, 12, and 16. These were judged to be reasonably similar; at least 12 was similar to 8, and 16 was similar to 12.

### 3.3.2 Second example

The night of December 4/5, 1966 was disturbed prior to midnight have a  $\sim 200$   $\gamma$  positive bay at 1920 and an unusual, sharp, 400  $\gamma$  positive bay peaking at about 2247. After midnight it was relatively undisturbed. The College narrow beam riometer (cf. Berkey, 1968) showed strong absorption that started at 2236 and had maximum values of 2.9 dB at 2245 and 2249-2250; it then quickly recovered.

Shortly after 1900 a weak diffuse envelope could be just discerned on the all-sky camera film spreading south through the zenith

from an arc in the low north. This arc became brighter after 2200 and was jointed by several others. In one of the arcs a high frequency flicker was observed both visually and with the TV system. At 2240 the most predominant feature was one bright arc ( $> 100$  kR in  $\lambda 4278$ ) through the zenith. Fast flickering of small segments was readily evident in this arc.

At 2245 the arc containing the flickering forms was aligned east-west through the zenith. At this time the all-sky camera record showed the start of an apparent poleward expansion: by 2246 the arc(s) had expanded to  $30^\circ\text{N}$  of the zenith; by 2249 to  $60^\circ\text{N}$  of the zenith; the average expansion velocity was  $750$  m/sec. Then the arcs on the south side faded so that by 2252 all bright features were more than  $60^\circ\text{N}$  of the zenith; scattered remnants remained near the zenith.

Photocells attached to the projection screen during TV film analysis revealed quasi-periodic variations as rapid as 8 cps. More noticeably than with the February 22, 1966 display, some of the small patches moved quite rapidly; one was measured to travel from west to east at  $\sim 7$  km/sec.

It seemed apparent that there was some close association between the flickering aurora and the ionospheric absorption measured by the  $6^\circ$  beam riometer centered on the zenith. During the flickering the TV camera was moved in elevation along the meridian to record the best flickering. At 2209 this was at elevation  $40^\circ\text{N}$ ; from 2221

until 2250 it was generally centered within  $15^\circ$  of the zenith, although this meant that the  $6^\circ$  riometer beam and the TV field ( $14^\circ$  in the north-south direction) often did not overlap. Additionally, the riometer site is some 10 km northeast of the television site. Keeping in mind these points, arbitrary indices (0-4) for the visual quality of the flickering as seen in the TV film were assigned for times between 2221 and 2250 (there was no flickering after 2250). The indices were assigned as follows:

- 0 : glow
- 1 : structures like those that occur during flickering,  
i.e. patches commonly 1-2 km across
- 2 : weak flickering
- 3 : moderate flickering
- 4 : strong flickering

The indices were then plotted with the absorption (Fig. 3.20).

Allowing for the crude manner in which the indices were assigned, and the fact that the riometer beam and TV field often did not overlap, one can see that the agreement between the quality of the flickering and the amount of absorption was very good. In other words, the precipitation of large fluxes of energetic electrons was associated with the precipitation of highly time-structured fluxes of auroral energy electrons. Whether or not the energetic electron fluxes were highly time-structured is a matter of conjecture, although the rocket results of Evans (1967) may suggest that they were (cf. section 3.2.3).

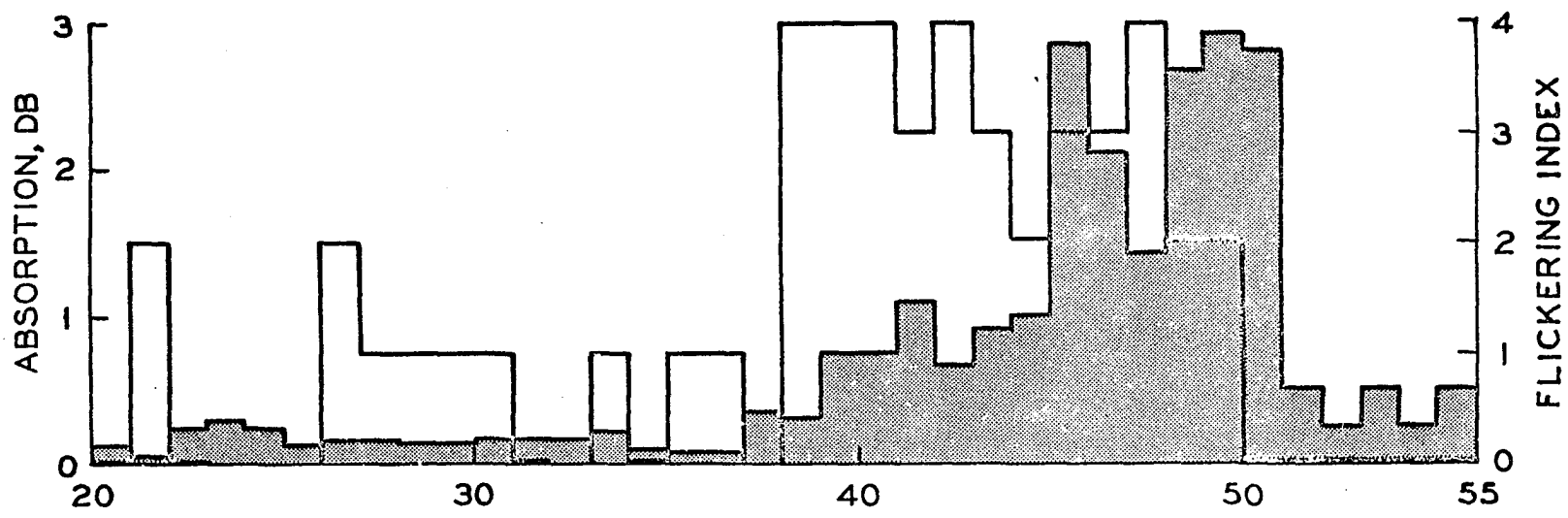


Figure 3.20 Plots of the flickering index and the narrow beam rliometer absorption (shaded).

Evidence for the precipitation of large fluxes of protons was provided by the  $\lambda 4861 \text{ H}_\beta$  zenith photometer operated by Professors Belon and Romick: the trace showed several large spikes between 2242 and 2249 with intensities up to 650 R.

### 3.3.3 Discussion

Flickering auroras have been observed from College as part of bright features ( $\sim 100 \text{ kR}$ ) seen before midnight on active days ( $\Sigma K_p \sim 30$ ). They were made of numerous small patches 1-2 km that underwent rapid changes ( $\sim 10 \text{ cps}$ ) in size and shape, and were accompanied by ionospheric absorption ( $\sim 1-3 \text{ dB}$ ).

Very recently (Evans, 1967) there have been rocket observations of a strong, purely temporal, 10 cps periodicity in the precipitation of auroral zone electrons. The rocket was flown into a "breakup phase" aurora at 2256 local time at Ft. Churchill. By examining electron fluxes of different energies and allowing for velocity dispersion, Evans placed the source of the periodicity at  $< 1500 \text{ km}$  from the earth. It seems likely that if the aurora had been subjected to television observations it would have appeared as a flickering aurora.

## Chapter 4

### FAST AURORAL WAVES: OBSERVATIONS

"An arch of brilliant red light stretched across the sky from N.N.E. to W.S.W., and pale waves of light rolled across the sky almost to the southern horizon." Paulin at London, England, 1870 (Newton, 1958).

Fast auroral waves will be defined to be east-west aligned waves of luminosity that rapidly travel equatorwards parallel to the earth's surface. Most often they appear to emanate from arcs or glows. On occasions they may occur concurrent with pulsating or diffuse auroras. They have occurred too infrequently to warrant mention in the International Auroral Atlas (1963). Quite possibly they could be added to the category "pulsing auroras" as a type p5 after pulsating, flaming, flickering, and streaming auroras.

The first reported observation appears beneath the title above. Comparatively recently we have the observation of Parsons and Fenton (1953), two visual observers at Macquarie Island (geomagnetic coordinates:  $61^{\circ}06'S$ ,  $243^{\circ}06'E$ ) who, on March 2, 1951, observed that "very distinct waves following each other at intervals of about one second swept from approximately  $20^{\circ}$  south of the zenith to low in the northern sky." This display lasted from 0000 to 0037 L.T.

Soon after, on January 24, 1952, Heppner (1954) at College (geomagnetic coordinates:  $64^{\circ}36'N$ ,  $256^{\circ}18'E$ ) visually observed an arc to be "pulsating violently with two distinct types of motion." One type was described as "segments of the arc were ejected southward in a continuous manner resembling waves of light which died out with increasing distance." The display lasted from 0330 to 0442 L.T.

Fast auroral waves can occur with pulsating and diffuse auroras and an example of this phenomenon observed near FranzJosef's Land was described by Weyprecht who wintered with the Austrian-Hungarian Arctic Expedition in 1872-73 (Chapman and Bartels (1940)) "through these fragments drive the waves of light". Similarly, Parsons and Fenton (1953) described "waves which brightened scattered areas of glow momentarily as they passed."

When searching through documented auroral observations one rapidly becomes aware that some of the descriptions could apply equally well to both fast auroral waves and flaming auroras. A sure way of distinguishing a fast auroral wave display from flaming auroras is to see if the moving luminosity passes through the magnetic zenith; if it does than it cannot be due to flaming alone, there must be a horizontal component. As an example of this, the 1726 observation of de Mairan (1754) in France can be cited. He described an extensive diffuse display that to him resembled a great fluid that was traversed by waves from the horizon, "and above all from the north up to the zenith." Another is the April 16, 1938, New Zealand observation of Geddes (1939) of "an entirely different type" of flaming which was from the south and consisted of a bodily movement of the whole arc towards the zenith, a height of  $50^\circ$  being reached in about half a second". Both of these observations satisfy the fast auroral wave condition that the motion be equatorward. However, since no mention is made of the motion going beyond the magnetic zenith it remains possible that it was field aligned.

On the other hand, fast moving auroral forms described to be flaming auroras may sometimes be fast auroral waves. For instance, Evans (1963) described careful observations on the  $\lambda 3914$ - $\lambda 5577$  time delay for flaming auroras and found a mean value of  $0.67 \pm 0.06$  sec. However, during a discussion with him on fast auroral waves he pointed out that it was actually these that he had been observing.

Several years ago Georgio (1959) reported on observations of a rare phenomenon described as the wave-like movement of luminescent formations. One record showed the waves to travel from  $40^\circ$  south of the zenith to the zenith at 14 km/sec. Because of their slow speed and poleward motion these would not be described here as fast auroral waves.

Instrument-supported observations on fast auroral waves were not made until 1964 when photometers having separated fields of view were used at this Institute to obtain wave velocities, widths, repetition rates, and distances traveled (Cresswell and Belon, 1966). From 1964 until the present time a program of observations on clear moonless night yielded six fast auroral wave displays.

Accounts of the observations from the six wave displays are presented in chronological order in the following sections. To aid the reader, each observation is preceded by a brief abstract. Following each observation are details of the distribution of auroras over Alaska at various epochs for the night considered. These were determined from data from the all-sky camera network; not all

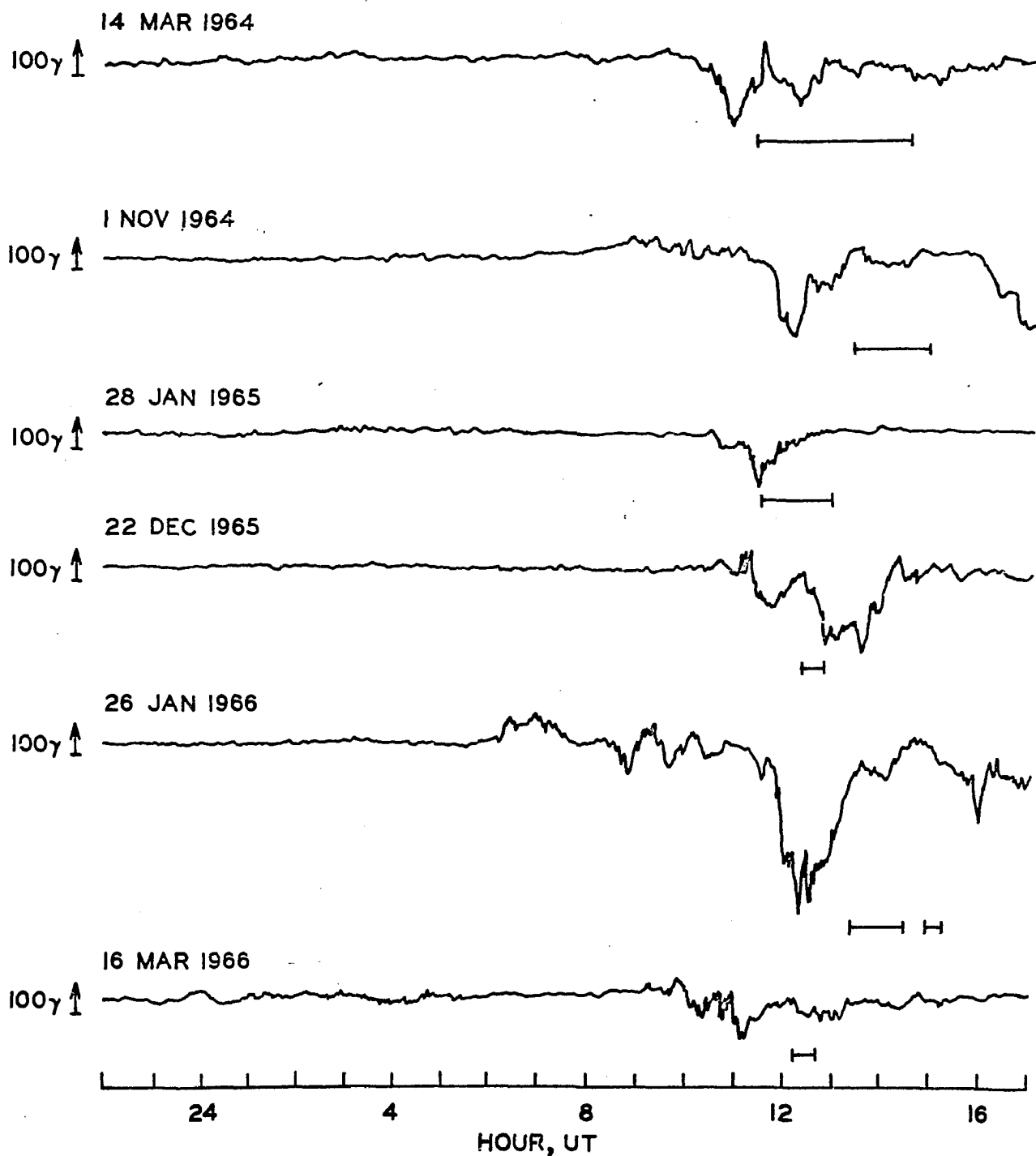


Figure 4.1 The College magnetograph H component traces for the nights on which wave displays occurred. The times that waves were seen or recorded are marked by bars. Subtract 10 hours for Alaska Standard Time.

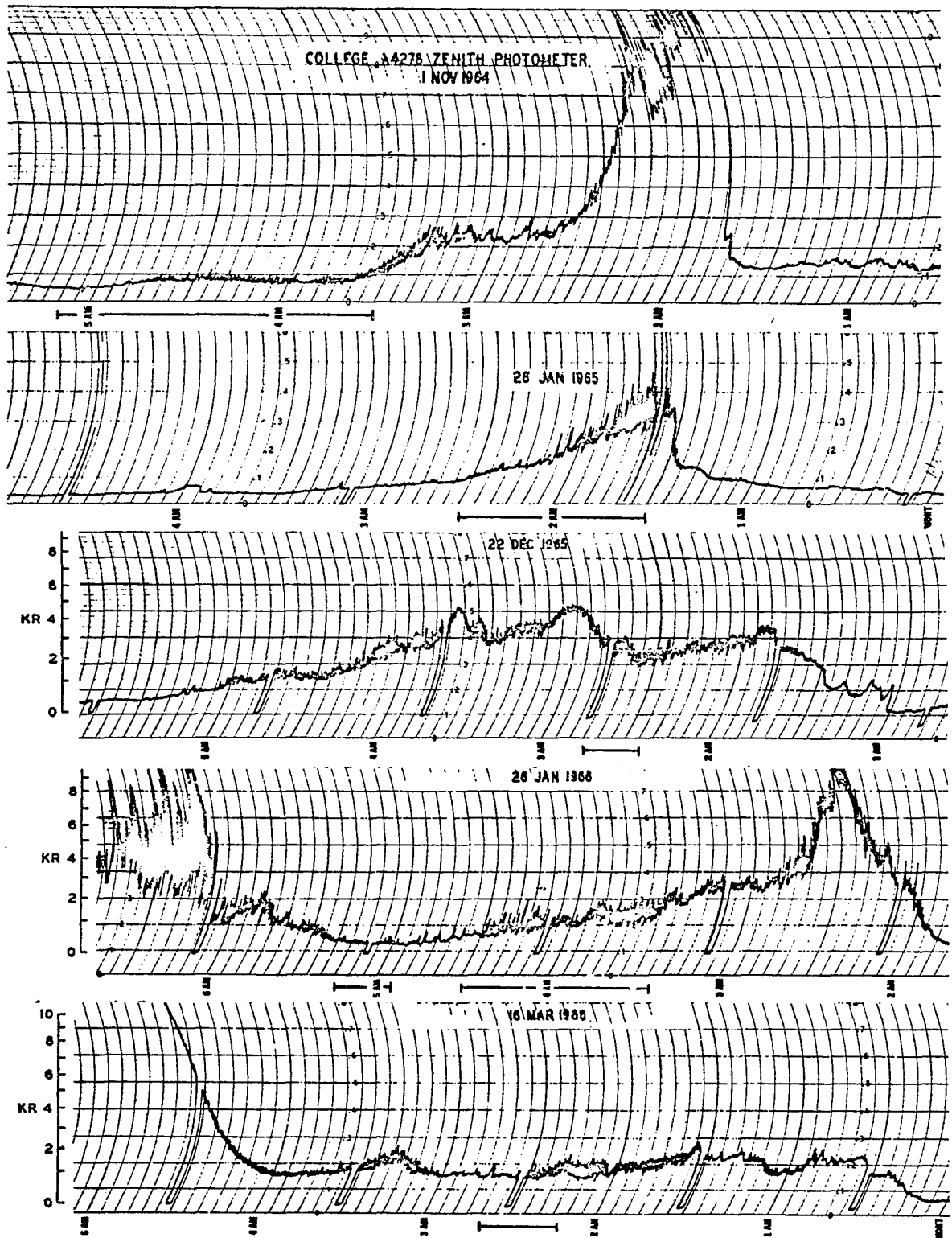


Figure 4.2 The College  $\lambda 4278$  zenith photometer traces for the last five nights on which wave displays occurred. The times that waves were seen or recorded are marked by bars.

stations could be used, those that were are marked on the respective maps. Except where stated otherwise, only information gleaned from the all-sky films is plotted; subvisual envelopes detected with the College photometers are not plotted. The distributions are discussed in the light of the substorm picture of Akasofu and co-workers (see Chapter 1.).

There is a section devoted to a comparison of nights when waves did occur to those when they did not. The final section is a summary of the observational properties of the waves.

The magnetogram H traces and the  $\lambda 4278$  zenith photometer traces for the wave displays are presented in Figs. 4.1 and 4.2.

#### 4.1 March 14, 1964

##### Abstract

A fast auroral wave display was seen from 0130 until it disappeared into the dawn continuum at 0430. The display was preceded by a substorm onset over northern Alaska which was followed by the southward spread of a diffuse envelope. This then weakened, except to the north, leaving a northern arc. Waves were recorded at 0130 in the College zenith and seen to come apparently from the arc and to travel  $\approx 250$  km into the southern sky. At this time the substorm negative bay had almost recovered. A smaller negative bay was registered shortly after 0130 and lasted until 0250.

The photometer provided the following information about the waves:

Velocity: 50-300 km/sec.

Frequency: about 1/sec.

Width: 30-200 km.

### Observation

At 0130 on the morning of March 14, 1964, fast moving waves of weak luminosity oriented E-W were observed moving south (equatorward) from a stable homogeneous arc about  $50^\circ$  north of the zenith to about  $50^\circ$  south of the zenith, a distance of  $\sim 250$  km. They were too weak to be seen going farther. Soon after 0130 the four-field photometer was directed at the zenith so that the velocity of the waves could be determined. From this time, until they disappeared into the dawn continuum at 0430, the waves were recorded at a rate of one per second. The intensity of the waves remained constant enough for the amplifiers to be set to an optimum and left essentially untouched for two and one-half hours.

Velocity determinations assuming a height of 100 km showed the waves to have velocities in the range 50-300 km/sec with 150 km/sec most common. The separation of small intensity variations in the waves was as little as 5-10 km while the width of the waves was as much as 150 km. To the eye the waves typically appeared much narrower, of the order of 10 km. Figure 4.3 shows a series of three waves having velocities of 60-70 km/sec and widths (measured start to finish, not half peak) 30, 45 and 100 km respectively.

During the period when the waves were seen the northern arc was remarkably stable. This can be seen in Fig. 4.4 which shows a series of all-sky camera photographs at thirty minute intervals before and during the wave display.\* With visual observations these can be interpreted as follows: at 0030 an arc in the north became active and remained active for about ten minutes. As it became quiet it was joined by a weak corona which is visible in the 0100 picture. At 0130 only a homogeneous arc of IBC -II remained and extended from 20° to 40° elevation. It was at this time that the waves were first seen, but of course the long all-sky camera exposures could not record them.

Information on likely altitudes of the waves is provided by the Huet zenith spectrograph (Fig. 4.5). Until about 0100 only the strong oxygen  $\lambda 5577$  line and the mercury line (from street lamp contamination) are readily evident. There is some evidence of  $N_2^+$  1 N.G.  $\lambda 4278$ , the oxygen red lines, and  $O_2^+$  1 N.G.

After 0100, when the weak corona formed, until nautical twilight, when the operation of the spectrograph was terminated, emissions indicative of low altitude auroras were enhanced, viz, the red  $N_2$  1 P.G. and the  $O_2^+$  1 N.G. near 6000A. Also suggesting a low altitude aurora is the large  $\lambda 5577/6300$  ratio. The absence of the hydrogen

---

\* When printing, the 0431 frame was given a longer exposure than the other frames.

lines at 6563A and 4861A rules out the possibility of excitation by energetic proton bombardment.

The College magnetogram for the morning of March 14 (Fig. 4.1) shows the waves to have occurred on the recovery side of a negative bay that had a maximum value at 0100. The magnetogram did not register the passage of the waves through the zenith because its time constant is considerably longer than one second and possibly because the disturbance caused by the waves was small. Fast run (one inch per minute) and sensitive (comparable to 5 gammas full scale) earth current recordings did not show fluctuations which could be directly associated with the waves.

#### Distributions of auroras over Alaska March 14, 1964

The Barrow film showed a poleward expansion to be taking place at 0030 while at the same time the northern arc from College was brightening and folding (Fig. 4.6a). In the wake of the poleward expansion were diffuse forms. The College magnetogram H trace was in the process of going gradually negative. Following the break-up, a diffuse envelope spread over northern Alaska and the Arctic Ocean. At 0100 (Fig. 4.6b) it had just passed the College zenith and was growing southward at just less than 100 m/sec; it did not appear to be growing near Kotzebue at that time. It stopped 60 km south of College and then weakened except to the north.

At 0130, when waves were seen at College, (the wavy arrows in Fig. 4.6c), the northern part of Alaska was covered by a diffuse

envelope containing some forms showing an E-W alignment. The meridional extent of the envelope was about 500 km: waves could be seen 200 km south of it. The College H trace at this time had almost recovered from a negative bay.

By 0300 the envelope had contracted mainly from the north to a width of about 200 km (Fig. 4.6d). Structural details could not be discerned due to the large zenith angles from all stations. Waves were still visible over College and the H trace had recovered after a second negative bay.

In summary, a substorm onset was registered around 0030. Another, though west of Barrow, may have caused the second negative bay shortly after 0200 (by which time the first had recovered). Eastward drifting patches, often characteristic of the substorm morning side were absent.

#### Imp 1 Measurements on March 14, 1964

During the wave display of March 14, 1964, the Imp 1 satellite was on an inbound orbit between 17 and 13  $R_e$  some 65° east of the midnight meridian; its local time was therefore about 0420 (Anderson, 1965, Figure 9; Anderson, private communication). Possibly significant is the fact that the substorm onset at 0030 over Alaska appears to be followed by the appearance of an 'electron island' at the satellite with a fast rise commencing at ~0045. Later, from ~0130-0230, another flux increase was measured, this time not having the

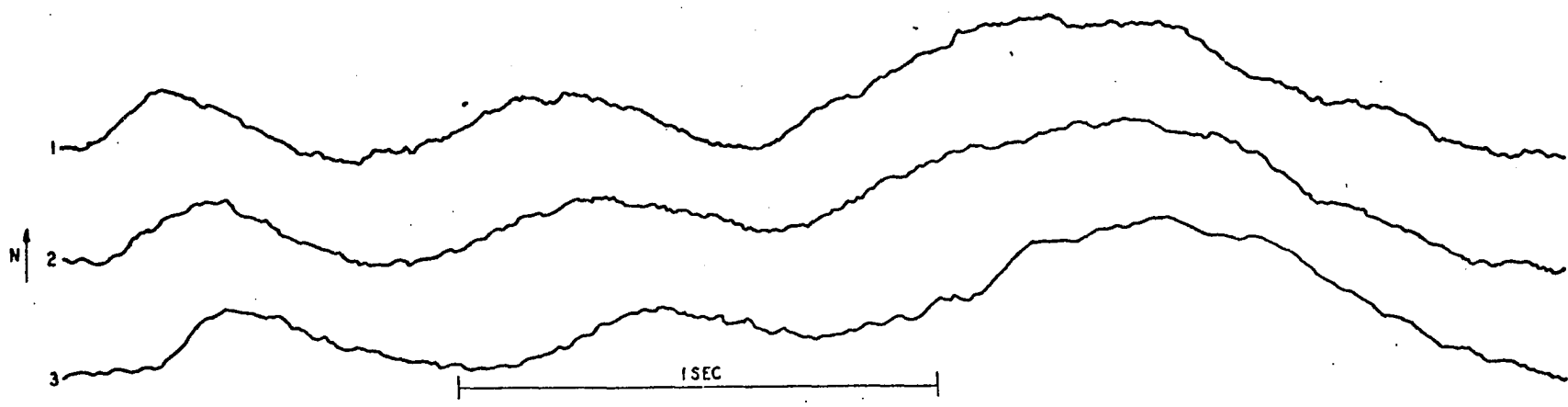


Figure 4.3 A tracing of the photometer records of three fields of view showing luminous waves having velocities of 60-70 km/sec and widths 30, 45, and 100 km respectively. The three  $1\frac{1}{2}^\circ$  fields of view intersect the 100 km altitude level at  $\sim 5$  km intervals.

## COLLEGE, MARCH 14, 1964

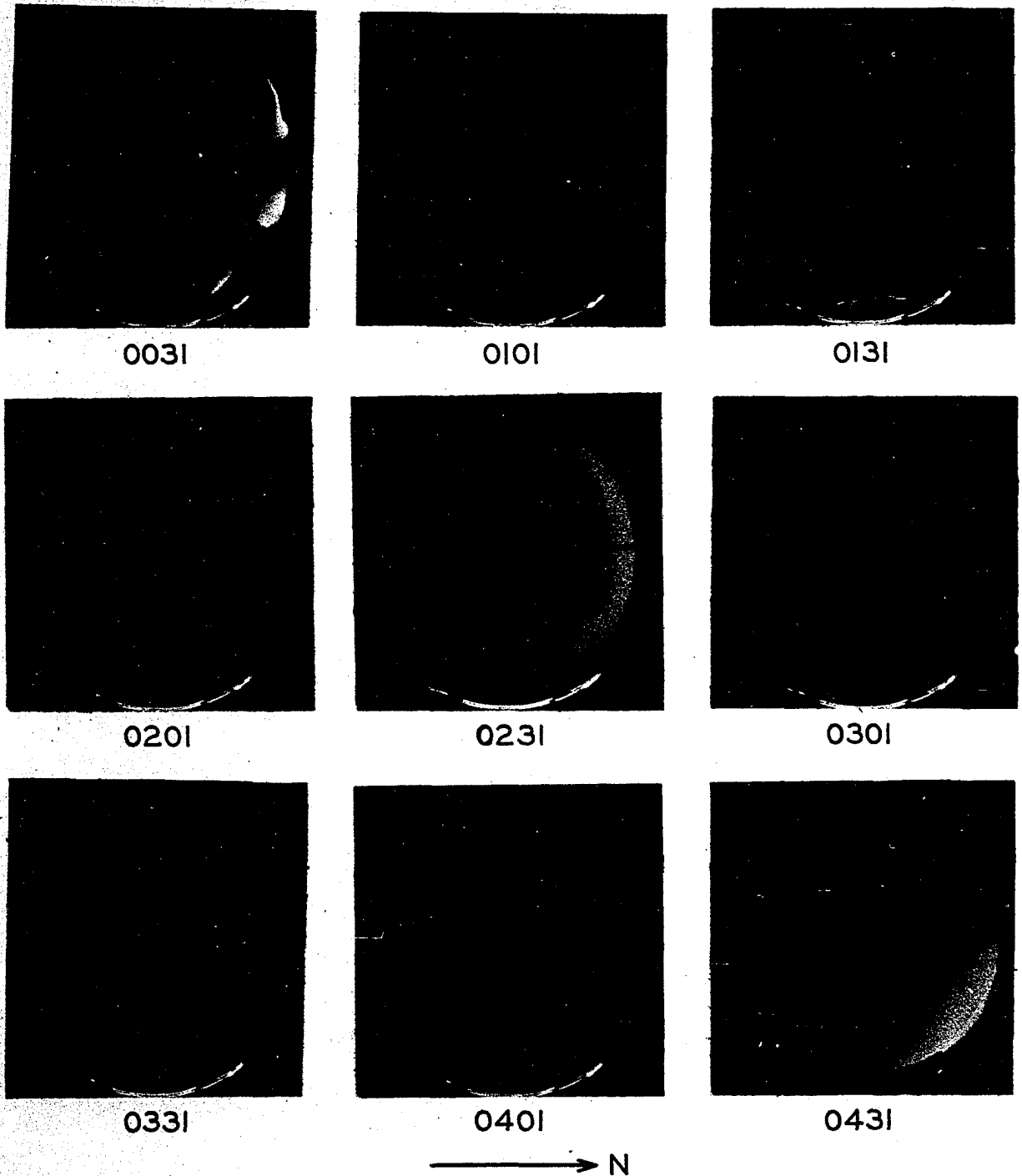


Figure 4.4 A series of all-sky camera photographs at 30 minute intervals taken before and during the period when the waves were seen.

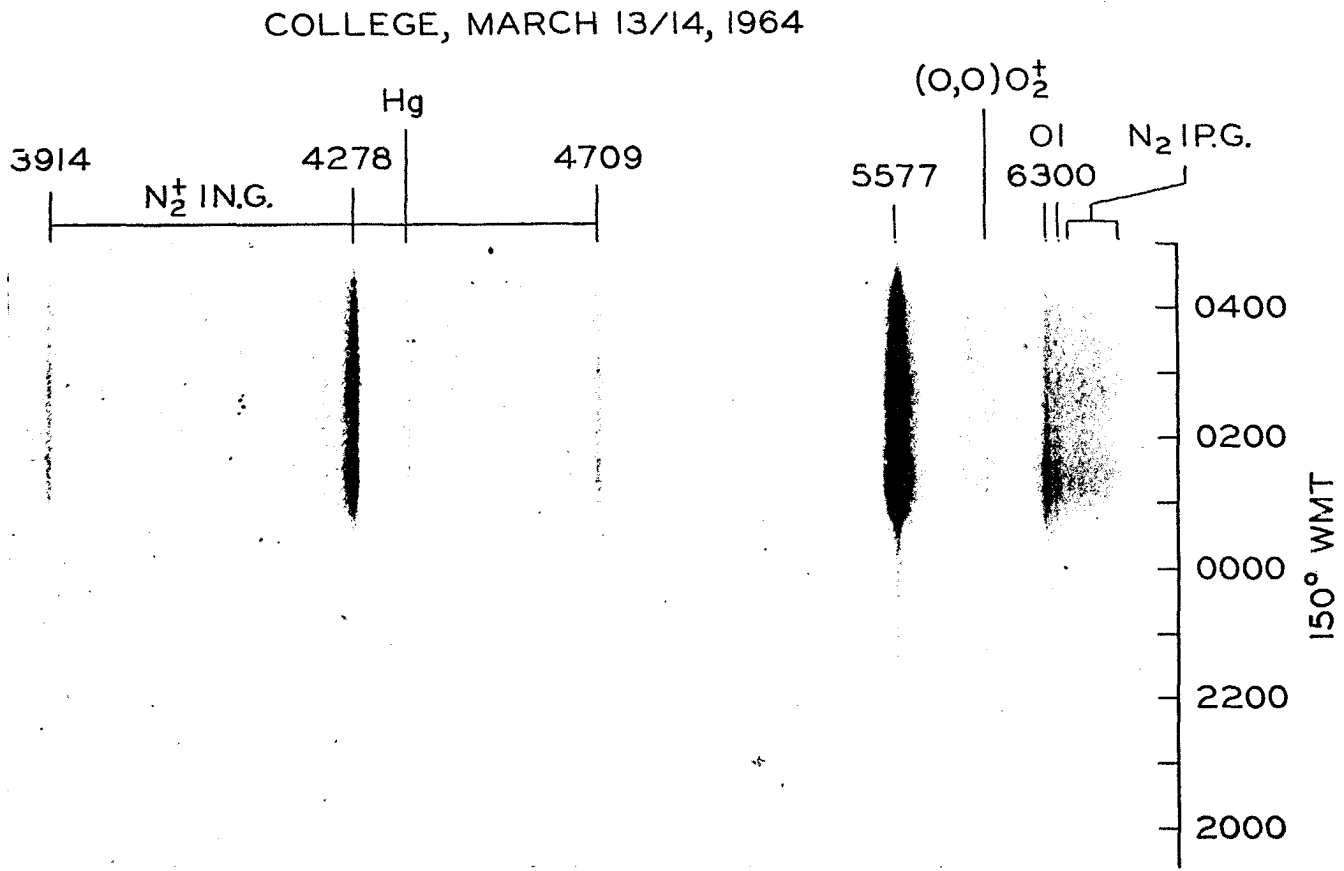


Figure 4.5 The Huet zenith spectrum for the night of March 13/14, 1964.

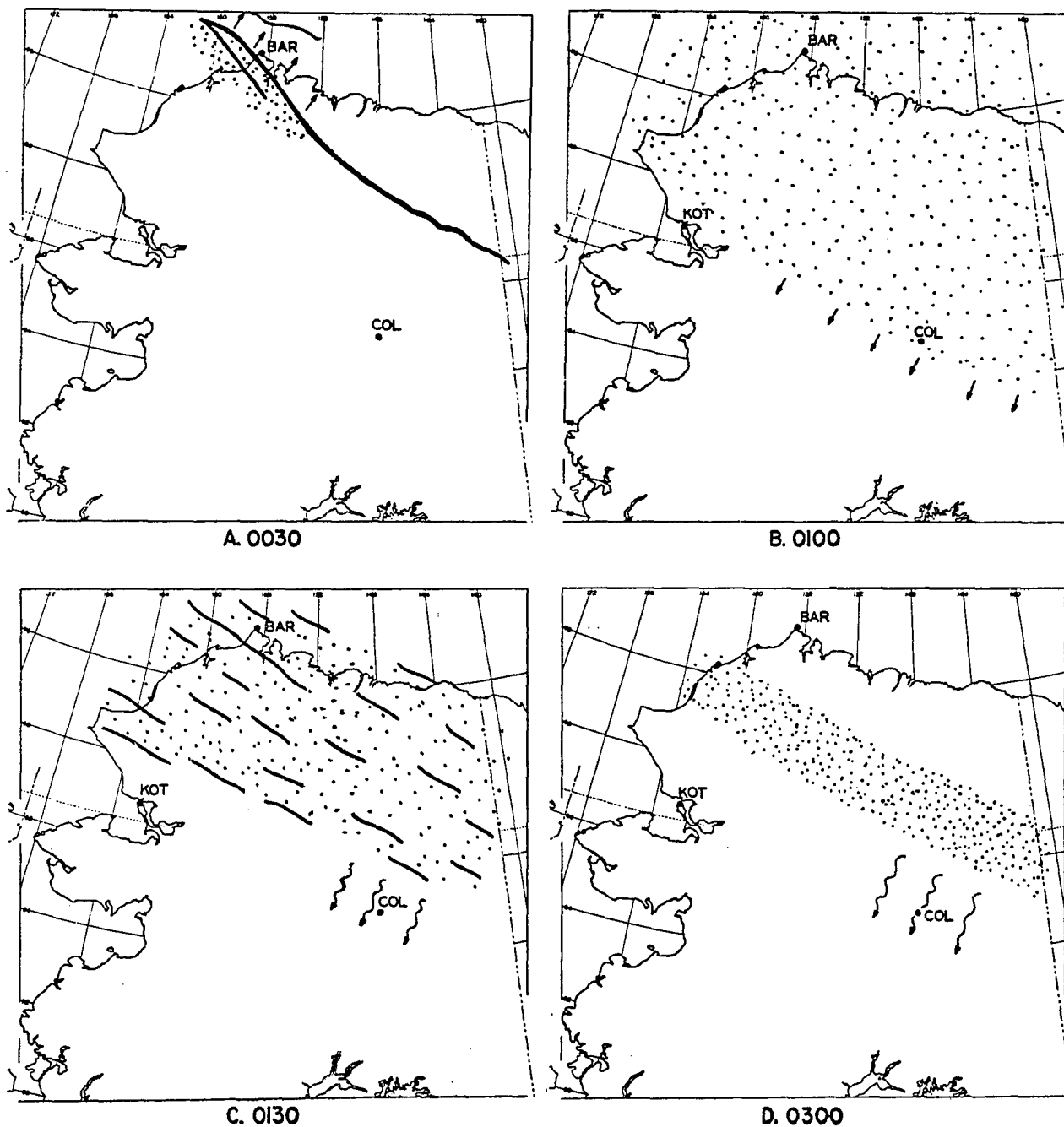


Figure 4.6 The distribution of auroras over Alaska at several epochs during the March 14, 1964, display. Arrows near a feature show it to be moving; wavy arrows show fast auroral waves; dots show diffuseness.

characteristic fast rise of an 'electron island'. This may have been associated with the second negative bay at College at this time.

4.2 November 1, 1964

#### Abstract

A fast auroral wave display was recorded from 0330 until 0510. It followed a substorm onset over College at 0200 and then the southward spread of a diffuse envelope. This contracted from both the north and the south until it was restricted to a band about 200 km wide across Alaska north of College. Waves were detected at College at 0330 when the substorm negative bay had essentially recovered.

The wave path (the region traversed by waves) was found to migrate northward in step with the contraction of the diffuse envelope. The velocities of the waves were 60-70 km/sec and many were found to travel at least 100 km and in so doing passed through the College magnetic zenith. This confirmed visual impressions that the motion was horizontal rather than field aligned.

#### The Observation

The photometer records of the March 14, 1964 wave display did not give proof that the waves travelled horizontally over large distances. In order to prove that they do, on November 1, 1964, one photometer was fixed at 30°N of the zenith while the other, with two fields separated by 6°, was set at various places along the meridian.

Quite early in the night (1830) a weak arc was seen to the north. Over the next few hours it slowly became brighter; at 2115 it was  $70^{\circ}\text{N}$  of the zenith with a diffuse envelope reaching to the zenith. At 0150 the arc was quite bright and passed through the zenith causing a rapid increase in intensity as seen by the College  $\lambda 4278$  zenith photometer (Fig. 4.2). The magnetogram showed the start of a large negative bay at this time (Fig. 4.1). By 0200 a great part of the sky at College (Fig. 4.7) and the southern sky at Ft. Yukon (Fig. 4.8) was covered by a very bright diffuse glow. At 0230 the diffuseness was more marked but the intensity had decreased. Gradually the diffuse envelope migrated north and was beyond the College zenith by 0330. At this time waves, very nearly sub-visual, were seen. Fig. 4.9 shows the trace at slow chart speed starting at 0334 from the  $30^{\circ}\text{N}$  and  $23^{\circ}\text{S}$  photometer fields of view which, for an assumed height of 100 km, are respectively 58 km north and 42 km south of the zenith. Features A, B, C, and D were selected to be good examples and run at a faster chart speed for display in Figs. 9b and 9c. The respective velocities were 60, 60, 60, and 65 km/sec. Note in examples C and D the combination and separation of waves that occur as they progress southward. These changes, and the tendency for the waves to retain only their gross identity (see Fig. 4.9a) are not unexpected in the light of the March 14, 1964, observations where changes in shape and speed could be seen between fields separated by a mere  $3^{\circ}$ .

At about 0335 the intensity of the waves reaching  $23^{\circ}\text{S}$  was seen to decrease, and so at 0341 the photometer was moved to the zenith where the wave intensity was greater (Fig. 4.10). At 0412 the photometer was directed  $35^{\circ}\text{S}$  of the zenith and there it detected only the strongest of the waves seen by the  $30^{\circ}\text{N}$  photometer. At 0418 the photometer was moved back to the zenith and essentially all the waves seen by the  $30^{\circ}\text{N}$  photometer were seen there. One can conclude that the intensity of the waves dropped off markedly between the zenith and  $35^{\circ}\text{S}$  of the zenith and that the intensity of the waves reaching  $20^{\circ}\text{S}$ , although initially high, decreased slowly from about 0330.

Prior to 0455 waves were detectable between  $30^{\circ}\text{N}$  and the zenith. The zenith photometer was then moved to  $45^{\circ}\text{N}$ ; at 0500 it was moved to  $52^{\circ}\text{N}$ . Waves were detectable between these positions and  $30^{\circ}\text{N}$  but the intensity of the waves seen by the  $30^{\circ}\text{N}$  photometer at 0502 was only one fourth of what it saw at around 0340.

The behavior above could be taken to indicate that the wave path slowly moved northward from 0330 onwards. It could be that the wave path is anchored to the auroras over Ft. Yukon because these also slowly moved northward from 0330 (a transient brightening occurred at 0430).

A "Sonagram" spectral analysis was run on the wave data from the movable photometer for this night. The result (Fig. 4.11) is a noise-like spectrum with periods 1 second and greater.

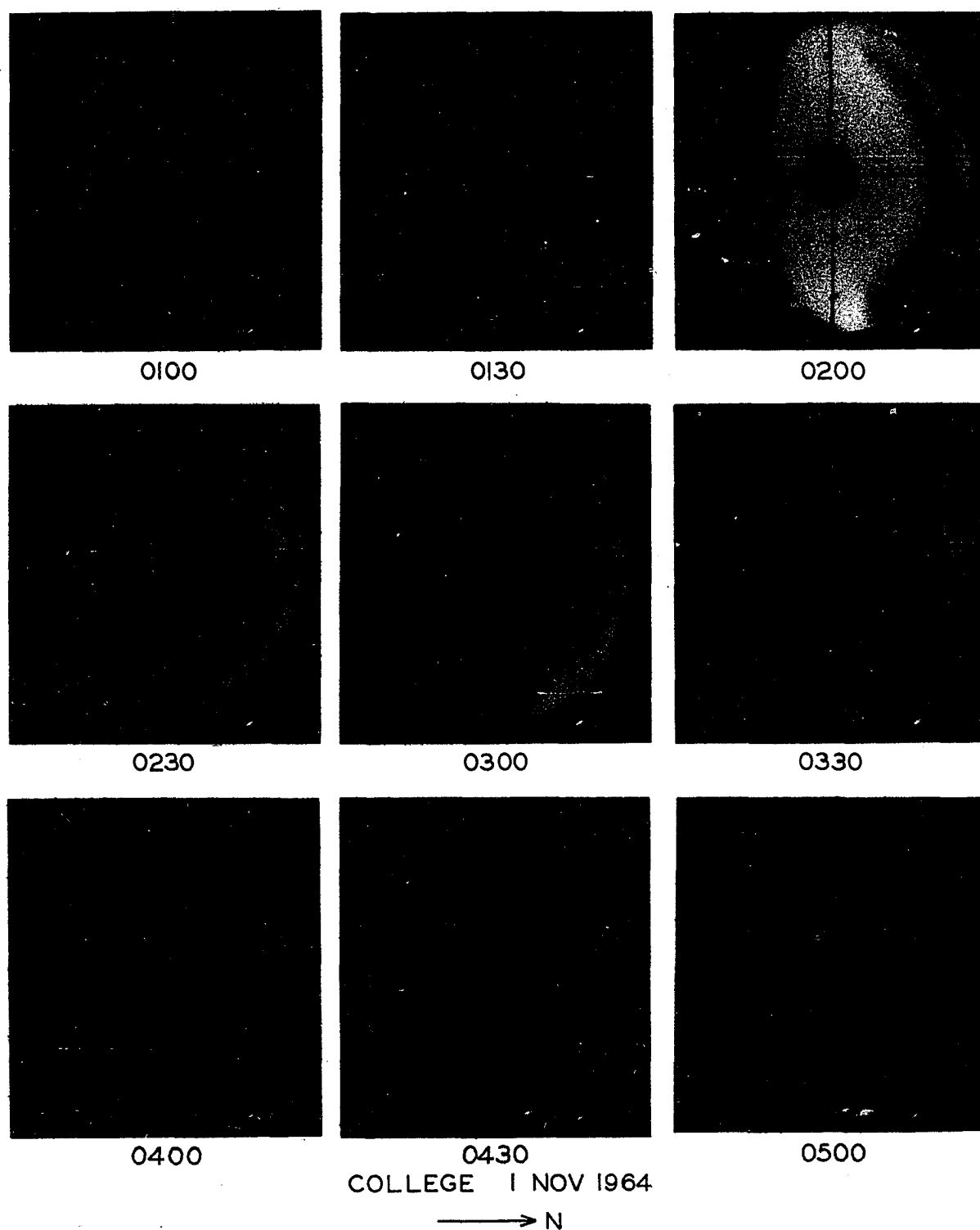


Figure 4.7 College all-sky camera frames at 30 minute intervals before and during the wave display November 1, 1964.

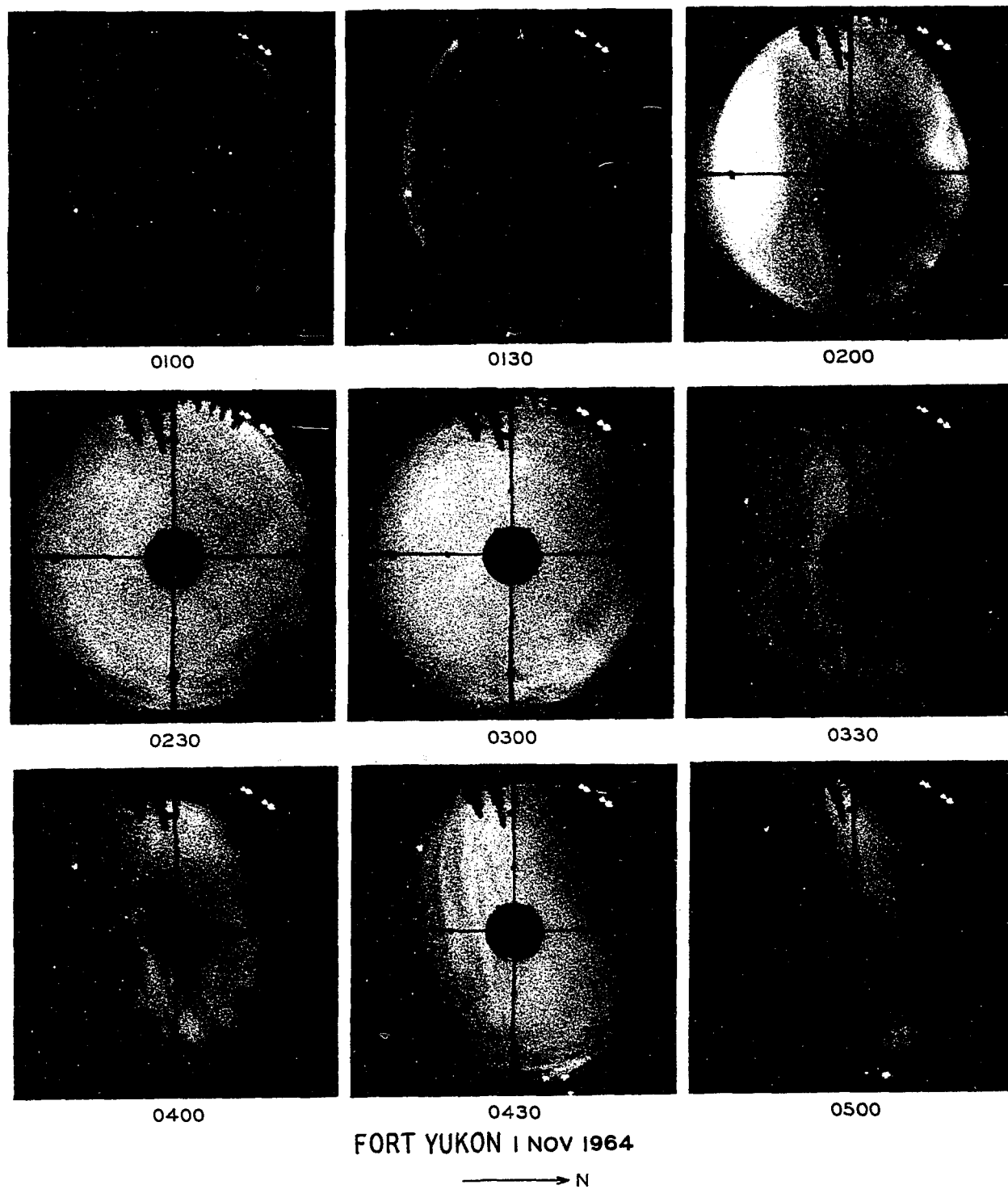


Figure 4.8 Ft. Yukon all-sky camera frames at 30 minute intervals before and during the wave display of November 1, 1964.

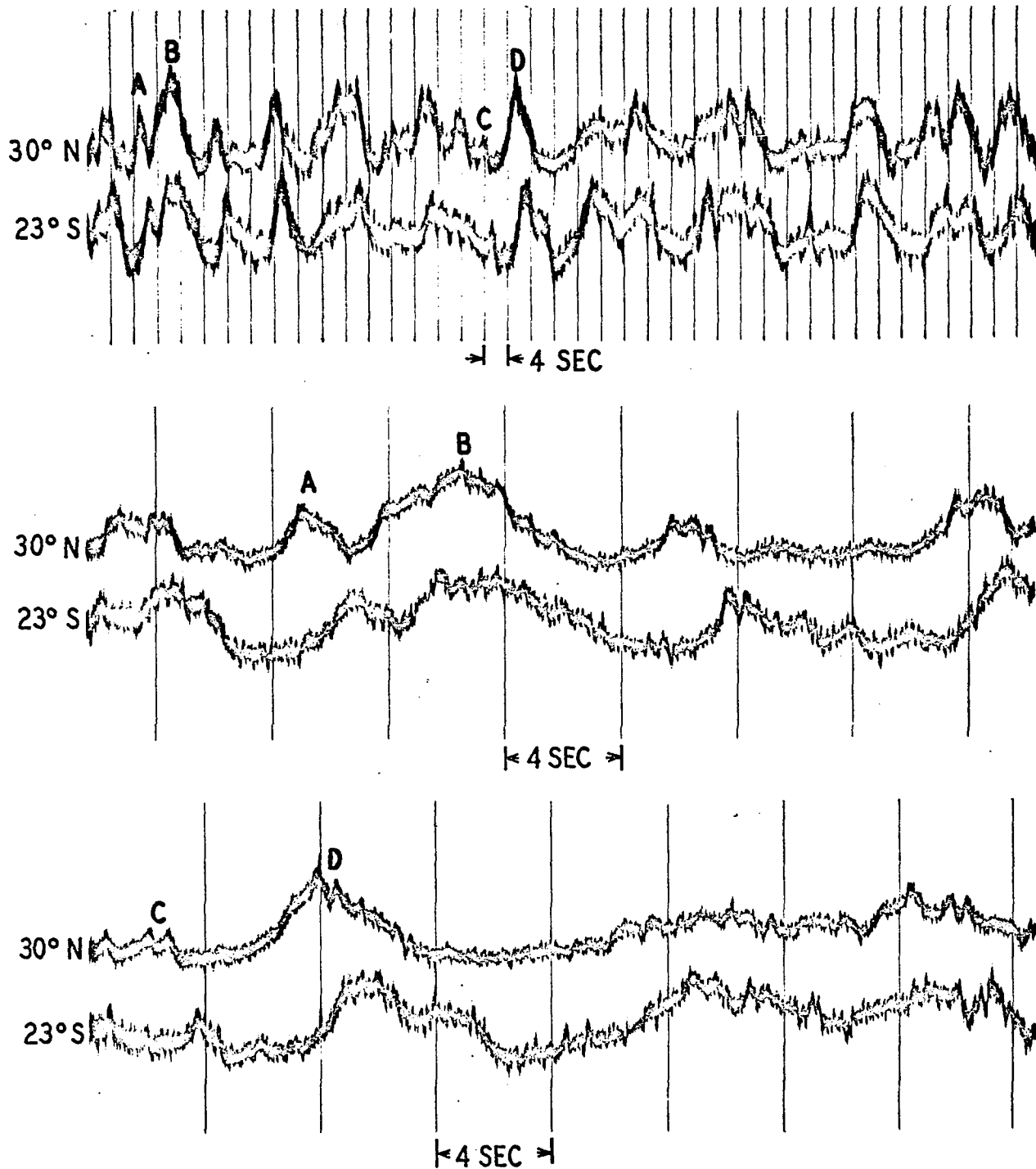


Figure 4.9 (A, B, C,) photometer traces starting at 0334 of fast auroral waves from  $1\ 1/2^\circ$  fields of view  $30^\circ\text{N}$  and  $23^\circ\text{S}$  of the College zenith. Traces (B) and (C) are fast-run samples selected from the slow-run trace (A). The velocities of the waves shown were commonly 60 km/sec.

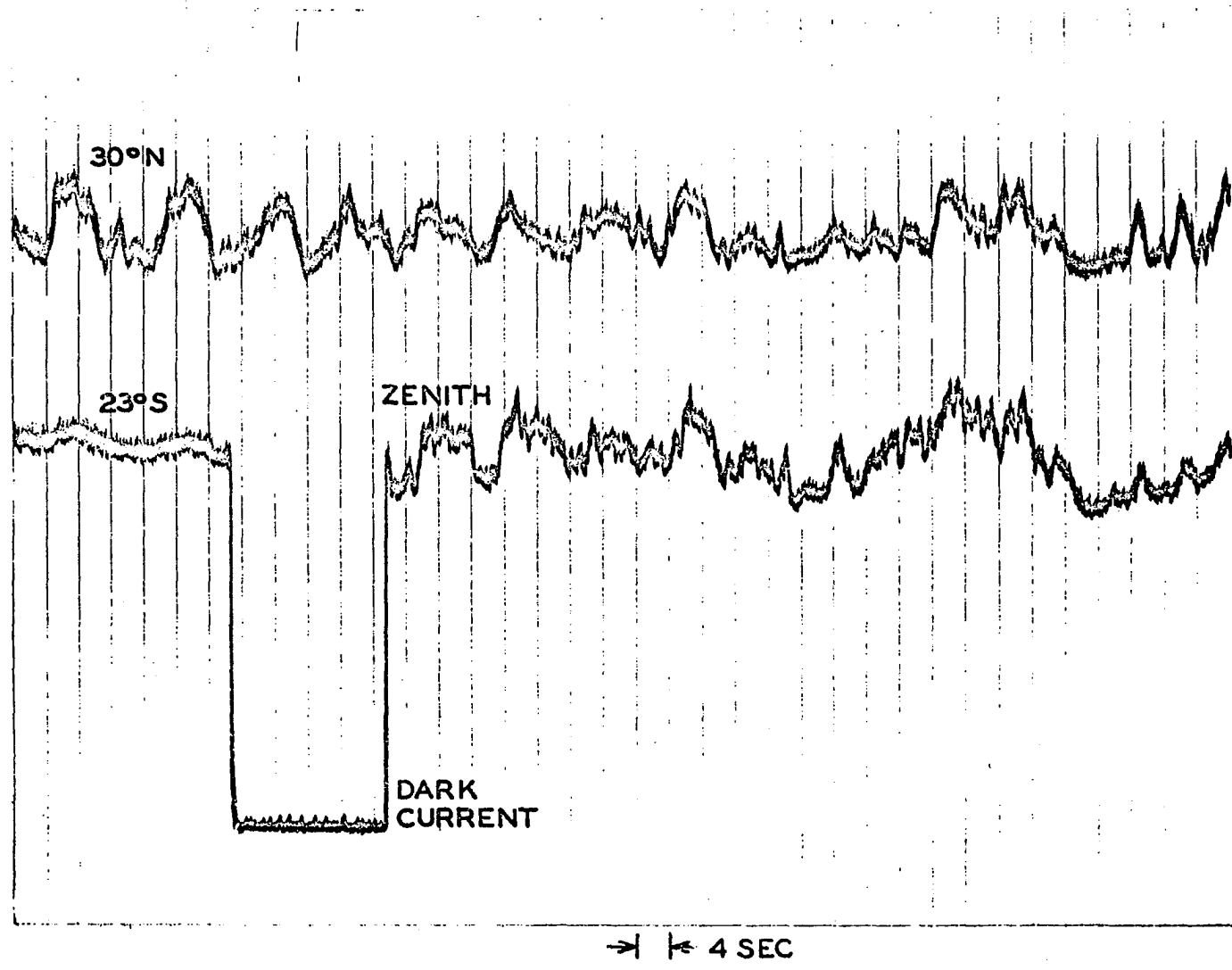


Figure 4.10 Photometer traces at 0341 showing the waves to travel to the zenith from the north, but to lose intensity farther south.

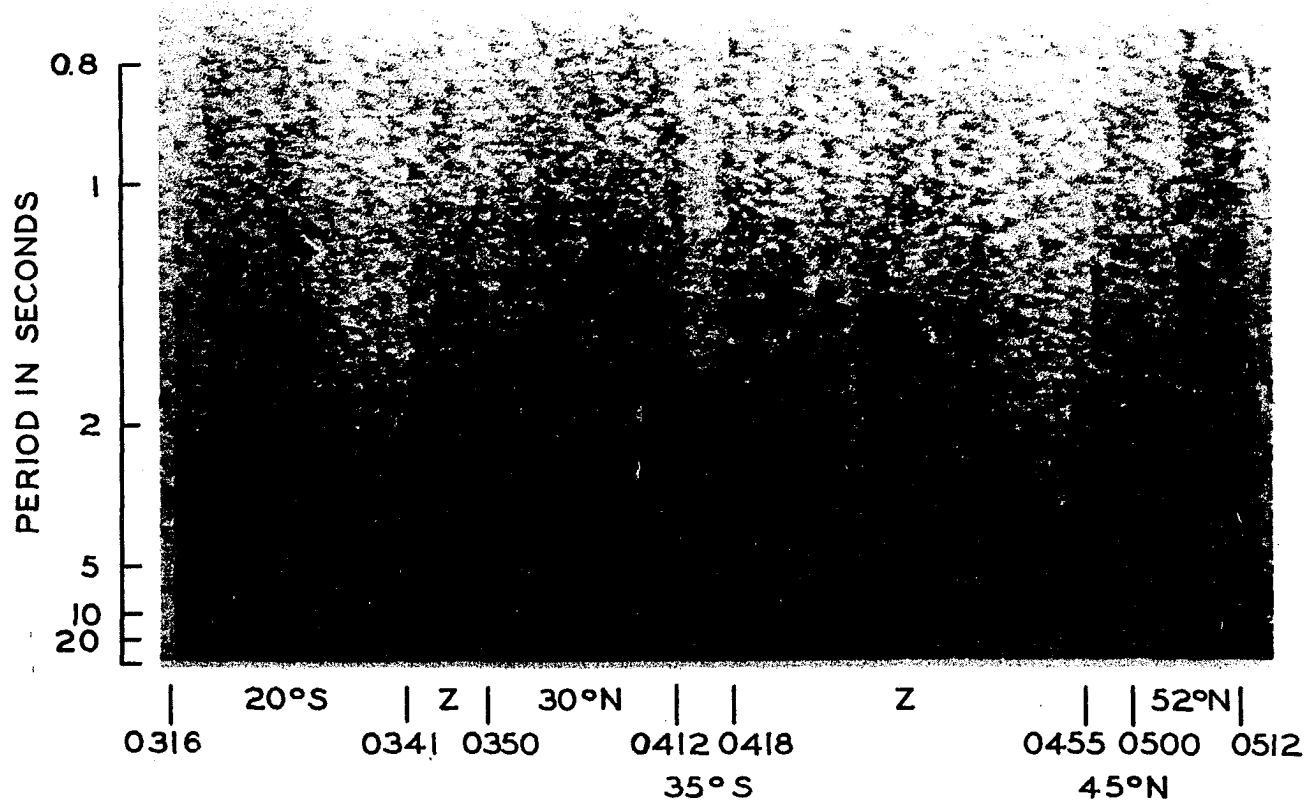


Figure 4.11 A "sonagram" showing the frequency spectrum of the fast auroral waves of November 1, 1964. The photometer was directed at a number of places during the display.

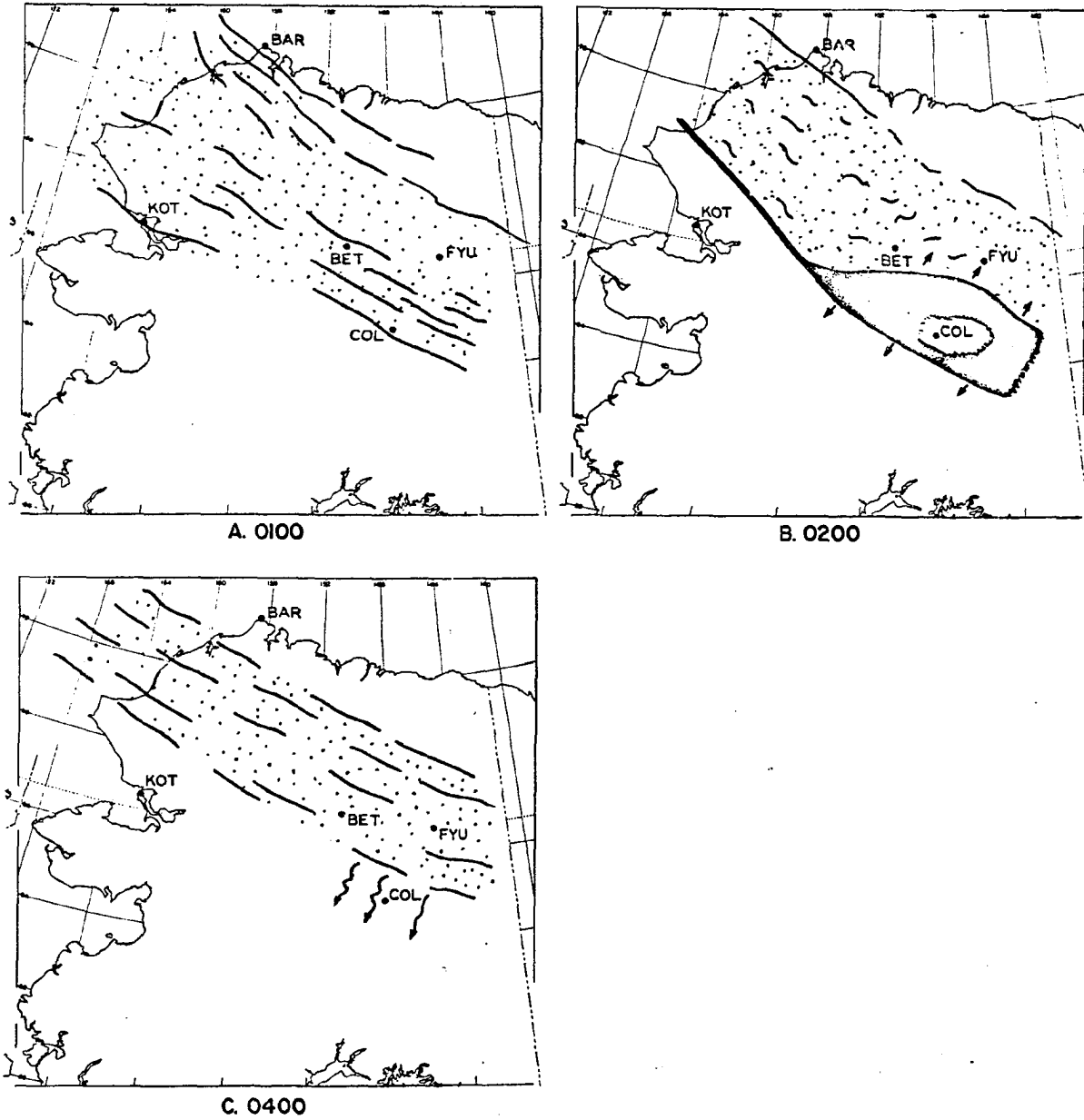


Figure 4.12 The distribution of auroras over Alaska at several epochs during the November 1, 1964 display. Arrows near a feature indicate it to be moving; wavy arrows indicate fast auroral waves; dots indicate diffuseness.

Distribution of auroras over Alaska: November 1, 1964

A diffuse envelope containing several E-W arcs was over northern Alaska at 0100 (Fig. 4.12a). Prior to 0200 the southern edge of the envelope moved southward and brightened to form an arc. This brightened and rapidly expanded, indicating a substorm onset over College (Fig. 4.12 b). When the intensity decreased the sky was covered by a diffuse envelope some 700 km in meridional extent (not shown). The envelope contracted from both the north and the south and waves were detected at College at 0330, apparently coming from the envelope. As it contracted northward, so did the wave propagation path. The envelope contained some E-W forms (Fig. 4.12c).

4.3 January 28, 1965Abstract

A fast auroral wave display was seen between 0130 and 0300. Evidence from all-sky cameras indicated that there was a substorm at 0015 over northern Alaska which was followed by the southward spread of a diffuse envelope. This contained weak pulsating forms and was traversed by fast auroral waves having velocities of 50-100 km/sec. The waves only reached the southern edge of the envelope; as it contracted to the north so did the region in which waves were detectable. The time that the waves were seen corresponded to the recovery phase of the substorm negative bay.

The Observation

This night was preceded by four in which the aurora never reached the College zenith (from the north). For more than half of this

night the auroral activity was confined to an arc low on the northern horizon. At 0100 a brightening which extended slightly southward occurred in the western end of the arc and drifted eastward at an average velocity of 330 m/s; it disappeared after 0112. Between 0115 and 0145 the southern boundary of the arc spread southward at about 100 m/s until the sky between  $45^{\circ}\text{S}$  and  $60^{\circ}\text{N}$  of the zenith was covered by diffuse forms. The diffuse forms were pulsating, and through the entire display passed very weak southward-traveling waves.

The display was monitored by both an image orthicon television system having a  $14^{\circ}$  field of view and a photometer (Type II, Sec. 3.1) having four fields of view, each  $1\ 1/2^{\circ}$  diameter, on a  $6^{\circ}$  diameter circle. Neither instrument was ideal for the task of sorting out in situ pulsations from waves. The waves had a photometric meridional extent of 50-200 km, greatly exceeding the television field of view of 25 km in the zenith, and their leading and trailing edges were not sharply defined on the television films, making these useless for velocity estimates. In the case of the photometer, the fields were too close together, resulting in very small time separation between fields. The in situ pulsations added a complication because their photometer traces are the same as those for infinitely-fast moving waves. From some of the better photometer records it was possible to determine that the waves traveled at 50-100 km/sec.

From both the photometer and television data it appeared that the waves only reached the southern edge of the diffuse envelope because as the latter weakened and contracted to the north through the fields of view, so the detection of waves ceased.

The College magnetogram H trace and  $\lambda 4278$  zenith photometer trace are shown in Figs. 4.1 and 4.2 respectively.

Distribution of auroras over Alaska: January 28, 1965

A westward traveling surge was in the Barrow vicinity at 0015. Its appearance would seem to indicate a substorm onset farther east (Fig. 4.13a). From Ft. Yukon however, the evidence was for only a mild breakup in the north. The College H trace was slightly positive and did not go negative until 0030. Consulting Figure 1.1 one can see that this behavior may agree with the Akasofu et al picture because at low latitude the H trace can be positive even after the surge has crossed the meridian.

At 0030 (not shown) the sky north of Ft. Yukon was covered by a diffuse envelope; within this were several bright forms. The envelope spread southward and passed over College at about 0130 (Fig. 4.13b) and was seen there to be traversed by fast auroral waves.

Later the envelope contracted back over College. At 0500 only a diffuse arc was evident some 200 km north of Ft. Yukon.

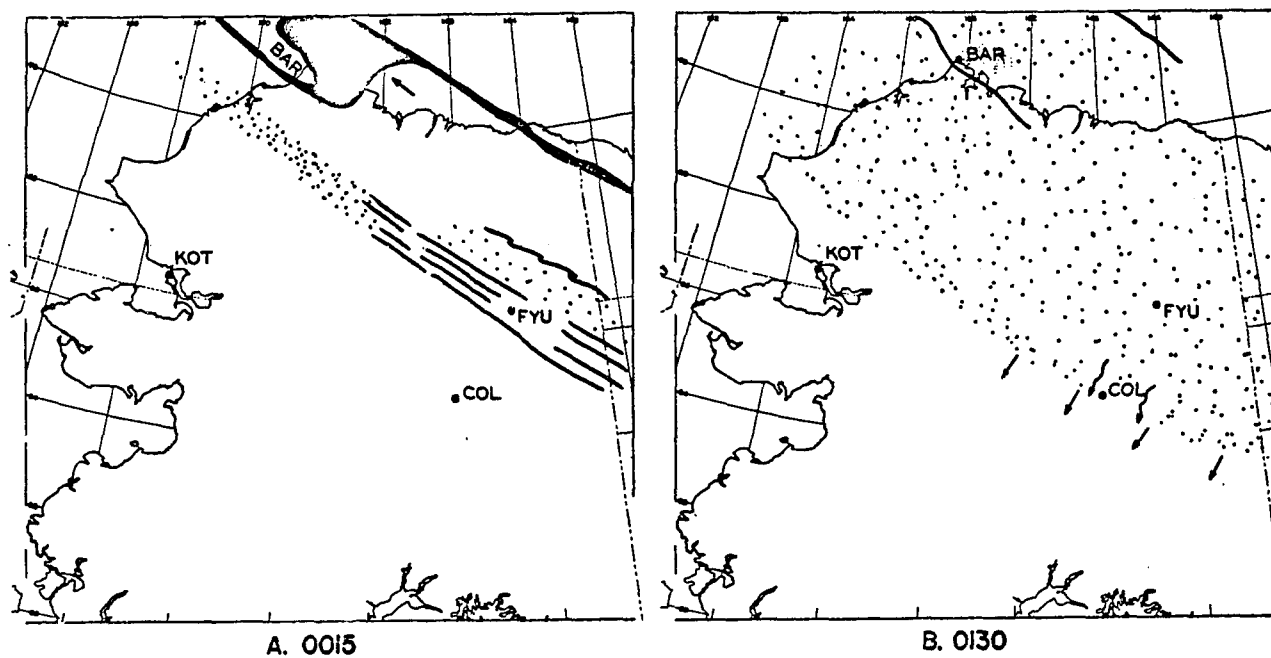


Figure 4.13 The distribution of auroras over Alaska at two epochs during the January 28, 1965, display. Arrows near a feature indicate it to be moving; wavy arrows indicate fast auroral waves; dots indicate diffuseness.

4.4 December 22, 1965

Abstract

Fast auroral waves were recorded from 0225 until shortly after 0245. The display followed a substorm onset at 0100 in the northernmost of two arcs that stretched across northern Alaska. An envelope of diffuse features spread south to cover most of northern Alaska by 0130. The waves were seen following the recovery of the substorm negative bay but the display was apparently interrupted by another substorm onset. This led to the formation of eastward drifting patches.

The photometer records confirmed visual impressions that the waves only traveled a short distance ( $< 50$  km) initially. As the display progressed, the waves were recorded to travel in excess of 100 km. The waves were relatively slow, having velocities of 50-75 km/sec. A significant finding, made possible by the use of the new wave photometer, was that the waves did not originate in the northern arc accompanying the display. For example, at 0245, progressing southward along the meridian, there was first a bright arc, then a low intensity region almost free of temporal variations, then a pulsating aurora region, and finally the wave propagation path.

The Observation

This wave display differed from what we have come to think of as a "typical" display in that waves were seen going overhead

while a quite active auroral display (IBC II-III) took place about  $60^{\circ}\text{N}$  of the zenith. Visually, the waves gave the impression of having a limited east-west extent ( $\sim 50$  km) and each one did not seem to propagate very far.

The wave photometer was not operating until 0225, some ten minutes after the first visual observation of the waves. At this time the patches that had been overhead at 0200 had disappeared (see the all-sky camera sequence in Fig. 4.14) so that the majority of the luminosity variations can be ascribed to waves. The wave photometer records at this time (Fig. 4.15a) show the fields to be seeing fluctuations of similar high frequency. There do not seem to be any good examples of waves traveling a full 50 km from one field to the next.

At 0234, however, the waves had started to travel at least 100 km and influence all three southernmost fields while the northernmost field showed slow variations probably due to pulsating patches (Fig. 4.15b). The southern three fields showed many examples of fine structure carry-over, some of which have been marked alphabetically and are associated with velocities of 50-60 km/sec.

At 0245 only the two southernmost fields showed any similarities (Fig. 4.15c). Field 1 was almost undisturbed (although its IP21 anode current was a factor of 10 higher than the night sky level) while field 2 was greatly disturbed, possibly as the result of pulsating features. In general, most of the similarities between

fields 3 and 4 are in gross structure only, but waves A-C are examples of fine structure carry-over; the associated velocities are respectively 60, 75 and 70 km/sec. From 0200 to 0240 the southward shift of the wave path may be related to the southward shift of the northern arc.

At 0255 a visual observation revealed the presence of both pulsating patches and waves which resulted in four dissimilar traces from the wave photometer. By 0304 a diffuse envelope covered the sky down to about  $80^{\circ}\text{S}$  of the zenith (see also Fig. 4.14) and no waves could be seen. From this time until after 0500 pulsating patches and diffuse features covered most of the sky and caused the fluctuations seen on the  $\lambda 4278$  zenith photometer trace (Fig. 4.2).

The magnetogram for this night (Fig. 4.1) shows undisturbed traces until 0030. During the time that waves were seen there commenced a negative bay in H that lasted until shortly after 0400.

The meridian-scanning photometer showed that at 0240 the northern arc was extremely strong in  $\lambda 5577$  and contained measureable  $H_{\beta}$ .

#### Distribution of auroras over Alaska: December 22, 1965

At 0100 a breakup, indicating a substorm onset, occurred in the more northern of two main arcs that stretched across Alaska (Fig. 4.16a). By 0130 diffuse features covered most of northern Alaska. Waves were recorded at College from 0225 until shortly after 0245. Prior to 0230, at a time of almost complete recovery of the negative bay, a bright arc formed 200 km north of College.

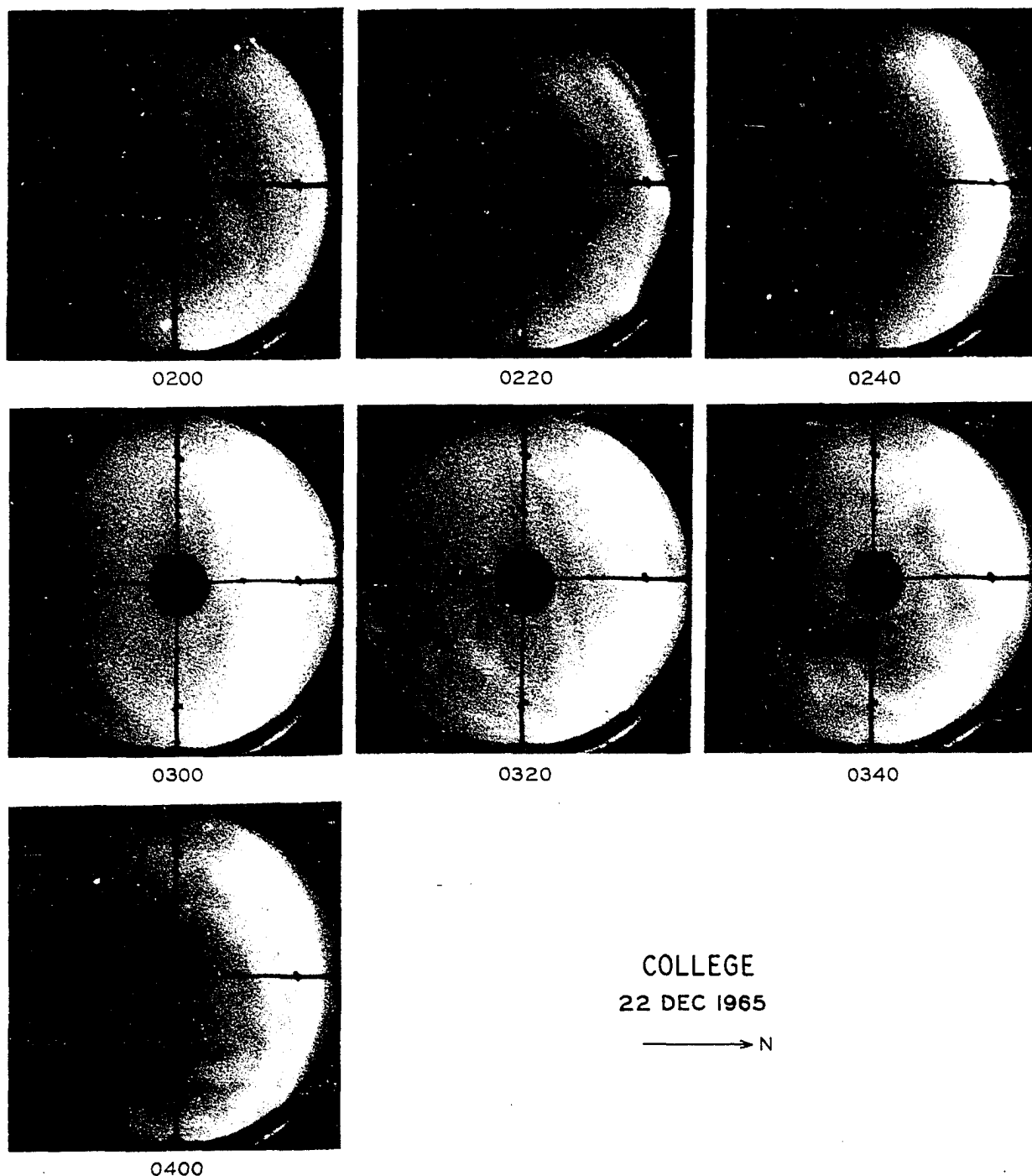


Figure 4.14 A series of all-sky camera pictures covering part of the December 22, 1965, auroral display. The quality of the wave photometer traces was best around 0240. The evidence for patches before and after this time is quite clear.

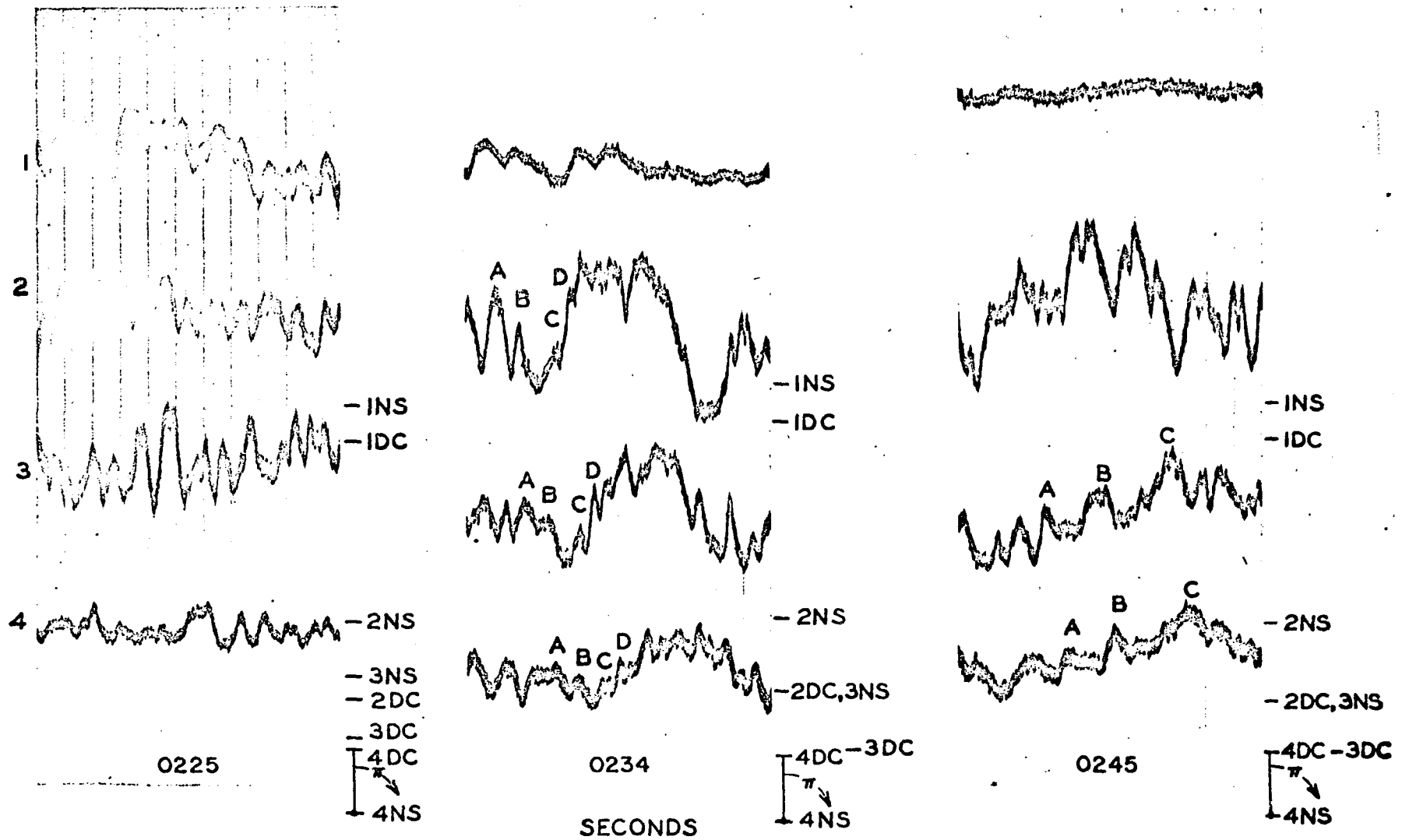


Figure 4.15 Wave photometer records for December 22, 1965. 'NS' and 'DC' respectively refer to night sky and dark current deflections (A) 0225, wave motions were seen visually but the waves must have traveled less than 50 km. (B) 0234, waves can be seen to cross the 3 southernmost fields. The slow variations on channel 1 are probably due to pulsating patches. Waves A-D traveled at 50-60 km/sec. (C) 0245, channel 3 and 4 only were traversed by waves. Channel 1 indicates a steady signal 10 times the night sky value while channel 2 is greatly disturbed, possibly the result of pulsating auroras.

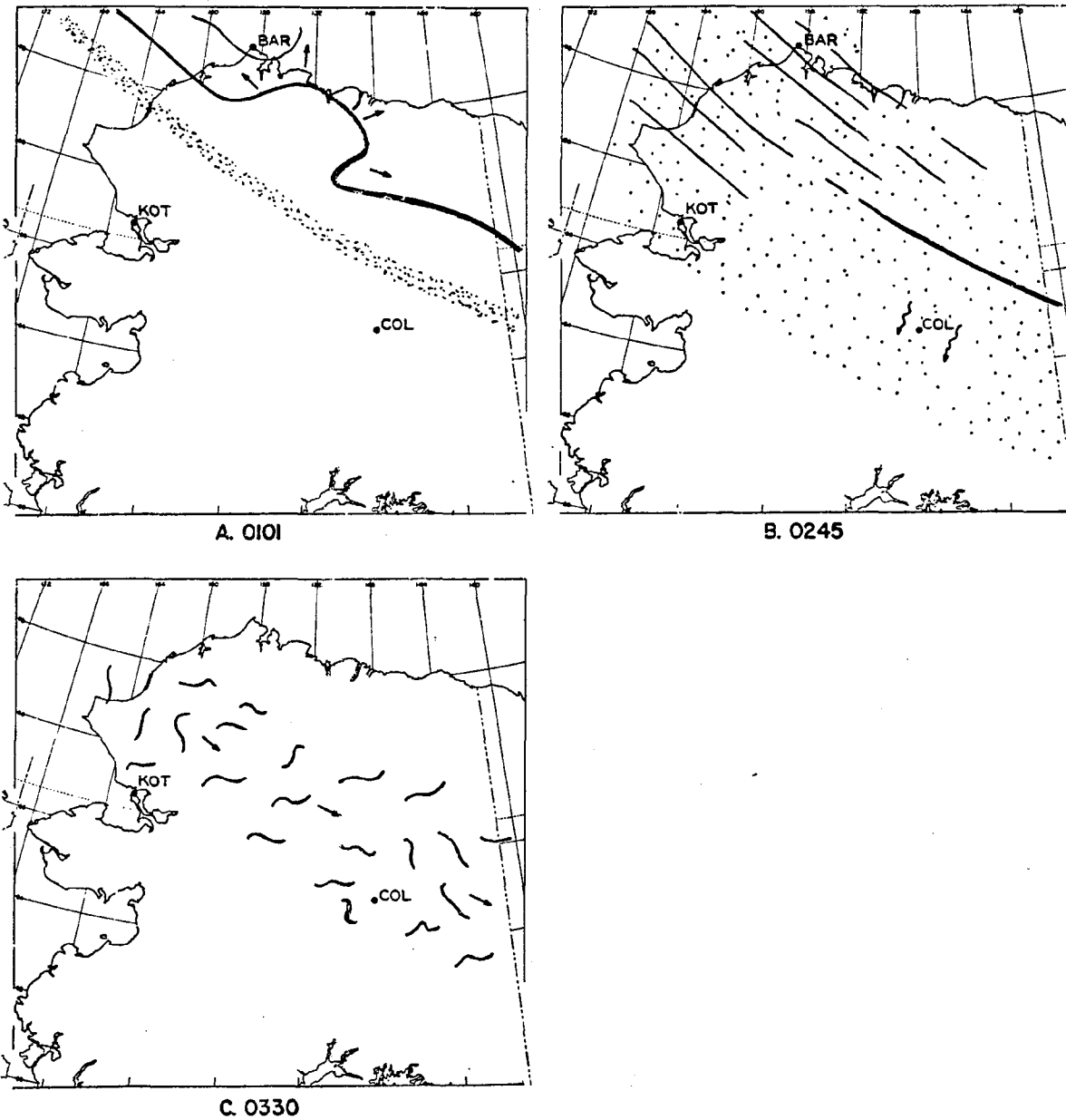


Figure 4.16 The distribution of auroras over Alaska at several epochs during the December 22, 1965, display. Arrows near a feature indicate it to be moving; wavy arrows indicate fast auroral waves; dots indicate diffuseness.

The Barrow film showed a poleward expansion to take place between 0234 and 0241 reaching the zenith at 0239. The expansive phase seen to the north from College did not appear to commence until 0249. The time difference may place the substorm onset closer to Barrow's meridian. The distribution at 0245 (Fig. 4.16b) shows a diffuse envelope, a bright arc north from College and weaker arcs near Barrow. The College H trace at this time was on a sharp negative excursion.

After 0250 the H trace showed a gradual recovery and patches appeared; Fig. 4.16c for 0330 shows them to cover a west-east band across Alaska. Barrow became cloud covered after 0250 but, even so, an apparent poleward expansion could be discerned at 0345. The College H trace went sharply negative at about this time but no change of the patches was evident.

By 0430 several arcs were 200 km north of College; a few patches were further south. Gradually these arcs moved north and were 300 km distant at twilight, ~ 0720.

#### 4.5 January 26, 1966

##### Abstract

Fast auroral waves were recorded quite strongly from 0324 until about 0430 and then weakly from about 0456 until 0515. Pulsating auroras caused sporadic contamination of the records. A substorm onset occurred just north of College at 0200. Following this onset a diffuse envelope containing several weak patches migrated southward,

stopping some 100 km south of College at 0245. This slowly weakened leaving just an arc to the north. Waves were first detected at 0324. Eastward drifting patches appeared south of the arc at 0515, about the time that waves were last seen. They were probably associated with a substorm to the far west.

At the start of the wave display only the two northern fields recorded waves. As the display proceeded the southern fields progressively detected waves also. In other words, the southern edge of the wave propagation path progressed southwards; its velocity of progression being about 100 m/sec. During the second wave period (0456-0515) only the two northern fields detected waves.

The waves were measured to have velocities ranging from 75 to 200 km/sec with 100-150 km/sec being most common. Waves that propagated over the entire 150 km monitored by the photometer and that were suitable for velocity measurements were not common. Among the examples found, two showed a slight slowing down and one showed first a slight speeding up, then a slowing down.

#### The Observation

At 1930 a quiet arc was seen to the north. It developed folds and brightened at 2240 but at 0000 had reverted to its former state. At 0200 diffuse features moved south through the zenith and brightened, this being evident on the College  $\lambda 4278$  zenith photometer record (Fig. 4.2). The southward move was accompanied by the start of a large negative bay of the College magnetogram H trace (Fig. 4.1).

At 0230 east-west aligned arc-like features were seen to be rapidly pulsating (about 1 cps). This type of behavior lasted until about 0320; the wave photometer records at 0303 are shown in Fig. 4.17a. The northern field shows slow pulsations, fields 2 and 3 show rapid variations, and field 4 shows very little except some 2 cps tape recorder noise. There is no convincing evidence for fast auroral waves.

Fast auroral waves were seen by eye at 0330 but subsequent inspection of the wave photometer records showed that waves traversed the two northern fields as early as 0324 (Fig. 4.17b). Some of the gross features of the waves seen by these fields carried over to field 3 but were much weaker. Good carry-over of fine structure was evident between 1 and 2 with wave A being noteworthy. Measuring from the start of the recorded pulses wave A was found to have a velocity of 300 km/sec. However, it is possible that the left side spike of A on channel 2 may be another wave that started between fields 1 and 2. Other waves were found to have traveled at  $\sim 100$  km/sec.

Figure 4.17c shows the wave photometer records for 0330 with no gain adjustment in the interim from 0324. Significantly, field 3 had started to strongly record the passage of waves, these having velocities in the vicinity of 125 km/sec. Field 4 poses a problem as yet unsolved. It shows small slow variations similar to the other fields but having the wrong phase relationship to them to be

caused by waves. A tentative explanation is that field 4 was affected by reflections in the plastic dome over the wave photometer.

By 0340 waves were crossing all fields (Fig. 4.18a) showing that, in the course of twenty minutes, the path of propagation of the waves had shifted 100 km to the south. A similar shift was evident in the arcs over Ft. Yukon, thus indicating that the wave path and the arcs move together. Figure 4.18a reveals gross structure carry-over from fields 1 to 4 as well as a great deal of fine structure carry-over. Wave A is a good example of the latter.

At 0356 (Fig. 4.18b) the rate of fluctuations seen by the wave photometer was greater than previously. Possibly some fluctuations were due to weak patches seen near the zenith during a brief visual observation at 0347. Many, however, were directly ascribable to the passage of waves across the sky. Here a good example is wave A. As seen in field 1 it appeared as a single peak but as it progressed southward two peaks could be seen. The first wave component was faster than the second and both showed initially (before field 3) a positive acceleration and then (after field 3) a negative acceleration. The two components had average velocities of 140 and 110 km/sec but between successive fields their velocities can be listed: 1-2,  $140 \pm 10$  and  $90 \pm 10$  km/sec; 2-3,  $170 \pm 25$  and  $125 \pm 10$  km/sec; 3-4  $130 \pm 10$  and  $110 \pm 10$  km/sec.

According to visual observations all patches had disappeared by 0414. The wave photometer record at this time (Fig. 4.18c) showed the passage of strong waves across all four fields (during transcription from magnetic tape to paper chart the gains had to be reduced to prevent the traces crossing in a confusing fashion). Fine structure changes between fields of view are evident. The best example of fine structure carry-over, in this case from fields 2 to 4, is wave A with successive velocities 140 and 100 km/sec.

At 0420 (Fig. 4.19a) waves were less frequent and weaker and although wave A crossed all four fields, other waves at this time crossed only two fields. Other spikes are ascribable to either in situ pulsations or waves crossing only one field. Wave A as seen by fields 2 and 3 had two prominent components; the velocities of these were 125 and 200 km/sec respectively. The other waves had similar velocities.

At 0435 visual inspection of the sky revealed no waves. The wave photometer traces for this time (not shown) showed asynchronous pulsations on the four channels that were probably caused by pulsating patches. However, from about 0456 until 0515, traces 1 and 2 showed many similarities which, when examined closely, were concluded to be due to the passage of weak waves. Waves around 0500 (Fig. 4.19b) had velocities from 70-125 km/sec. After 0515 all variations were apparently due to in situ patches.

At 0535 the all-sky camera records showed patches to be forming off the northern arc and by 0600 these were well defined, oddly shaped (as is usual), brighter, and apparently drifting eastward. Figure 4.2 shows them to have been pulsing quite strongly, although many of the variations were no doubt due to patches drifting through the field of view.

The all-sky cameras from both College and Ft. Yukon showed that the northern arc seen from College was not homogeneous, as appeared visually, but rather composed of numerous thin arcs over Ft. Yukon.

The frequency-time display of telluric current activity (Heacock and Hessler, 1966) showed high frequencies up to the instrumental limit (0.2 cps) to occur from just prior to 0200 until 0430. From the preceding account we know that this period corresponds to that of visual overhead auroras whether they were diffuse features, patches, or fast waves. It may be significant that only fast waves were present for the last 15-20 minutes of the above period and so they were possibly related to telluric current activity.

Distribution of auroras over Alaska: January 26, 1966

On several occasions in the evening active auroras reached as far south as the College zenith. At 0100 there was a broad diffuse arc some 200 km north of College. This slowly brightened, moved 100 km southward and then suddenly broadened as if it was

the center of a substorm onset (Fig. 4.20a). The H trace at this time was on a sharp negative excursion. To the west was a weak diffuse envelope containing some patches discernible near Kotzebue and some arc-like forms near Barrow. After the onset a diffuse envelope migrated south and appeared to stop at 0245 (Fig. 4.20b).

At 0230 an unusual N-S folded feature appeared in the Barrow eastern sky and traveled westward, much as would a westward surge. Possibly it was a type of surge and was associated with the substorm onset at College described above. It reached the Barrow zenith at 0234 and was traveling there at approximately 400 m/sec.

Apart from the above surge, a diffuse envelope containing some patches remained until about 0345, when there was a broad mainly-diffuse arc north from College. South of the arc were several small, weak patches but these soon disappeared. The negative bay had recovered by this time. Waves were seen from 0324 until 0430 and from 0456 until 0515. The distribution at 0420 appears in Fig. 4.20c.

From about 0515 eastward drifting patches appeared south of the arc, many appearing to be attached to it. As time progressed patches could be seen farther south; the distribution at 0620 appears in Fig. 4.20d. As seen on the all-sky camera films the patches were quite bright (cf. zenith photometer trace, Fig. 4.2) and had much detailed structure. They were visible until the dawn continuum became too bright at about 0700.

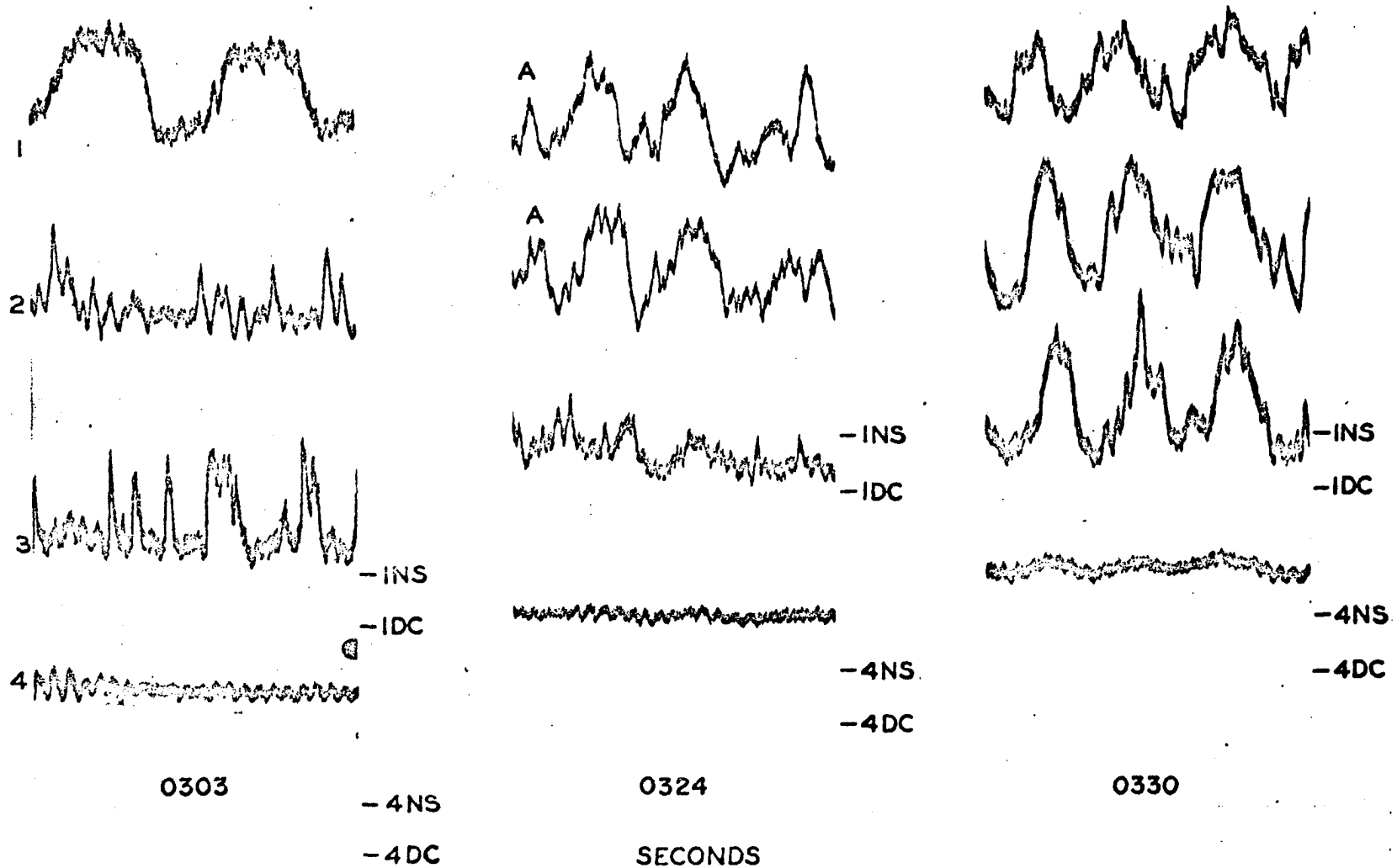


Figure 4.17 Wave photometer records for January 26, 1966. 'NS' and 'DC' respectively refer to night sky and dark current deflections. (A) 0303, fields 1-3 show various types of pulsations while 4 shows steady low intensity except for some 2 cps tape recorder noise. (B) 0324, fields 1 and 2 show convincing evidence for waves but these did not reach fields 3 and 4. Example A had a velocity of 150 km/sec. (C) 0330, the wave path reached south to include field 3 with 1 and 2. There were no gain changes between 0324 and 0330.

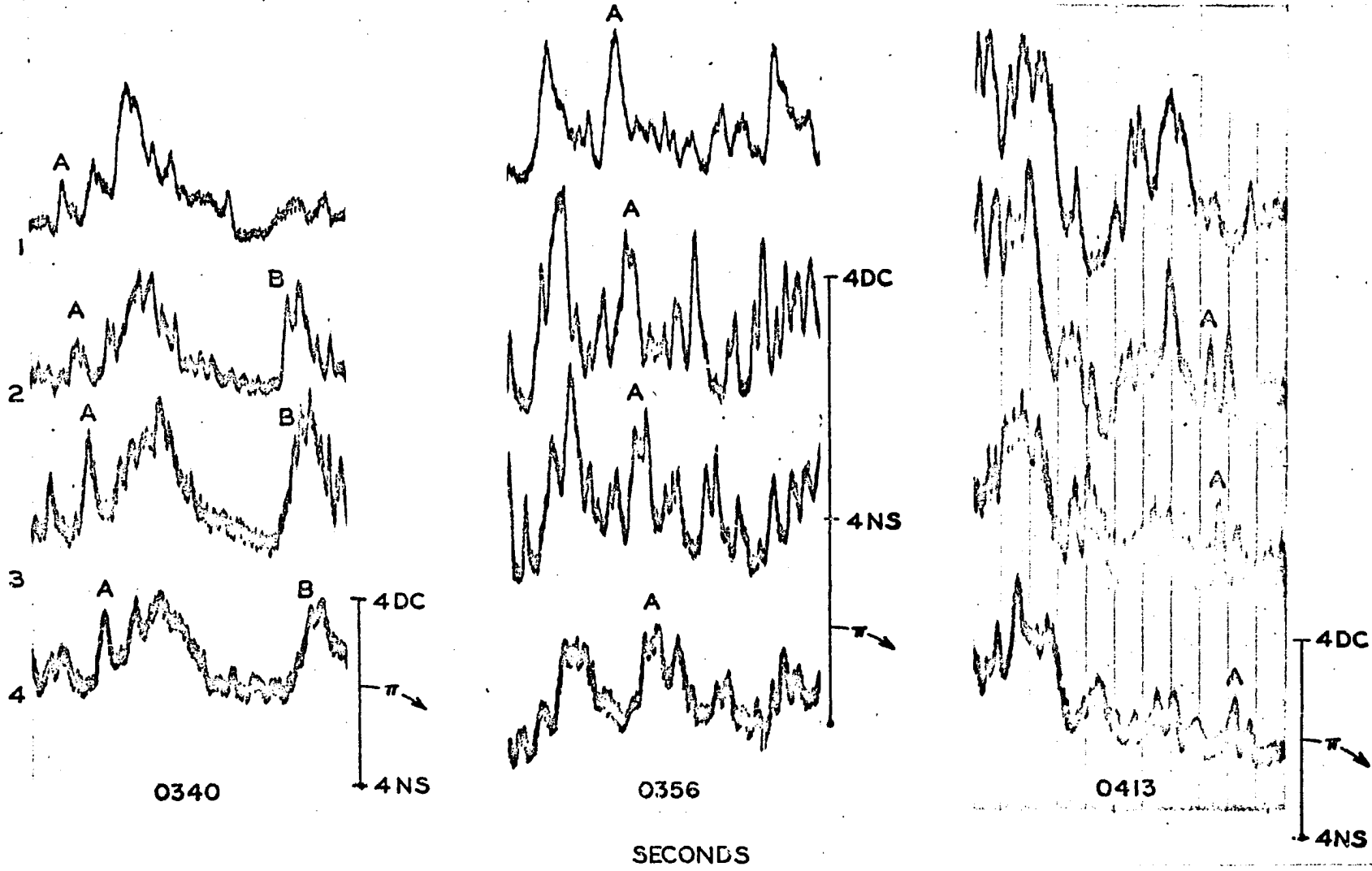


Figure 4.18 Wave photometer records for January 26, 1966. 'NS' and 'DC' respectively refer to night sky and dark current deflections. (A) 0340, the wave path had continued to spread south and included all fields of view. Wave A's velocities between the fields were 150, 150, and 100 km/sec respectively. Wave B had velocity 140 km/sec. (B) 0356, wave A had two components and shows how consecutive waves can have different velocities. (C) 0413, wave A traveled at 140 km/sec between fields 2 and 3 and 100 km/sec between 3 and 4.

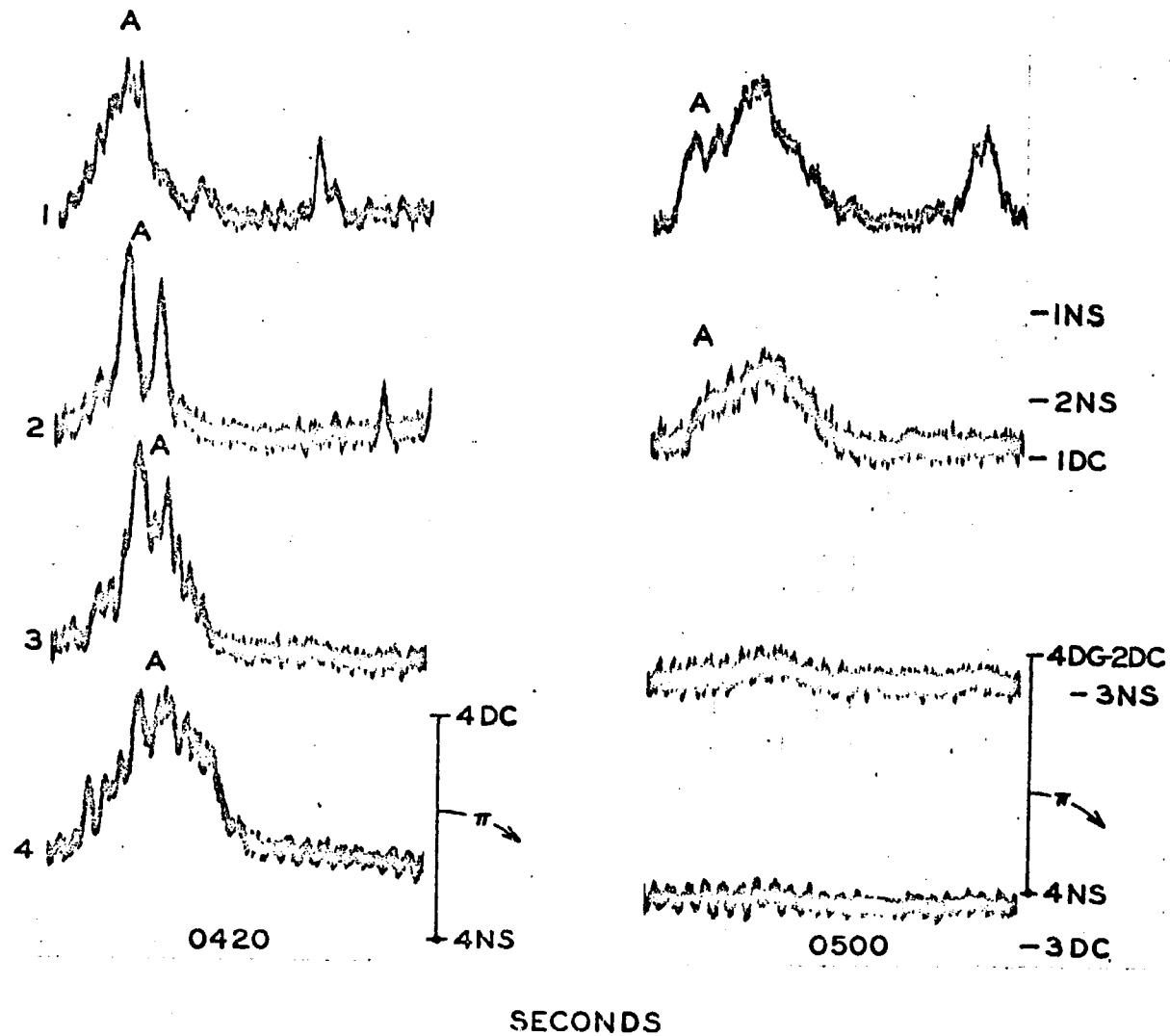


Figure 4.19 Wave photometer records for January 26, 1966. 'NS' and 'DC' respectively refer to night sky and dark current deflections. (A) 0420, the waves were less frequent than before. (B) 0500, infrequent waves crossed fields 1 and 2. The three southernmost fields are down to or below night sky levels (determined on another night).

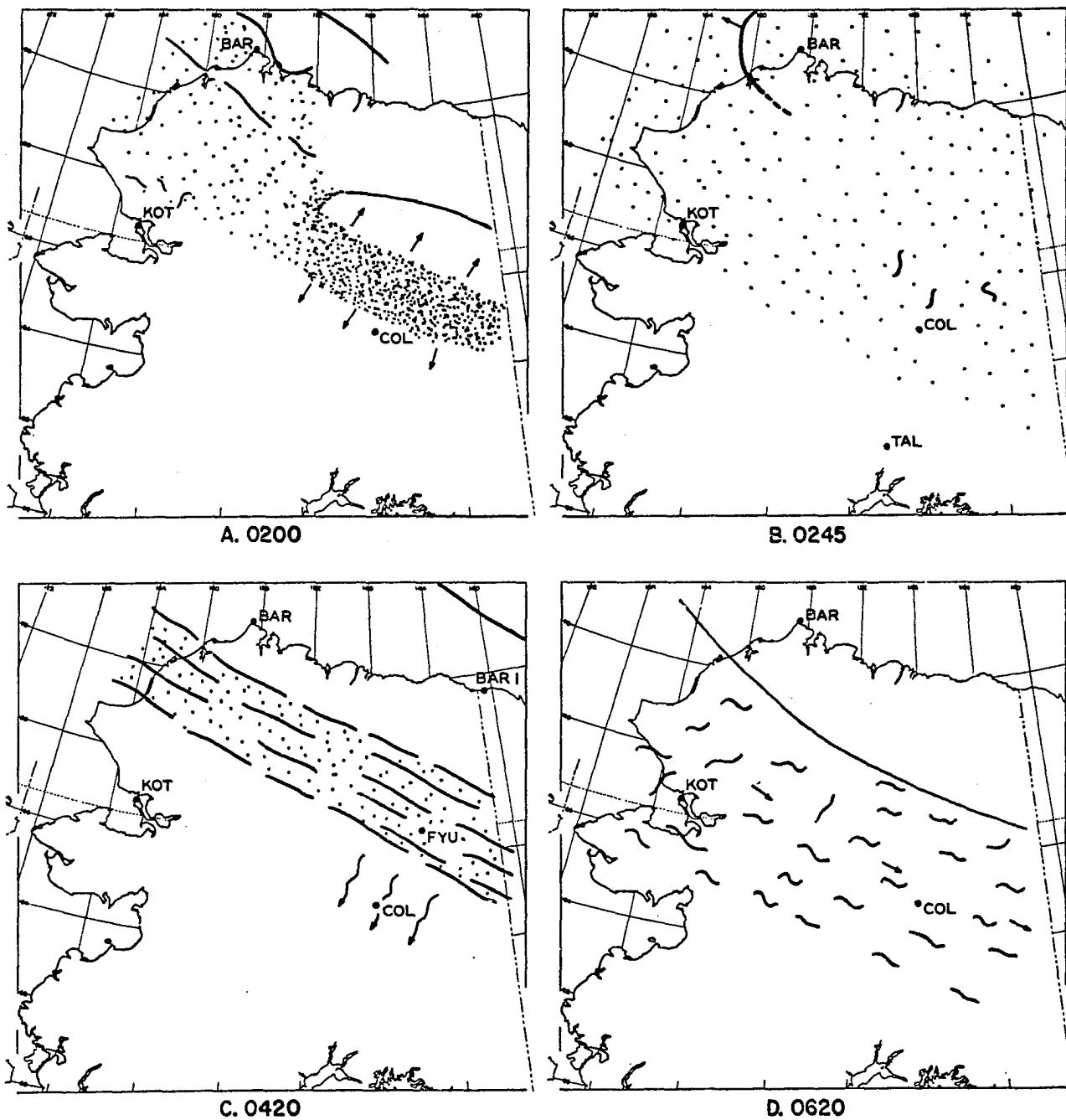


Figure 4.20 The distribution of auroras over Alaska at several epochs during the January 26, 1966 display. Arrows near a feature indicate it to be moving; wavy arrows indicate fast auroral waves; dots indicate diffuseness.

#### 4.6 March 16, 1966

##### Abstract

Fast auroral waves were recorded from 0214 until 0241. They were measured to have velocities in the range 40-100 km/sec. The wave propagation path had a N-S width slightly more than 100 km and migrated southward until it was beyond the photometer fields of view. A simple calculation showed the migration velocity to be about 100 m/sec. The display was preceded by a substorm onset that occurred at 0015 near Barrow. This was followed by the southward migration of a diffuse envelope that later weakened while an arc formed to the north of College. Waves were then recorded to pass over College.

##### The Observation

In a number of ways the auroral activity prior to the wave display was similar to that for the March 14, 1964, display. Consequently it was anticipated that a wave display would take place.

A weak arc first appeared low in the north at 2100 and developed several folds from 2240 to 0000. Diffuse features spread overhead from the north at 0030. These remained until 0200 and at 0210 fast auroral waves were seen visually.

On examining the College  $\lambda 4278$  zenith photometer (Fig. 4.2), low intensity pulsations can be seen from 0135 until 0200. The pulsations then stop for several minutes and slightly larger ones start and continue until 0230. It is tentatively suggested that

the former pulsations were associated with diffuse features and the latter with waves. A visual observation at 0247 showed that the waves had ceased. From several minutes after 0300 until twilight more pulsations occurred but these were probably due to diffuse and weak features which were also seen visually. During the time that waves were seen the magnetogram (Fig. 4.1) showed a small negative bay.

The wave photometer record for 0219 (Fig. 4.21a) showed that the waves recorded by the northern fields (2 and 3; 1 was inoperative) had lost a great deal of their intensity by the time they reached the southern field. Several minutes later at 0223 (Fig. 4.21b) the southern field was starting to detect the waves more strongly together with some of the fine structure seen by field 3.

Shortly after this, at 0228, the quality of the field 2 trace deteriorated, presumably the result of the wave propagation path shifting southwards (Fig. 4.21c). The fine structure carry-over from field 3 to 4 was very good with the waves having velocities around 50 km/sec. Another sample (Fig. 4.22a) at 0230 shows essentially the same behavior except perhaps the fine structure carry-over from 3 to 4 was even better. The waves had velocities of 60-70 km/sec.

At 0238 (Fig. 4.22b) field 4 was seeing wave-like variations while 3 was undisturbed and 2 almost undisturbed. It is suggested

that the wave propagation path had migrated farther southwards beyond field 3 and that field 2 was seeing some type of in situ pulsation.

Field 4 continued to see wave type fluctuations until 0241. After this it was essentially undisturbed until 0250. From this time on the three channels at first appeared to be influenced only by weak in situ pulsations, but closer investigation showed that there may also have been a slow (25-50 km/sec) wave motion (Fig. 4.22c).

Pairs of all-sky camera frames from College and Ft. Yukon for 0228, 0252 and 0310 are shown in Fig. 4.23. As was the case in the 26 January 1966 display, the homogeneous arc seen visually from College was actually numerous thin arcs over Ft. Yukon. Since the wave propagation path migrated southwards, the fact that the arcs over Ft. Yukon also moved southwards between the frames for 0228 and 0252 may be significant. The College meridian scanning photometer indicated a measureable amount of  $H_{\beta}$  in the arcs.

For a short period during the wave display the image orthicon television system was used. The direct view TV camera apparently lacked the sensitivity to detect the waves. The TV spectrograph, however, produced spectra of the waves from a four second integration time during which three waves crossed the field of view. The spectrum showed  $\lambda 6300$ , 5577, 5200, 4709, and 4278, together with a little  $H_{\beta}$ .

The frequency-time display of telluric current activity (Heacock and Hessler, 1966) showed frequencies higher than 0.10 cps to occur from 0015-0500 with peaks at 0030 and 0200. The former peak corresponds to the time at which diffuse features came overhead from the north, and the latter to the time when weak patches were overhead. If anything, the telluric current activity decreased during the wave display and increased again when weak patches were over most of the sky after 0300.

Distribution of auroras over Alaska: March 16, 1966

At 2303 an arc some 400 km north of College started to develop large folds that seemed to indicate a substorm onset. At Barrow an arc in the zenith brightened at 2308 and a westward surge appeared in the east at 2313. After coming to within 100 km of the Barrow meridian the surge stopped. Shortly after, it started moving again (Fig. 4.24a) and passed over Barrow at 2348.

Thirty minutes later another substorm was in progress, this time the onset appeared to be at Barrow. At least from the limited camera network, it seemed that the substorm propagated eastward as both a moving fold and a growing arc (Fig. 4.24b). Diffuse features were equatorward of the main discrete features.

After this time most of northern Alaska gradually became covered with diffuse features, occasionally some would brighten. Figure 4.24c shows the distribution at 0040, at which time the diffuse envelope was still spreading southward near College.

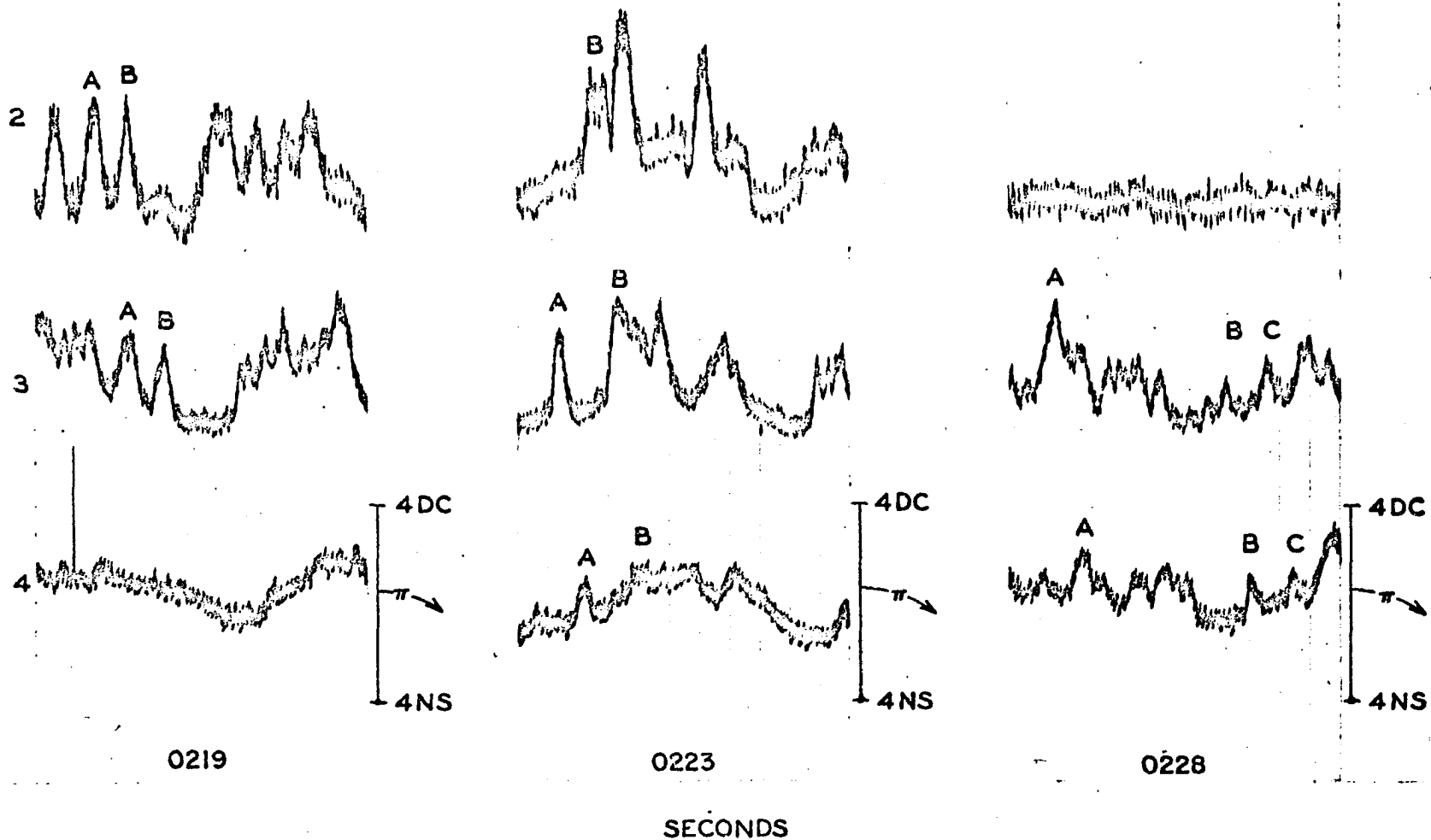


Figure 4.21 Wave photometer records for March 16, 1966. 'NS' and 'DC' respectively refer to night sky and dark current deflections. (A) 0219, channel 1 was inoperative. Waves crossing fields 2 and 3 seem to have lost intensity and fine structure by the time they reached 4. Waves A and B traveled at 40-45 km/sec. (B) 0223, the fine structure carry-over between fields 3 and 4 had improved. Wave A traveled at 60 km/sec and B at 60 km/sec between 2 and 3 and 75 km/sec between 3 and 4. (C) 0228, the signal from field 2 had deteriorated, possibly because the wave path had migrated southward. The waves shown had velocities around 50 km/sec.

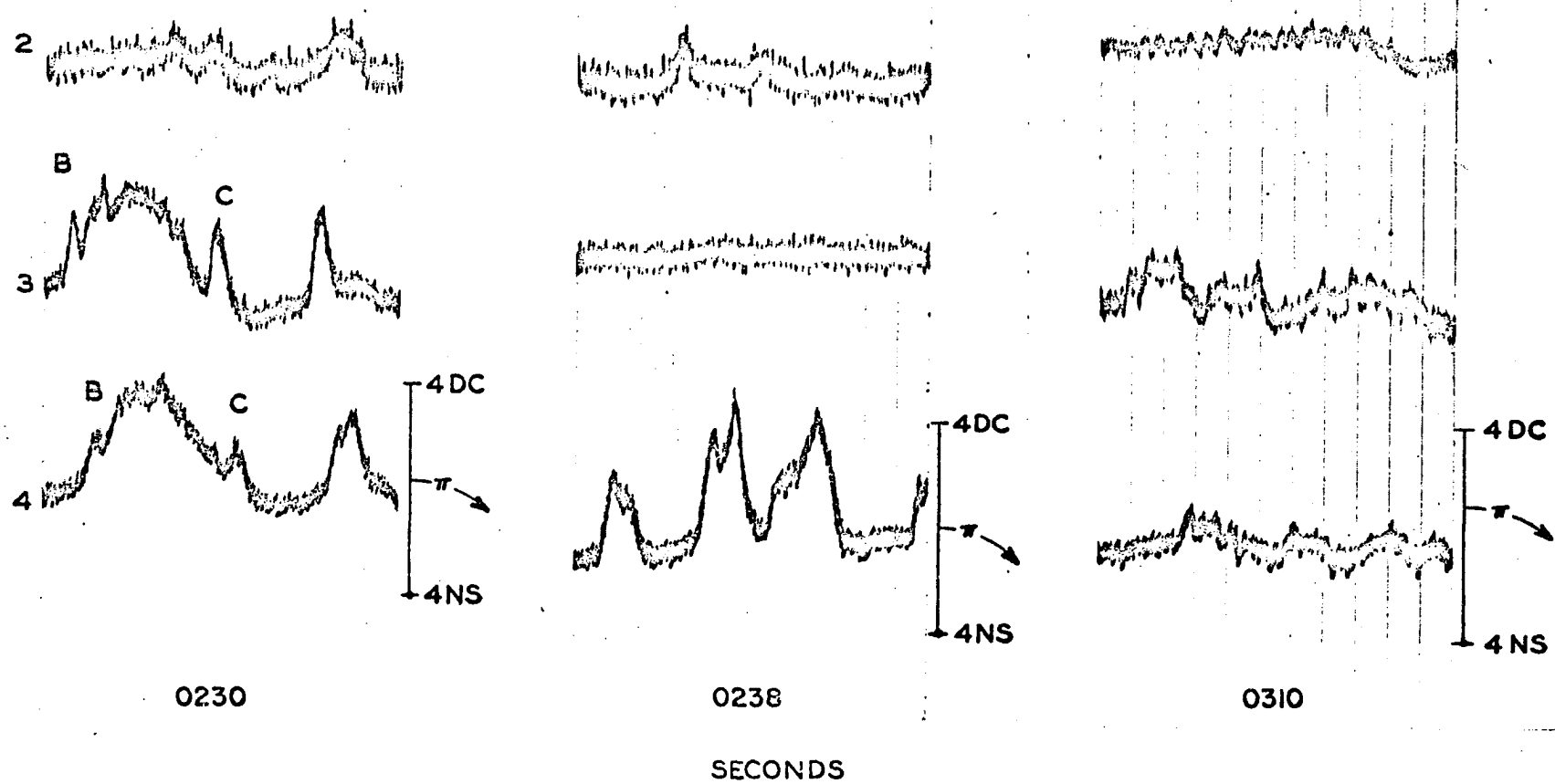


Figure 4.22 Wave photometer records for March 16, 1966. 'NS' and 'DC' respectively refer to night sky and dark current deflections. (A) 0230, the fine structure carry-over between fields 3 and 4 had improved. The waves marked had velocities of 60-70 km/sec. (B) 0238, only field 4 recorded wave-like variations. Field 2 may have recorded in situ pulsations. (C) 0310, there may have been a slow (25-50 km/sec) wave-like motion.

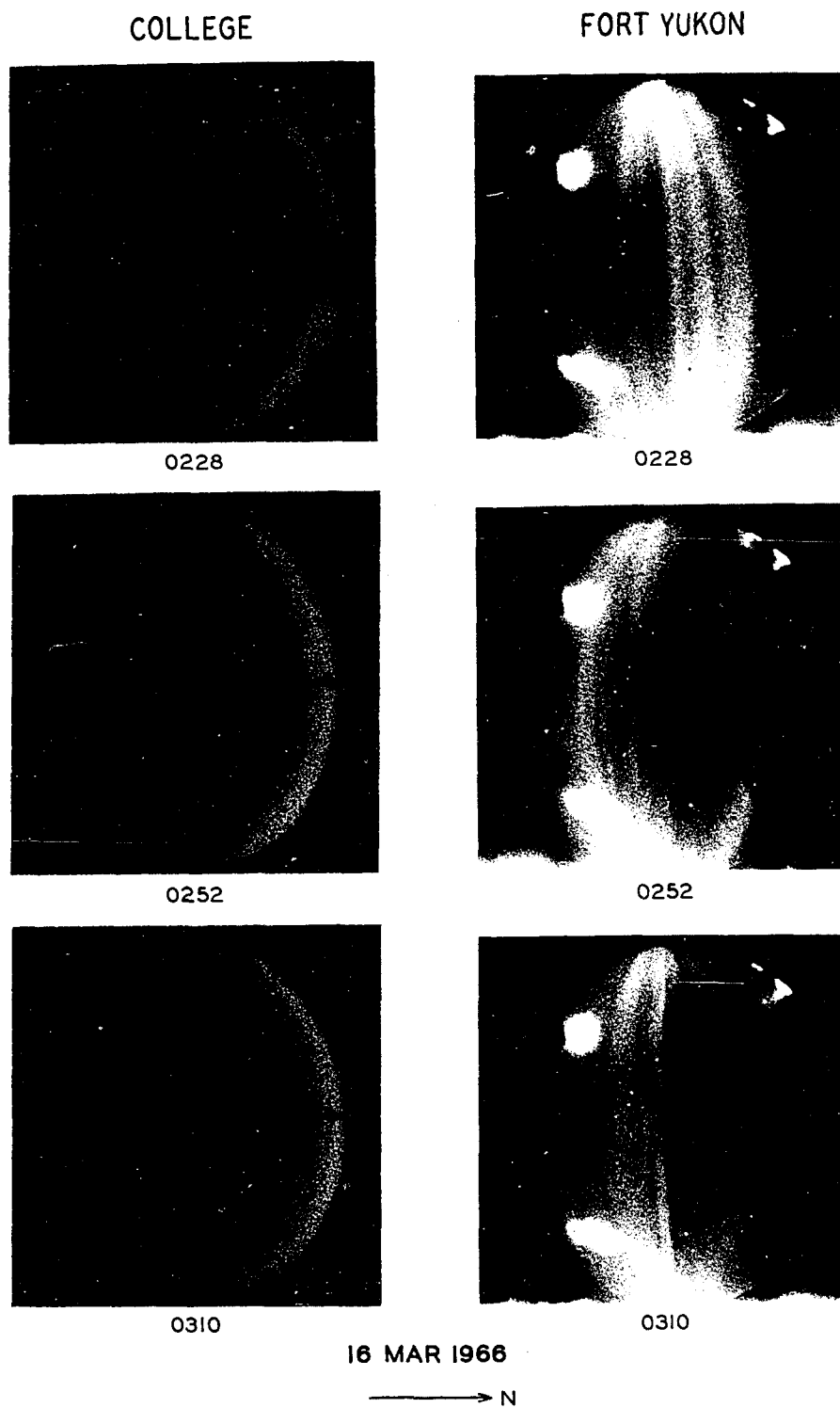


Figure 4.23 Pairs of all-sky camera frames from College and Ft. Yukon during and after the wave display. The "homogeneous" arc seen from College was, in fact, multiple arcs over Ft. Yukon.

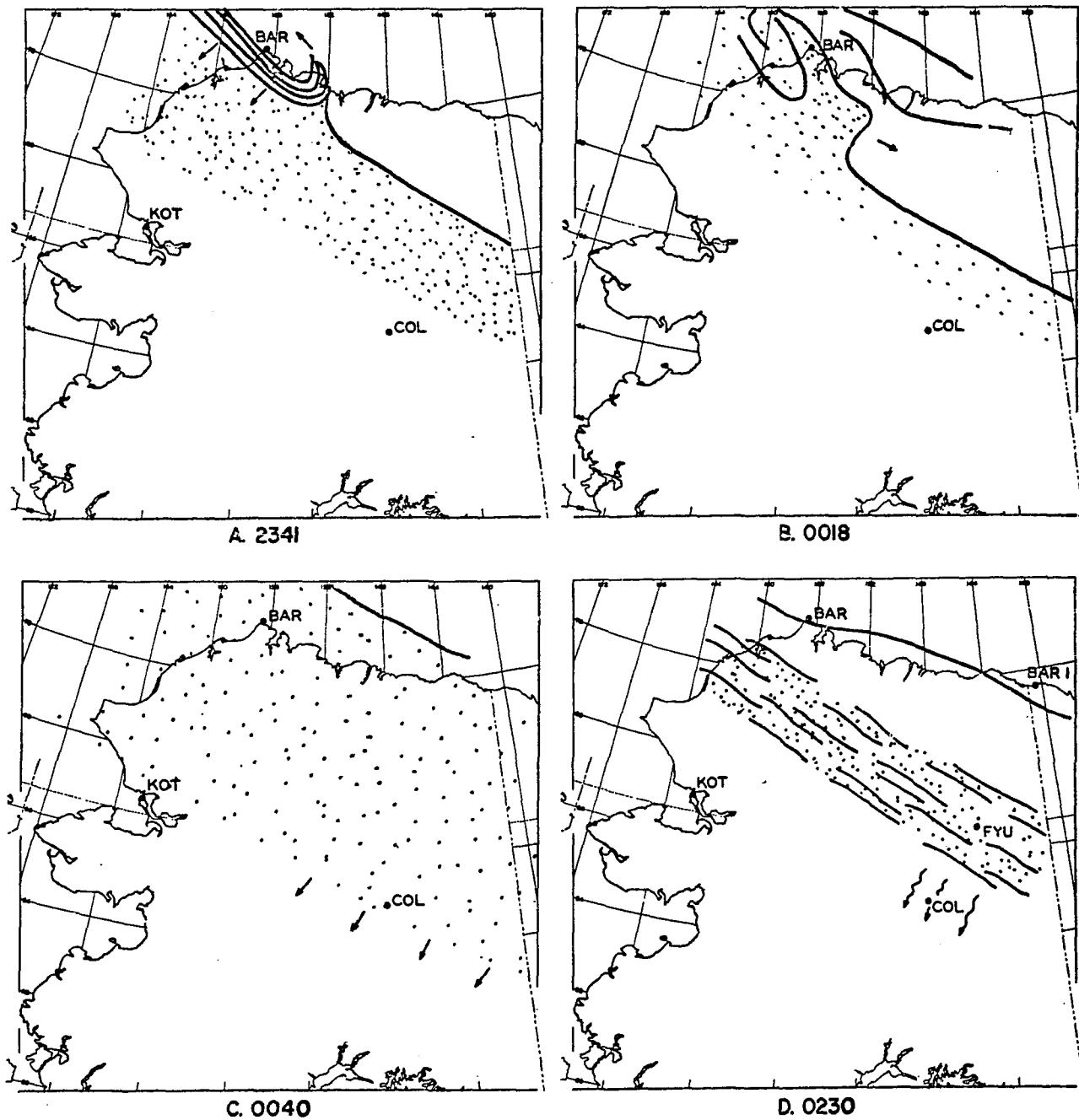


Figure 4.24 The distribution of auroras over Alaska at several epochs during the March 16, 1966 display. Arrows near a feature indicate it to be moving; wavy arrows indicate fast auroral waves; dots indicate diffuseness.

From about 0145 a diffuse arc started to form north of College while the weak, diffuse envelope remained farther south. The distribution at 0230, ignoring the very weak southern envelope, is shown in Fig. 4.24d. It consisted of a diffuse band across Alaska that contained some arc-like features. Waves were propagating over College at this time. In the far north was a discrete arc. The diffuse band or arc remained until the dawn continuum masked it at 0420.

#### 4.7 Nights when waves did not occur

Several nights will be briefly described in turn and then later compared as a whole with the nights when waves did occur.

##### November 30, 1965

The magnetogram registered quiet conditions prior to 0100 (Fig. 4.25). After 0130 the H trace went increasingly more negative, reaching a maximum depression at  $\sim$ 0240. The recovery from this point was ragged and took until 0600.

The all-sky camera revealed an arc in the low northern sky at 1900. By 2330 it was at  $20^{\circ}$ N. It developed rayed structure at 0045 and was at  $30^{\circ}$ N at 0120 and in the zenith at 0150; some scattered rays were in the north. At 0156 the arc registered an apparent substorm onset: brightening, then folds, then poleward expansion. By 0206 patches had already formed and soon covered most of the sky. They lasted almost until dawn and had intensities up to 10 kR in  $\lambda$ 4278.

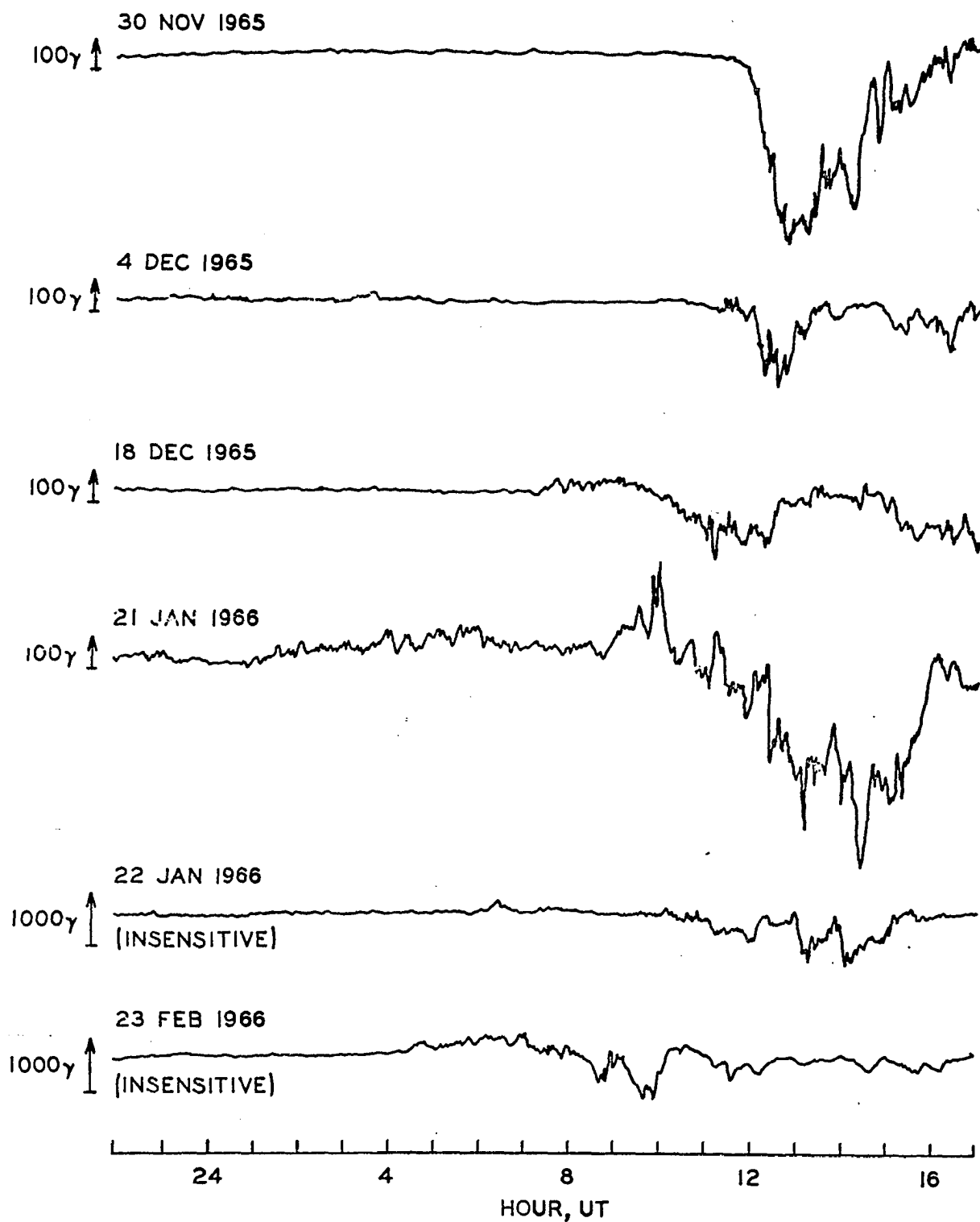


Figure 4.25 The College magnetograph H component traces for the nights discussed in Sec. 4.7. Note that the two bottom traces are from the insensitive (storm) magnetograph. Subtract 10 hours for Alaska Standard Time.

Wave photometer recording could not be commenced until 0256. The records showed many different types of pulsations but never any evidence for fast auroral waves.

December 4, 1965

The magnetogram showed quiet conditions before midnight with a slight positive step at  $\sim 2350$  (Fig. 4.25). Negative bays occurred from  $\sim 0200$ -  $0330$  and from  $\sim 0500$  onwards. The period  $0400 - 0500$  was relatively undisturbed.

The all-sky camera first revealed an arc at elevation  $30^{\circ}\text{N}$  at 0100. It moved to  $45^{\circ}$  and apparently registered a substorm onset at 0115 when it brightened, developed folds, and expanded northward. Luminosity ( $\sim 3\text{kR}$ ) in the form of diffuseness and arcs reached the zenith shortly afterwards.

At 0205 eastward drifting patches formed on the southern edge of the display ( $\sim 45^{\circ}\text{S}$ ). By 0230 they filled the southern half of the sky. At 0250 the western half of the sky was filled by patches which drifted slowly eastward. These were large and distinct and did not visually appear to pulsate at all (see however Section 3.1.9).

At 0400 an arc started to form at  $30^{\circ}\text{N}$  elevation while elsewhere were weak pulsating patches. The patches disappeared by 0415 and the zenith photometer recorded almost only the nightsky continuum. The wave photometer, however, showed weak pulsating auroras to be over most of the sky, particularly in the north. It showed no evidence at all for fast auroral waves. At 0545 more large patches started to form until, by 0630, the entire sky was covered.

December 18, 1965

The magnetogram was disturbed from 2100 onwards (Fig. 4.25). A negative bay commenced gradually at 2300 and reached maximum depression at 0100. It quickly recovered at 0230 although conditions were slightly disturbed. A second large negative bay started from about 0500.

At 2100 an arc was at  $5-10^{\circ}\text{N}$ . A diffuse envelope traveled southward through the zenith at 2200. It was several hundred kilometers wide and seemed to disappear at the southern horizon at 2230.

The northern sky up to  $60^{\circ}$  became diffuse by 2330 and at 0030 a bright arc moved south into the zenith. A slight fold developed and traveled east leaving the zenith region diffuse. At 0120 a diffuse (4 kR) envelope containing pulsating patches extended to  $30^{\circ}\text{S}$ . The envelope contracted to the north to form an arc at  $30^{\circ}$  similar to the ones that accompany wave displays.

The zenith photometer registered variations less than 50 R on a 500 R background. The wave photometer showed the variations to be in situ and not wave-like.

At 0520 eastward drifting patches were in the northern half of the sky. They covered the whole sky from 0600 until dawn.

January 21, 1966

The magnetogram showed generally disturbed conditions for the entire 24 hour period (Fig. 4.25). A positive bay occurred from  $\sim 2250$  until  $\sim 0015$  and then there commenced a ragged negative bay that did not recover until 0600.

At 1700 during evening twilight weak features were overhead and an arc was at 15°N. At 1840 an arc on the northern horizon was added to the display. Overhead was a diffuse envelope. The first arc had moved to 30°N at 2130 and at 2300 the intensity of the diffuse envelope and several new arcs in the sky increased.

A westward traveling surge started to go through a bright northern (30°N) arc at 2320. By 2340 the whole sky was diffusely bright (15 kR) with a bright arc in the zenith. The display became diffuse, patchy, and pulsating until ~ 0200 when an arc started to consolidate at 30°S; the zenith  $\lambda 4278$  intensity was only 1 kR.

The arc was brighter at 0220 while a much weaker rayed arc was in the zenith. At 0221 the southern arc registered an apparent sub-storm onset: folding, brightening, and rapid poleward expansion. The H trace correspondingly showed a very sudden negative decrease.

After this the whole sky was diffuse and patchy until dawn. Sometimes it was very bright, > 10 kR, and sometimes weak, ~ 3 kR. The period was characterized by almost continuous luminosity pulsations.

Several minutes around 0430 were characterized by the brightest pulsating patches observed during this study. They had period ~ 8 sec and ranged from a background of ~ 11 kR up to 22 kR in  $\lambda 4278$ .

#### January 22, 1966

The normal magnetogram at College exhibited disturbance for the entire 24 hour period. Referring to the less-confused storm magnetograms shows several negative bays after 0100; they commenced at

~ 0110, ~ 0300, and ~ 0400 (Fig. 4.25).

An arc on the northern horizon at 1900 was joined by a second arc at elevation  $25^{\circ}\text{N}$  at 2000. A diffuse envelope passed across the zenith going S at 2020 and at 2045 disappeared by drifting to the west. Only the northern arc remained. The aurora in the northern sky became diffuse up to elevation  $45^{\circ}\text{N}$  at 2130. This aurora spread through the zenith at 2345.

A bright arc formed in the zenith at 0009, developed folds in the east, and started a northward motion at 0014. It reached  $30^{\circ}\text{N}$  at 0024 and was then disturbed by a westward traveling surge at 0028. The sky quickly (0035) became covered by many bright arcs and then became diffusely bright ( $\geq 10$  kR).

Patches formed and then drifted westward at  $\sim 380$  m/sec between 0125 and 0135 to leave only weak diffuseness (5 kR); more patches "appeared".

By 0250 an arc started to consolidate at  $30^{\circ}\text{S}$ , apparently at the expense of the diffuse luminosity north of it (the zenith  $\lambda 4278$  intensity dropped to 1.5 kR). At 0300 the arc was complete. At 0301 there occurred a substorm onset. The arc expanded northwards from  $45^{\circ}$  to the zenith in 3 minutes ( $\sim 500$  m/sec). Eventually the whole sky was diffuse and bright (6-10 kR) with pulsations. The overall intensity fluctuated after this and was very high at 0400. At 0550 discrete eastward drifting patches had formed. They continued until dawn.

February 23, 1966

The magnetic field at College was disturbed for the entire 24 hour period. From 1800 until 0600 it was particularly disturbed (Fig. 4.25).

At 1850 there was a rayed arc at  $45^{\circ}\text{N}$  and a 3 kR diffuse envelope down to  $30^{\circ}\text{S}$ . The southern edge of the envelope had roughly a saw-tooth shape and was westward drifting. Bands broke off in the northern sky and moved westward around 2000. At 2030 multiple arcs formed in the northern sky. They covered most of the sky at 2100.

From 2130 to 2300 several loops and surges propagated westward. A surge around 2200 apparently went westward, then eastward, and finally continued westward. At 2300 there were bands scattered around the sky. By 0000 the display was diffuse; sporadic brightening occurred during the next two hours.

Patches covered the sky at 0230 but did not show evidence of eastward drifting until 0340. The display then remained essentially the same until dawn.

Waves were not seen at any time during the display. Several interesting types of pulsing auroras were recorded by the television system. Descriptions of these appear in Chapter 3.

#### Summary

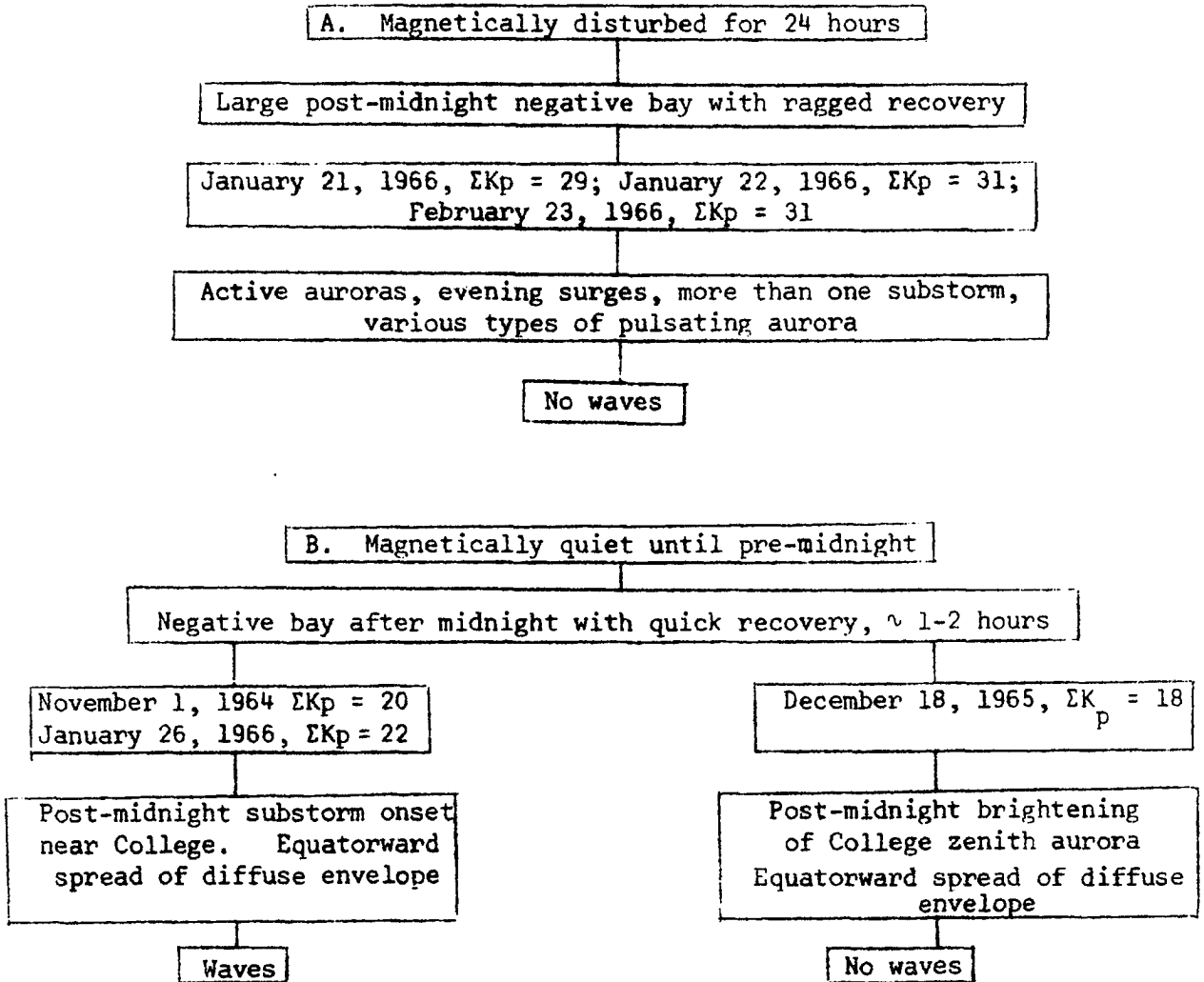
Taking these nights and the nights on which waves occurred it was possible to sort them according to the character of their magnetograms (Table 6). The following conclusions can be drawn about wave displays.

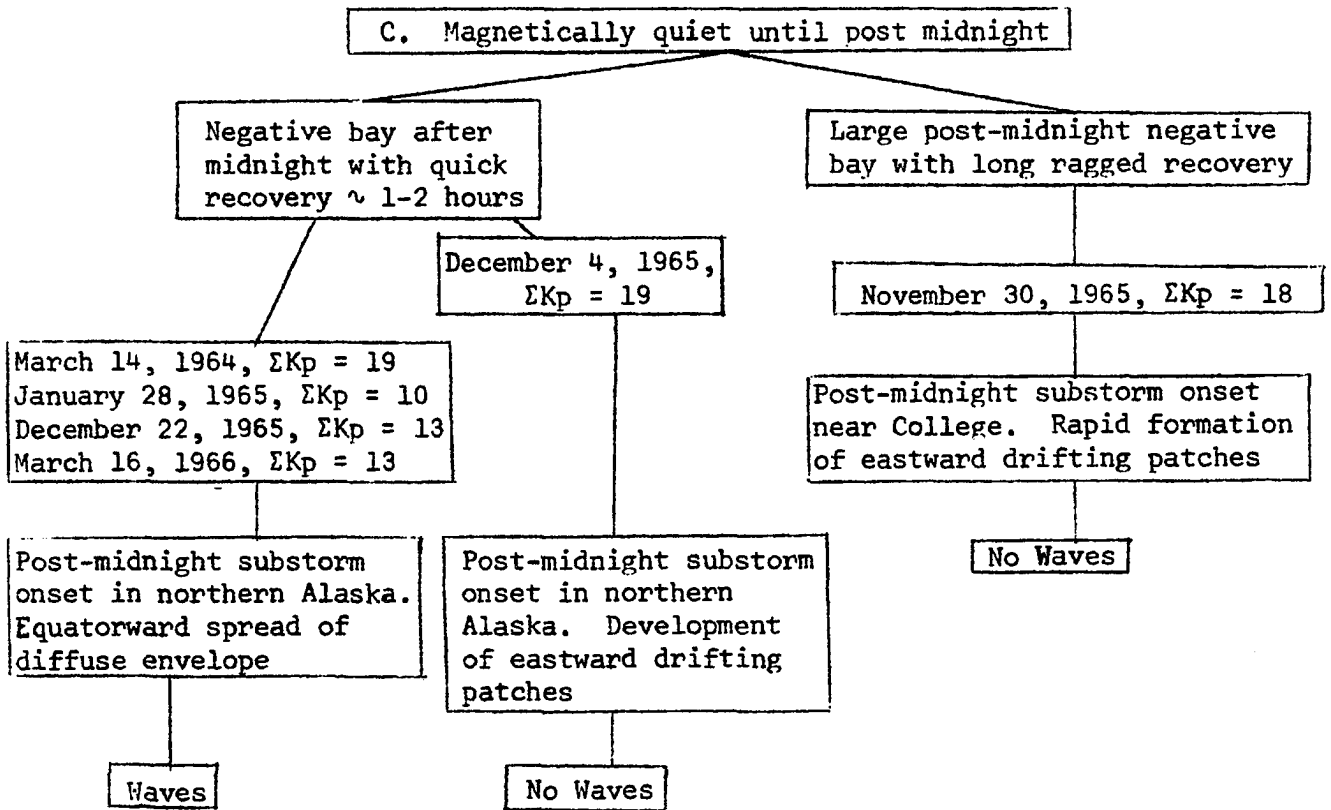
1. Waves only seem to occur on nights when the preceding 12 hours daytime was not magnetically disturbed at College.
2. They occur only, but not always, after the recovery of short-lived ( $\sim 1-2$  hours) post-midnight negative bays. The alternative is pulsating auroras.
3. They can occur when the sky contains weak diffuse pulsating auroras, but not when it contains distinct eastward drifting patches (as seen on the all-sky camera).

#### 4.8 Observational summary

Fast auroral waves are east-west aligned arc-like features that have been observed to propagate southward in the College vicinity after midnight on rare occasions. They occurred only when the preceding daylight hours, and often the evening hours, were magnetically undisturbed and only after a short-lived ( $\sim 1-2$  hour) substorm. In four of six cases wave displays were accompanied by a broad diffuse arc across Alaska; in this were often arc-like forms. South of the broad arc was a 300-400 km wide band of sub-visual glow ( $I_{4278} \sim 1\text{kR}$ ) and it was part of this width that was traversed by fast auroral waves. The region traversed, defined to be the wave path, was not fixed but could be observed to progress either north or south when suitable photometers were used.

A comparison of the magnetic and auroral conditions for the nights with and without waves





In all four cases the wave display followed a substorm whose onset appeared to be somewhere over Alaska: in two cases near College; in the other two near the north coast. Sometime after the onset, a diffuse envelope, perhaps containing weak pulsating patches, spread southward and generally passed College. With the recovery of the negative bay this envelope grew weaker and there was a tendency for an arc-like feature to form north of College. The wave display started about 2 hours after the onset, by which time the substorm negative bay recovery was essentially complete. Once started the wave display lasted up to 3 hours. In none of the cases did distinct, large, eastward drifting patches occur over Alaska in the time between substorm onset and wave display. The diffuse envelope, however, sometimes contained diffuse weak patches.

Of the remaining two cases, December 22, 1965, was essentially the same as above except that the northern arc was bright, apparently due to a substorm onset in progress near Barrow. This promptly caused large patches to form and the waves ceased. The final case, January 28, 1965, was unique because, following a moderate substorm onset in northern Alaska, a diffuse envelope containing pulsating patches and waves migrated first southward over College and then back northward.

Onset times and display durations are summarized in Table 7.

Table 7  
Fast Auroral Wave Display Summary

<u>Display</u>	<u>Substorm Onset</u>	<u>Time of Maximum Southern Excursion of Diffuse Envelope</u>	<u>Waves Observed</u>	<u>Wave Path Migration</u>
March 14, 1964	0030	~0115	0130-0430 (dawn)	
November 1, 1964	0200	~0250	0330-0510	S → N
January 28, 1965	0015	~0145	~0130-0230	S → N
December 22, 1965	0100	~0245	0225-0245	N → S
January 26, 1966	0200	~0245	0324-0430, 0456-0515	N → S
March 16, 1966	2340	~0100	0214-0241	N → S

#### Planetary Magnetic Disturbance

The 3-hr-range index  $K_p$  at the times of the wave displays ranged from 1 to 3. The  $K_p$  sum for the days of wave displays ranged from 10 to 22. According to Akasofu (1964) such activity will place the centerline of the auroral oval at or above the auroral zone in the midnight sector ( $dp \text{ lat} = 67^\circ$ ). This agrees with the present observations: all substorm onsets took place in the northern half of Alaska. From the preceding paragraphs it has been seen that the waves are observed on the equatorward edge of the auroral oval. At times of enhanced overall storm conditions in the magnetosphere the oval expands and so, given suitable conditions, waves

could perhaps be observed at lower latitudes. This is borne out by wave observations at Yerkes, Wisconsin ( $\lambda_m = 53.25^\circ\text{N}$ ) by C. R. Wilson (private communication); at Boston, Massachusetts ( $\lambda_m = 56^\circ\text{N}$ ) by B. P. Sandford (private communication); and at London, England by Paulin, (see the quotation at the start of this chapter).

#### The Wave Path

Situated in the sub-visual glow is the wave path over which the waves propagate. The start of the wave path is indicated by a wave acquiring detectable intensity, while the end is indicated by it losing this intensity. The path length can exceed 150 km and it can be separated from the northern arc by 100 km or more. It has been observed to progress north or south during a display with velocities of about 100 m/sec. Since the northern arc appeared to similarly progress it may have been that a contraction or expansion of the auroral oval was witnessed.

The sub-visual glow region containing the wave path also at times contained weak diffuse, pulsating auroras. It is emphasized that they were weak and diffuse and not, for instance, like the patches of 0600, January 26, 1966.

#### Microscopic Properties

These can be listed as follows:

Frequency: about 1/sec, although some intensity fluctuations caused by waves passing through the photometer fields of view can be as high as 4 cps (January 26, 1966; Fig. 4.18b).

Distance traveled by a particular wave: can exceed 150 km.

Width: commonly 30-200 km. Several overlapping waves may sometimes appear to exceed 200 km.

Intensity: generally <1 kR in  $\lambda 4278$  above the glow which has a similar value. The photometers (eg. channel 4, January 26, 1966) showed the waves to be up to three times as bright as the sub-visual glow.

Spectra: indicative of electron precipitation at low altitudes. Weak Balmer  $H_{\beta}$  is sometimes detected.

Range of velocities:  $\sim$  50-300 km/sec

Most common velocity: may vary from one display to the next. For instance on January 26, 1966 it appeared to be 120 km/sec while on March 16, 1966 it was 70 km/sec.

Velocity changes of particular waves: There does not seem to be any evidence to show consistent speeding up or slowing down of waves as they proceed southward. In general, the quality of the waves on the last three displays (when the Type III photometer was used) was inferior to that for the November 1, 1964, display when it was possible to have two fields of view separated by 100 km and see only slight changes in the wave profiles. During the last three displays it has often been difficult to follow the waves across two fields separated by 50 km. One has the impression

that the waves often traveled only short distances. However, several examples of waves traveling a full 150 km were obtained and these showed both speeding up and slowing down of waves as they proceeded southward.

#### Schematic Auroral Distribution

A number of the features described in this summary have been combined to sketch a model distribution of auroras over Alaska at times of fast auroral wave displays (Fig. 4.26). Only a short E-W section confined to the College vicinity is shown. However, it seems likely, after examining the all-sky camera records, that waves could be simultaneously detected over a region with an east-west elongation of 1500-2000 km. Verification will have to await future observations.

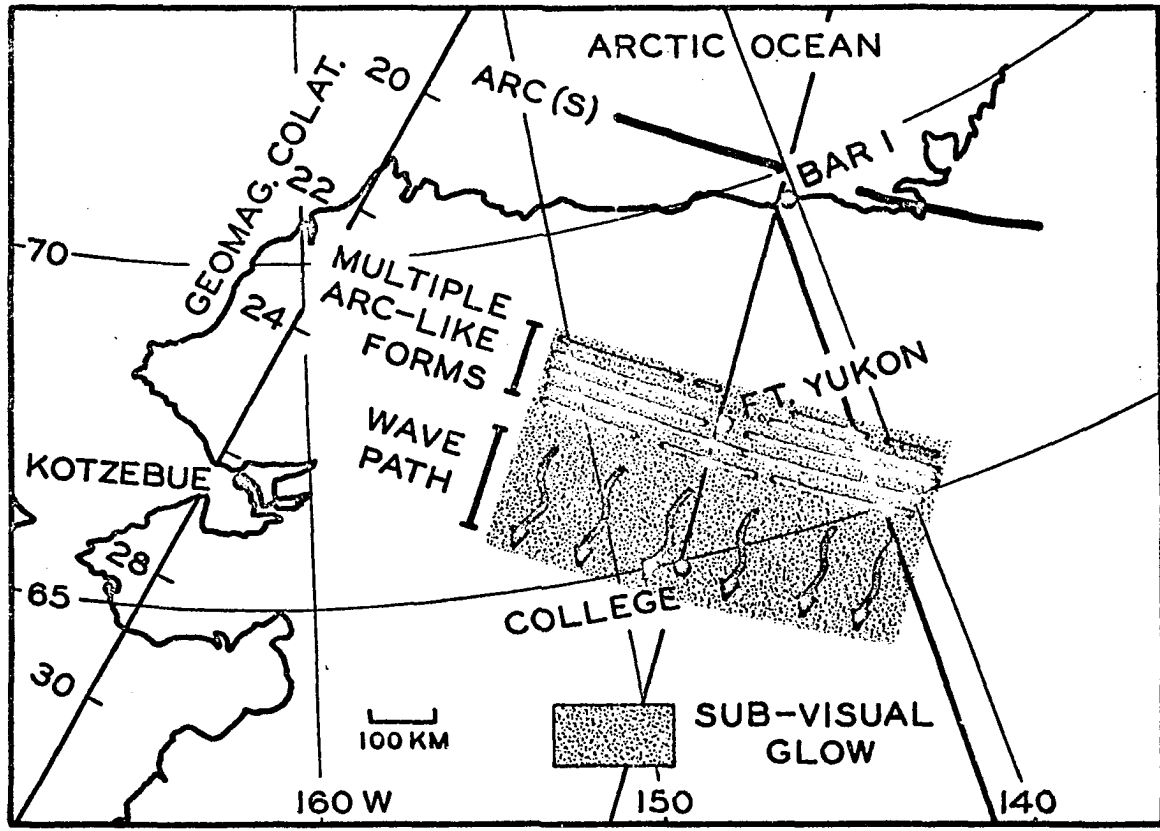


Figure 4.26 A model distribution of the auroras over part of Alaska during a fast auroral wave display. The length of the wave path within which all waves propagate is variable, as is its position within the sub-visual glow. The sub-visual glow may contain weak pulsating patches as well as waves. Its intensity is commonly  $I_{4278} \approx 1 \text{ kR}$  while that of the waves is  $I_{4278} < 1 \text{ kR}$ .

## Chapter 5

### -FAST AURORAL WAVES: DISCUSSION

In this discussion the wave properties will first be related to precipitating electron patterns as they enter the atmosphere. Later the electron patterns will be related to possible electron sources in the magnetosphere.

#### 5.1 Electron precipitation patterns

Spectra taken during fast auroral wave displays indicated the waves probably to be the result of electron precipitation into the atmosphere. Since charged particles are constrained to travel along magnetic field lines, the apparent motion of an auroral wave must be due to the cross-sectional shape of the precipitating electron bunch. A schematic example is given in Fig. 5.1a: the apparent velocity,  $v_w$ , of the wave is related to the downward velocity,  $v_e$ , of the slab of electrons, and the angle,  $\alpha$ , that the slab makes to the horizontal:

$$v_w = \frac{v_e}{\tan \alpha}$$

For example, taking  $v_w = 100$  km/sec and 5 keV electrons, for which  $v_e \approx 4 \times 10^4$  km/sec, it can be found that  $\alpha$  is  $89^\circ 50'$ . The horizontal dimension of the diagram is revealed by this to be greatly exaggerated.

#### Overtaking

It was not uncommon for the observations to reveal one wave being overtaken by another. In this case each wave can be related

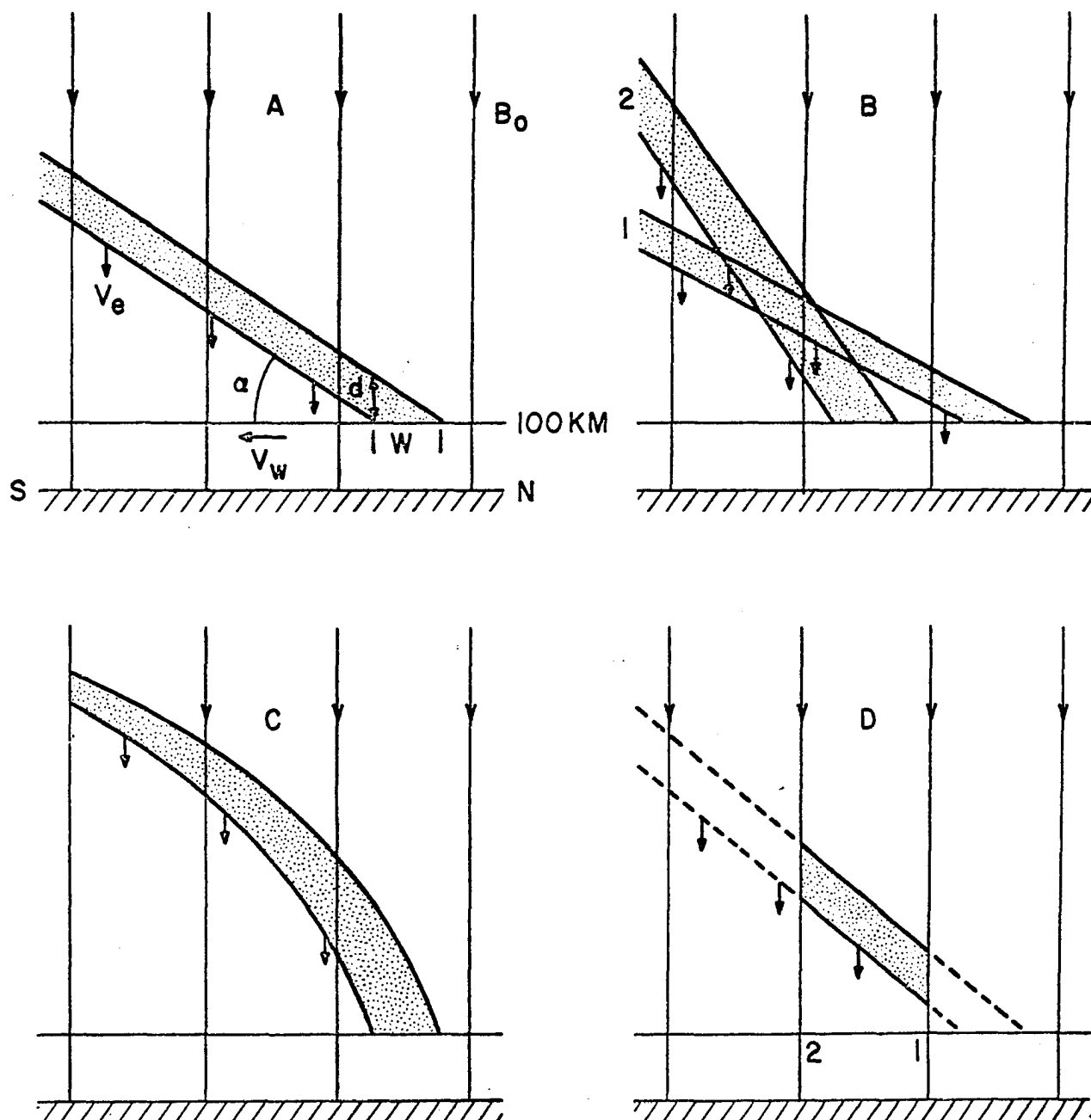


Figure 5.1 Schematic pictures showing the orientation of precipitating electron slabs required to produce some of the fast auroral wave properties: (A) Wave velocity and width. (B) Overtaking. (C) Speeding up. (D) Wave Path. The horizontal dimension of the diagram is greatly exaggerated because  $\alpha$  is almost  $90^\circ$ .

to an incoming slab of electrons. Assuming  $v_e$  to be the same for both slabs, then the difference would be in the angle  $\alpha$ :

$$v_{w1} = \frac{v_e}{\tan \alpha_1} \quad , \quad v_{w2} = \frac{v_e}{\tan \alpha_2}$$

Fig. 5.1b presents this result schematically;  $v_{w1}$  exceeds  $v_{w2}$  and so  $\alpha_1$  is less than  $\alpha_2$ .

On the other hand the effect could be related to the electrons in the two slabs being of different energies. For example we can see what this would mean for the observation of 0356 on January 26, 1966 (Fig. 4.18b). A single wave seen by the northern field of view split into two components with average velocities 110 and 140 km/sec as it progressed southward. Suppose the 110 km/sec component was due to 5 kev ( $4.1 \times 10^4$  km/sec) electrons. If  $\alpha$  was the same for both slabs then the electrons associated with the 140 km/sec wave would have velocity  $\frac{140}{110} \times 4.1 \times 10^4 = 5.2 \times 10^4$  km/sec. This velocity corresponds to  $\sim 7.5$  kev electrons.

#### Velocity changes

The data on velocity changes of waves were scanty but did reveal both the speeding up and slowing down of waves as they progressed southward. The speeding up of a wave can result from two effects; either the angle  $\alpha$  made with the 100 km level gradually decreases, or the velocity,  $v_e$ , increases towards lower L values (towards the left side of the diagrams). The effect of  $\alpha$ 's decrease with time for constant  $v_e$  is shown in Fig. 5.1c.

### Widths

The apparent width of the wave is  $W$  (in Fig. 5.1a). It is related to the distance between the front and rear surfaces of the slab as measured along the field lines.

$$W = \frac{d}{\tan \alpha}$$

Alternatively it can be thought of as the product of the time that a point in the atmosphere stays "illuminated" by electrons (and therefore the time that it illuminates visible radiation) with the apparent velocity of the wave,  $v_w$ ,

$$\begin{aligned} W &= t \times v_w \\ &= \frac{d}{v_e} \times \frac{v_e}{\tan \alpha} = \frac{d}{\tan \alpha} \end{aligned}$$

as above.

### The wave path

In describing the observations the region that was traversed by the fast auroral waves was called the wave path. It appeared that north and south of this the waves had little, if any, intensity. Fig. 4.17b for 0324 on January 26, 1966, reveals the decrease of intensity of the waves as they travel between fields of view 2 and 3.

An intensity decrease of this type could be related to a change of the electron density in the slab as shown in Fig. 5.1d. Assuming the dotted region, only, to produce measureable luminosity, the wave path would be measured to be between points 1 and 2.

### Intensity

Chamberlain (1961), page 283, calculated that an aurora of brightness 100 kR in  $\lambda 3914$  had an energy of ionization deposited into it of  $2.5 \times 10^{14}$  ev/cm<sup>2</sup>-sec. From the fast auroral wave observations the  $\lambda 3914$  intensity is about 1 kR, and so the energy deposited is  $2.5 \times 10^{12}$  ev/cm<sup>2</sup>-sec. Using the result that the energy spectrum of the incident electron stream peaks between 1 and 4 kev (Belon, Romick, and Rees, 1966) gives the rate of precipitation of electrons into a fast auroral wave to be about  $10^9$ /cm<sup>2</sup>-sec.

Referring back to Fig. 5.1, this number could give an indication of the electron density in the slab. For the present we will treat the artificial case where the field lines do not diverge. This will give a density that will apply only near the 100 km level; farther out field line divergence will cause it to be too high.

Taking 5 kev electrons and assuming the wave width to be 100 km and the velocity to be 100 km/sec then the time of illumination,  $t$ , will be 1 sec. The distance,  $d$ , will be  $4 \times 10^4$  km and a 1 cm<sup>2</sup> column of this length will contain  $10^9$  electrons that are injected into the atmosphere in 1 sec. The equivalent electron density will be  $10^9/4 \times 10^9$ /cm<sup>3</sup> or  $0.25$ /cm<sup>3</sup>.

### 5.2 Electron sources

Having discussed the idealized configuration of the electron slabs as they enter the atmosphere it is necessary to consider electron

sources. Two regions of the nightside magnetosphere will be discussed: The first, the equatorial plane vicinity, is suggested by many magnetospheric models to be where charged particles are either introduced from the tail, or untrapped by mechanisms propagating in from it. The other, the altitude region less than  $1 R_e$ , is favored by many recent rocket and balloon observations of precipitating electrons in different energy bands (c.f. Section 3.2.3). The importance of the two regions will be explored in the following sections.

### 5.2.1 Equatorial plane vicinity

An important factor favoring this vicinity over any other is simply that the hydromagnetic velocity in the plane projects down the field lines to the atmosphere to a value that is within the observed fast auroral wave velocity range. Elsewhere it greatly exceeds values in the range. This point can be clarified by assuming a dipole field and referring to the results of Bostick et al (1964). Field lines from the College vicinity, it can be shown, diverge by a factor of  $\sim 22$  in going to the equatorial plane. The hydromagnetic velocity on the College field line where it crosses the equatorial plane is, from Bostick et al,  $\sim 10^3$  km/sec. Thus an electron source propagating at  $V_A$  to lower L in the equatorial plane could give rise to a fast auroral wave with velocity  $\sim 50$  km/sec.

Away from the equatorial plane, but on the same field lines, the magnetic field is stronger and so the hydromagnetic velocity

is proportionally higher. Also, the field line divergence factor is smaller. Both these features could combine to produce faster auroral waves; at latitude  $30^\circ$  an increase of a factor of three would result. Thus, if the electron source propagated in simultaneously at several latitudes then overtaking of auroral waves would result.

At higher latitudes the scaled hydromagnetic velocity rapidly exceeds the fast auroral wave upper limit,  $\sim 300$  km/sec. This holds until altitudes down to several hundred km. Here the hydromagnetic velocity is of the same order as the fast auroral wave velocity. Two factors rule out such a low altitude source: one is that the ambient field is so large that an extremely large perturbation field would be required to untrap electrons. The other is that Injun 3 satellite measurements (O'Brien, 1964) showed no evidence for particle acceleration below  $10^3$  km.

Having given this introduction the mechanisms of electron injection and electron untrapping near the equatorial plane will be examined.

#### Electron injection

The injection into the magnetosphere of fresh electrons during an electron precipitation event was concluded from Injun-series observations (O'Brien, 1964) to be more likely than the untrapping of previously trapped electrons. Such injection has been discussed in recent field line merging models (Atkinson, 1966, Axford, 1966, Piddington, 1967). Particles in the tail initially possessing

small pitch angles are Fermi accelerated on collapsing field lines in a manner that leads to the auroral substorm poleward expansion. On the other hand, particles having large pitch angles become betatron accelerated as they are carried into the trapping region at velocity  $\sim V_A$  on collapsing field lines. This results in high density regions of electrons with anisotropic (flat) pitch angle distributions. According to Brice (1964) and Kennel and Petschek (1966) such conditions lead to the generation of whistler mode noise which then, by resonance with the gyrating electrons, causes rapid pitch angle diffusion which results in precipitation.

This mechanism could possibly cause fast auroral waves if the electrons that were given the small pitch angles could transfer from the moving field line to ambient stationary ones.

#### Electron untrapping

Implicit in an auroral model employing electron untrapping is that at some earlier time energetic electrons either were injected into the magnetosphere or resulted from an unspecified acceleration process. O'Brien (1962, 1964) called the complete process the "leaky-bucket" model and showed that it did not seem important for electron precipitation events. Although this is so, the concept of electron untrapping has many attractive features as far as trying to explain fast auroral waves. For example, if the untrapping process is hydromagnetic in nature then, as shown earlier, the velocities in the equatorial plane project down to the atmosphere within the

fast auroral wave velocity range. Also, if the untrapping on any one field line takes place at several latitudes then different velocities will result and overtaking of waves could occur. Finally, the wave path could result from only field lines in a certain L value range carrying sufficient electrons of suitable energy.

In addition to conventional hydromagnetic waves are hydromagnetic shock waves which have several attractive features. Both types will be discussed in turn in the following sections.

#### Hydromagnetic waves

In the field line merging model, reconnected field lines collapse back to the earth somewhat analogously to stretched strings. They travel as hydromagnetic waves and are believed to be absorbed near the midnight meridian at latitude  $68^\circ$  (Piddington, 1965). Axford (1966) has suggested that plasma trapped on closed field lines that are overrun by collapsing field lines traveling as compressional waves would be compressed. Just as in the injection case, this would lead to betatron acceleration. The resulting anisotropic pitch angle distributions could produce electron precipitation as suggested by Brice (1964) and Kennel and Petschek (1966). The patterns produced on the atmosphere would propagate equatorwards with velocities in the fast auroral wave velocity range.

From the point of view of energy, we know from section 5.1 that the energy flux required to produce the luminosity of a fast auroral wave is about  $2.5 \times 10^{12} \text{ ev/cm}^2\text{-sec}$ . Since the magnetic

field at the equatorial plane is  $\sim 200\gamma$ , whereas that at the ionosphere is  $50,000\gamma$ , this energy flux is 1/250 times smaller at the equatorial plane, i.e.  $10^{10}$  ev/cm<sup>2</sup>-sec, or  $1.6 \times 10^{-2}$  ergs/cm<sup>2</sup>-sec. Taking this energy to be carried by electrons of from 1-4 kev, say 2.5 kev, the flux corresponds to an energy density of  $1.6 \times 10^{-2} / 2.5 \times 10^9$ , or  $6.4 \times 10^{-11}$  ergs/cm<sup>3</sup>. The energy density of a hydromagnetic wave is  $B^2/8\pi$  and taking, say, a  $25\gamma$  wave one gets  $2.5 \times 10^{-9}$  ergs/cm<sup>3</sup>, enough to give the fast auroral wave energy.

#### Hydromagnetic shock waves

Hydromagnetic shocks are known to exist in the solar wind and where the solar wind encounters the earth's magnetosphere. It does not seem altogether unlikely that they would occur in the tail region and near the trapping region boundary (cf. Anderson and Ness, 1966). They would result when compressional hydromagnetic waves entered regions of reduced magnetic field and then steepened. Such regions would result from the diamagnetic effects of concentrations of charged particles. Here we will examine, from the point of view of producing fast auroral waves, some of the consequences of the propagation of shocks in from the tail region. For us the shocks have two desirable features: they travel as compressional waves by definition faster than the local Alfvén velocity, and their fronts are very thin, possibly thin enough to cause violation of the magnetic moment invariants of trapped electrons.

Characteristics of shock wave propagation were discussed by Gee (1966). For the case of a shock traversing a medium at rest the Mach number of the flow (into the shock front) is given by

$$M^2 = \frac{2\eta}{3-\eta}$$

where

$$\eta = \frac{B_2}{B_1} = \frac{\rho_2}{\rho_1}$$

is the shock compression ratio from the back to the front of the shock. This would be the case for a shock which enters the trapping region from the tail.

Given a shock wave, then, the field compression could lead to betatron acceleration of trapped electrons on closed field lines. Precipitation of these by the method discussed in the previous section would lead to fast auroral waves faster than 50 km/sec, according to the Mach number of the shock.

The thickness of laboratory shock fronts has been investigated by Paul et al (1965). Its value for a Mach number of 2.5 was  $7 c/\omega_{pe}$  where  $\omega_{pe}$  is the electron plasma frequency. At earth distance  $5.5 R_e$

$$\frac{7c}{\omega_{pe}} = 7c \left( \frac{m_e}{4\pi n e^2} \right)^{1/2} \approx 4\text{km}$$

where  $n = 80/\text{cc}$  (from Hultqvist, 1966). This figure can be compared with that for an auroral-energy electron which is  $(1.0 - 1.5) \sin \theta$  km where  $\theta$  is the pitch angle. The two figures are comparable,

and under such conditions the magnetic moment invariant for the electron could break down resulting in scattering of the pitch angle. This also would lead to precipitation of electrons into an auroral wave-like pattern.

#### 5.2.2 Altitudes less than $1 R_e$

The importance of processes occurring at altitudes less than  $1 R_e$  has only recently become apparent (section 3.2.3). Rocket studies by Lampton (1967) that revealed no dispersion in the arrival times of electrons of different energies were interpreted by Parks (1967) to suggest the existence of a plasma instability less than  $1 R_e$  from the earth. The instability was believed to be triggered by VLF electromagnetic waves.

The only possible application of this mechanism to the production of fast auroral waves would be by a two step process: VLF waves would have to be produced at progressively lower L values somewhere on College vicinity field lines; the velocity of progression would have to project to the atmosphere and be within the fast auroral wave range. Once produced, the VLF waves could propagate down the field lines to the instability region. The instability would be produced at progressively lower L values and would, in turn, give rise to electron precipitation at progressively lower L values. The production of VLF waves has already been discussed as a by-product of betatron acceleration. The velocities involved projected to the atmosphere within the required range.

## Chapter 6

## CONCLUSIONS AND RECOMMENDATIONS

"One might as well try to record observations on a firework display". Simpson discussing a paper by Chree (1927).

6.1 ConclusionsPulsating auroras

Pulsating auroras are restricted primarily to the equatorward boundary of auroral displays in the midnight and morning sectors following substorm onsets. At such times the local horizontal magnetic field component is strongly negative or recovering from a negative bay. There seem to be at least four ways in which pulsating auroras can appear over a station: they can be left in the wake of a poleward expansion accompanying a substorm onset; they can be seen as patches that drift eastward through the zenith from the western horizon; they can occur in the diffuse glow produced as an arc in the north expands southward; or they can simply materialize up to 100 km south of such an arc and then commence drifting eastward.

Pulsating auroras can drift either east or west, but most commonly to the east. In this regard, the February 23, 1966, display is interesting because at 0340 the drift changed from west to east (section 4.7). Also it has been seen that it is possible to have eastward drifting patches in the southern sky accompanied by westward drifting patches in the northern sky.

A diffuse background of several kR in  $\lambda 4278$  invariably accompanies pulsating aurora displays. The pulsating auroras are superimposed

on this and are most readily recognized if their intensity fluctuates from this level to a maximum and down again. Their intensity above the background commonly ranges up to 10 kR in  $\lambda 4278$ ; the brightest ever seen were 11 kR above a 11 kR background (section 4.7). Often patches can be observed that do not appear to pulsate. This is because their intensity does not vary enough for the eye to register it: even a 3 kR 1 cps fluctuation on a 5 kR maximum signal above a 2 kR diffuse background can be missed.

Pulsating patches appear to take many forms but seem to fall into two main categories:

- (a) Those in which the growth and decay phases are simultaneous, or very nearly so, over the entire form.
- (b) Those in which the growth and decay phases are not simultaneous over the entire form. This results in apparent motion and changes in size and shape and is seen more frequently in large patches ( $\lambda$  50 km across) than in small ones.

Also, during the time that a patch is visible it sometimes has moving and in situ intensity variations within it. Photometer records of patches reveal quasi-periodic pulsations. Different patches commonly pulsate asynchronously.

The power spectrums for pulsating aurora displays peak roughly at 10 sec. Visually one has the impression that large patches ( $\approx$  50 km across) pulsate more slowly ( $\sim$  10 sec) than smaller ones. A narrow field of view photometer reveals relatively more of the shorter period components ( $\lesssim$  1 sec) than does a broad field. This is probably because the broad field would integrate many small patches pulsating rapidly while the narrow field would not. Also, small weak patches on the steady background of several kR that accompanies pulsating auroras would give a better signal to noise ratio with the small field of view.

The behavior of pulsating patches suggested to the writer that each is associated with a flux tube drifting in the magnetosphere. Quasi-periodically the trapped electron population of the tube is disturbed, causing some of it to precipitate and lead to brightening of the patch. Alternatively, as pointed out by Rosenberg (private communication), fresh electrons may be continuously injected into the tube to remain trapped until influenced by the modulation mechanism.

It is suggested that the shape of the leading and trailing edges of the precipitating electron bunches can give rise to the observed apparent velocities during the growth and decay phases. These shapes would result from the modulation mechanism starting and finishing at one side or another of the tube. Electron density inhomogeneities in the bunch would then produce the observed intensity fluctuations while the patch is visible.

### Flaming auroras

From the limited observations, flaming auroras appear to occur under the same conditions as pulsating auroras. The upward speed of flaming was 70-80 km/sec for an assumed starting height of 100 km.

Assuming multi-energy electrons to be released simultaneously from a point on the field line, a flaming effect can result. This is due to velocity dispersion and differential atmospheric penetration. The observed 70-80 km/sec could arise from a release point two thirds of the way between the ionosphere and the equatorial plane ( $6.4 R_e$ ). However, allowing the assumed starting height to range from 90-110 km would result in the release point ranging from the equatorial plane to  $2.5 R_e$  from the ionosphere.

### Flickering auroras

Flickering auroras have been observed infrequently as part of discrete bright features ( $\sim 100$  kR) seen before midnight on active days ( $\Sigma K_p \sim 30$ ). They were made up of numerous, scarcely separated, small patches 1-2 km across showing rapid changes ( $\sim 10$  cps) in both shape and intensity; sometimes they moved at up to  $\sim 10$  km/sec.

### Fast Auroral Waves

Fast auroral waves are east-west aligned arc-like features that have been observed to propagate southward in the College vicinity after midnight on rare occasions. They occurred only when the preceding daylight hours, and often the evening hours, were locally magnetically

undisturbed and only after a short-lived ( $\sim 1-2$  hour) substorm negative bay. In the majority of cases the wave displays were accompanied by a broad diffuse arc across Alaska; in this were often arc-like forms. South of the broad arc was a 300-400 km wide band of sub-visual glow ( $I_{4278} \lesssim 1\text{kR}$ ) and it was part of this width that was traversed by the waves. The region traversed, defined to be the wave path, was not fixed but could move north or south. The start of the wave path was indicated by a wave acquiring detectable intensity, while the end was indicated by it losing this intensity. The path length could exceed 150 km and it could be separated from the northern arc by 100 km or more.

The substorm onsets occurred over north-central Alaska. After the onset a diffuse envelope, perhaps containing weak pulsating patches, spread southward over College. With the recovery of the negative bay this envelope grew weaker and there was a tendency for an arc-like feature to form north of College. The wave display started about 2 hours after the onset, by which time the substorm negative bay recovery was often essentially complete. In none of the cases did distinct, large, eastward drifting patches occur over Alaska either in the time between substorm onset and wave display or during the wave display. In one case their appearance signaled the end of a wave display.

The microscopic properties of the waves can be listed as follows:

Frequency: about 1/sec

Distance traveled by a particular wave: can exceed 150 km.

Width: commonly 30-200 km. Several overlapping waves may sometimes appear to exceed 200 km.

Intensity: generally  $< 1$  kR in  $\lambda 4278$  above the glow which has a similar value.

Spectra: indicative of electron precipitation at low auroral altitudes. Weak Balmer  $H_{\beta}$  is sometimes detected.

Range of velocities:  $\sim 50$ -300 km/sec.

Most common velocity: may vary from one display to the next.

Velocity changes of particular waves: there does not seem to be any evidence to show consistent speeding up or slowing down of waves as they proceed southward.

A number of properties of the waves were related to the shape of the incoming slabs of precipitating electrons. Included among these are velocities, widths, velocity changes, overtaking, and the wave path. As far as the source of the slabs was concerned, consideration was given to both the equatorial plane vicinity and also much closer to the earth ( $\lesssim 1 R_e$ ). A factor thought to favor the equatorial plane vicinity was that the hydromagnetic velocity normal to the field there projects down the field lines to the atmosphere to give a value of 50 km/sec. This velocity increases

as one moves away from the equatorial plane vicinity. These sources of energetic electrons that propagate inwards at and near the equatorial plane with the hydromagnetic velocity could give fast auroral waves in the observed velocity range.

It was suggested that fresh energetic electrons were introduced into the magnetosphere on collapsing field lines as part of the field line merging model. The field lines collapse to the trapping region from the tail and lead to betatron acceleration of electrons trapped on them.

Alternatively the collapsing field lines traveling as hydro-magnetic waves overrun plasma trapped on closed field lines and lead to betatron acceleration and precipitation in patterns that travel equatorward. The possibility that such waves would travel as shock waves was considered. In this case trapped electrons could be untrapped due to the thinness of the wave front which would cause a violation of the first invariant.

For the acceleration or untrapping to take place at or less than  $1 R_e$  it was thought a complicated two step process would be required to produce the fast auroral waves.

## 6.2 Recommendations

1. One of the most promising experiments in the future is that of flying television systems on conjugate airplanes. Preliminary flights with all-sky cameras in March, 1967 yielded examples of

auroras showing surprisingly detailed conjugacy (Belon et al, 1967). Since pulsating auroras occur on the equatorward edge of auroral displays it is even more likely that they will be conjugate. Considering the ease of identifying conjugate forms from the early flights, it should be no great problem to identify patches  $\sim 50$  km across having distinctive shapes and pulsating in a temporally distinctive way.

Exact timing on both airplanes will make it possible to see if the brightening of a patch in one hemisphere is associated with a corresponding brightening in the other hemisphere. If the brightening is found to be simultaneous then the modulation mechanism would be at the equatorial plane, otherwise it would be nearer one ionosphere than the other. The actual amount will be indeterminate unless some assumption is made as to the energy of the electrons producing the patches. The next interesting observation will be to see if successive brightenings are due to modulation mechanisms situated at the same place on the field line. Finally, different patches can be studied to see where their respective modulation mechanisms are located.

2. By examining the dispersion in arrival times of electrons of different energies, the positions of the modulation mechanisms for the electron fluxes involved in pulsating auroras, flaming auroras, breakup auroras, and x-ray microbursts have been placed by various workers at almost anywhere on the observer's field line. More

observations are needed to determine if any one position is favored, and under what conditions. No position for the modulation mechanism for fast auroral waves is available. Satellite, rocket, or balloon observations of precipitating electrons coordinated with ground photometer observations are needed for this (as for the other auroras).

3. The flickering auroras had frequency variations near, and perhaps beyond, the upper frequency limit of the TV system. A high frequency photometer system attached to the TV camera mount to observe flickering auroras is needed.

4. A significant feature concerning the interpretation of fast auroral waves was that the hydromagnetic velocity normal to the field in the equatorial plane vicinity projected down the field lines to the atmosphere to give velocities in the fast auroral wave range. Satellite measurement of hydromagnetic waves and their influence on trapped electrons are recommended in the nightside equatorial plane vicinity.

5. The longitudinal extent of individual fast auroral waves is not known. One-station measurements with coupled two-field photometers tilted  $45^\circ$  east and west would show whether they are at least  $\sim 200$  km in longitudinal extent.

6. During the present sunspot maximum fast auroral wave displays may well be seen in sub-auroral regions. It is recommended that visual observers watch for them since a few observations could determine their role in the overall auroral-magnetic situation at such times.

## APPENDIX I

### MOTIONS OF ENERGETIC ELECTRONS IN THE GEOMAGNETIC FIELD

The drift velocity versus time of oscillations curve in Fig. 3.2 was calculated by following the steps outlined by Akasofu and Chapman (1961):

The time for one complete oscillation between the two mirror points is given by:

$$T_o = \frac{4\ell}{w} \quad (1)$$

$\ell$ : dimensionless arc length of spiraling particle from the equatorial plane to a mirror point

$w$ : particle velocity

$\ell$  has been calculated by Wentworth et al (1959; their Fig. 2) and for an equatorial pitch angle,  $\theta_e = 3^\circ 20'$  it is

$$\ell = 1.35 L \quad (2)$$

This particular pitch angle corresponds to a mirror altitude of 100 km on the  $L = 5.5 R_e$  field line.

For College  $L = 5.5 R_e$  and so the time of oscillation can be written

$$T_o = 1.90 \times 10^{10} / w \text{ sec} \quad (3)$$

The longitudinal displacement per oscillation is given by Alfvén and Fälthammar (1963), page 49:

$$\delta\lambda = \lambda - \lambda_o = (L/c_{st})^2 I_1(\phi_o) \text{ degrees} \quad (4)$$

They have plotted in their Fig. 2.8  $I_1(\phi_0)$  versus latitude for a series of values of the mirror latitudes  $\phi_0$ . Akasofu and Chapman pointed out that when  $\phi_0$  exceeds  $45^\circ$   $I_1(\phi_0)$  is nearly independent of  $\phi_0$ , with the approximate value of  $76^\circ$ . Thus

$$\delta\lambda = 4 \times 76^\circ \left( \frac{L}{c_{st}} \right)^2 \text{ degrees} \quad (5)$$

Substituting relevant values this becomes

$$\delta\lambda = 2.65 \times 10^{-12} \frac{w}{\sqrt{1 - \frac{w^2}{c^2}}} \text{ degrees} \quad (6)$$

The actual drift velocity,  $v_d$ , then comes from allowing for latitude (multiplying by  $\cos \lambda_m$ ), converting the angular drift to linear drift, and dividing by  $T_o$ :

$$v_d = \frac{\delta\lambda^\circ}{T_o} \times \frac{\pi}{180} \times 6.37 \times 10^6 \cos 65^\circ \quad (7)$$

i.e.

$$v_d = \frac{\delta\lambda^\circ}{T_o} \times 4.7 \times 10^4 \text{ meters/sec} \quad (8)$$

An alternative way to generate the drift velocity versus time of oscillation curve is to use the computations of Hamlin et al (1961). Using their approximations the drift velocity is

$$v_d = (2\pi \times 6370 \times \cos \lambda_m) \left( \frac{\gamma w L (1 + 0.43 \sin \theta_e)}{3.9 \times 10^9} \right) \text{ km/sec} \quad (9)$$

where for College L = 5.5,  $\lambda_m = 65^\circ$ , and  $\theta_e = 3^\circ 20'$  for mirroring at 100 km.  $W$  is the particle energy in electron volts

$$\begin{aligned} v_d &= 2.45 \times 10^{-5} \gamma W \text{ km/sec} \\ &= 2.45 \times 10^{-2} \gamma W \text{ m/sec} \end{aligned} \quad (10)$$

The time of oscillation (bounce period) is given by

$$\begin{aligned} T_o &= \frac{4R_e (1.3 - 0.56 \sin\theta_e)}{W} \\ &= \frac{17.7 \times 10^9}{W} \text{ sec} \end{aligned} \quad (11)$$

The values obtained from (10) and (11) lie close enough to those of the previous method that either may be used.

## BIBLIOGRAPHY

- Akasofu, S.-I., The latitudinal shift of the auroral belt, *J. Atmosph. Terr. Phys.*, 26, 1167-1174, 1964.
- Akasofu, S.-I., The aurora, *Scientific American*, 213(6), 54-62, 1965.
- Akasofu, S.-I., Electrodynamics of the magnetosphere: Geomagnetic storms, *Space Science Reviews*, 6, 21-143, 1966.
- Akasofu, S.-I. and S. Chapman, The ring current, geomagnetic disturbance, and the Van Allen radiation belts, *J. Geophys. Res.*, 66, 1321-1350, 1961.
- Akasofu, S.-I., C.-I. Meng and D. S. Kimball, Dynamics of the aurora - IV. Polar magnetic substorms and westward traveling surges, *J. Atmospheric Terrest. Phys.*, 28, 489-496, 1966.
- Alfvén, H. and C-G. Fälthammar, *Cosmical electrodynamics, fundamental principles*, Clarendon Press, Oxford, 1963.
- Anderson, K. A., Energetic electron fluxes in the tail of the geomagnetic field, *J. Geophys. Res.*, 70(19), 4741-4763, 1965.
- Anderson, K. A. and N. F. Ness, Correlation of magnetic fields and energetic electrons on the Imp 1 satellite, *J. Geophys. Res.*, 71(15), 3705-3727, 1966.
- Angot, A., "The Aurora Borealis", Kegan Paul, Trench, Trübner and Co. Ltd., London, pp. 14-20, 1896.
- Ansari, Z. A., The aurorally associated absorption of cosmic noise at College, Alaska, *J. Geophys. Res.*, 69(21), 4493-4513, 1964.
- Ashburn, E. V., Photometry of the aurora, *J. Geophys. Res.*, 60, 205-212, 1955.
- Atkinson, G., A theory of polar substorms, *J. Geophys. Res.*, 71(21), 5157-5164, 1966.
- Axford, W. I., The interaction between the solar wind and the magnetosphere, presented at the Advanced Study Institute on Aurora and Airglow, University of Keele, England, 1966.
- Axford, W. I. and C. O. Hines, A unifying theory of high-latitude geophysical phenomena and geomagnetic storms, *Can. J. Phys.*, 39, 1433-1464, 1961.
- Belon, A. E., G. J. Romick, C. S. Deehr, W. Murcray, and G. R. Cresswell, Spectrophotometry of atmospheric phenomena at high latitudes-vela, Geophysical Institute, University of Alaska Report UAG R-153, 1964.

- Belon, A. E., G. J. Romick and M. H. Rees, The energy spectrum of primary auroral electrons determined from auroral luminosity profiles, *Planet. Space Sci.*, 14, 597-615, 1966.
- Belon, A. E., K. B. Mather and N. W. Glass, The conjugacy of visual aurorae, *Antarctic Journal of the United States*, 2(4), 124-127, 1967.
- Berkey, F. T., Coordinated measurements of auroral absorption and luminosity using the narrow beam technique, *J. Geophys. Res.*, in press, 1968.
- Bostick, F. X., C. E. Prince and H. W. Smith, Propagation characteristics of plane small amplitude hydromagnetic disturbances in the earth's upper atmosphere, *Elect. Eng. Res. Lab. Sci. Rep. No. 135*, The University of Texas, 1964.
- Brice, N., Fundamentals of very low frequency generation mechanisms, *J. Geophys. Res.*, 69(21), 4515-4522, 1964.
- Brown, R. R., Electron precipitation in the auroral zone, *Space Science Reviews*, 5, 311-387, 1966.
- Bryant, D. A., H. L. Collin, G. M. Coutier and A. D. Johnstone, Evidence for velocity dispersion in auroral electrons, *Nature* 215, 45-46, 1967.
- Campbell, W. H. and M. H. Rees, A study of auroral coruscations, *J. Geophys. Res.*, 66, 41-55, 1961.
- Chamberlain, J. W., *Physics of the aurora and airglow*, Academic Press, New York and London, 1961.
- Chapman, S. and J. Bartels, "Geomagnetism", Clarendon Press, Oxford, pp. 452, 1940.
- Chree, C., Magnetic disturbance and aurora...at Cape Denison in 1912 and 1913, *Proc. Phys. Soc., London*, 39, 389-407, 1927.
- Cresswell, G. R. and A. E. Belon, Observations of fast auroral waves, *Planet. Space Sci.*, 14, 299-301, 1966.
- Davis, T. N., The application of image orthicon techniques to auroral observation, *Space Science Reviews*, 6, 222-247, 1966.
- de Mairan, "Traité Physique et Historique de L'Aurore Boréale", A Paris, de L'imprimerie Royale, Seconde Edition, pp. 136-137, 1754.

- Evans, David S., A 10-cps periodicity in the precipitation of auroral-zone electrons, *J. Geophys. Res.*, 72(17), 4281-4291, 1967.
- Evans, W. F. J., Auroral studies with a multichannel photometer, Thesis, University of Saskatchewan, p. 57, 1963.
- Flock, W. L., A. E. Belon and R. R. Heacock, Geomagnetic agitation and overhead aurora, Proceedings of the International Conference on the Ionosphere held at Imperial College, London, July 1962, 143-150, 1963.
- Geddes, M., Some characteristics of auroras in New Zealand, *Terrest. Magnetism and Atmospheric Elec.*, 44, 189-193, 1939.
- Gee, S., Bistatic-radar measurements of propagating interplanetary shock waves, *J. Geophys. Res.*, 71(11), 2729-2737, 1966.
- Georgio, N. V., Electrophotometric measurements in the auroral zone, Results of I.G.Y. Res.: Aurora and Airglow, 1, 30-40, 1959 (Also NASA Tech. Transl. F-76, 1962).
- Georgio, N. V., Coruscation regularities in aurorae, results of IGY researches: Aurora and Airglow, No. 8, 1962. (Also NASA Tech. Transl. F-201).
- Hamlin, D. A., R. Karplus, R. C. Vik and K. M. Watson, Mirror and azimuthal drift frequencies for geomagnetically trapped particles, *J. Geophys. Res.*, 66(1), 1-4, 1961.
- Heacock, R. R. and V. P. Hessler, Frequency-time displays of telluric current activity, Geophysical Institute, University of Alaska Report No. UAG C-43, 1966.
- Hepner, J. P., A study of the relationships between the aurora borealis and the geomagnetic disturbances caused by electric currents in the ionosphere, Thesis, California Institute of Technology, pp. 32, 1954.
- Hultqvist, B., Ionospheric absorption of cosmic radio noise, *Space Science Reviews*, 5, 771-817, 1966.
- International Auroral Atlas, Edinburgh, University Press, 1963.
- Johansen, O. E. and A. Omholt, A study of pulsating aurora, *Planet. Space Sci.*, 14, 207-215, 1966.
- Kendall, E. A., Description of aurora of 25 September 1827, *Quarterly Journal of Science, Literature and Art*, 392-407, October-December, 1827.

- Kennel, C. F. and H. E. Petschek, Limit on stably trapped particle fluxes, *J. Geophys. Res.*, 71(1), 1-28, 1966.
- Lampton, M., Rapid time structure in daytime auroral zone electrons, *Trans. A.G.U.*, 48(1), 180-181, 1967.
- Lovering, J., *Memoirs of the American Academy of Arts and Sciences*, Vol. X.-Part I, 1868.
- Murcray W. B., Some properties of the luminous aurora as measured by a photoelectric photometer, *J. Geophys. Res.*, 64, 955-959, 1959.
- Nadubovich, Y. A., Instantaneous light flux characteristics of auroras as revealed by all-sky electrophotometer observations, *Geomagnetism and Aeronomy*, 1, 465-471, 1961.
- Newton, H. W., "The Face of the Sun", Penguin Books, Middlesex, pp. 158, 1958.
- O'Brien, B. J., Lifetimes of outer-zone electrons and their precipitation into the atmosphere, *J. Geophys. Res.*, 67, 3687-3706, 1962.
- O'Brien, B. J., High-latitude geophysical studies with satellite Injun 3; 3. Precipitation of electrons into the atmosphere, *J. Geophys. Res.*, 69(1), 13-43, 1964.
- Omholt, A., Photometric observations of rayed and pulsating aurorae, *Astrophys. J.*, 126, 461-463, 1957.
- Omholt, A. and H. Pettersen, Characteristics of high frequency auroral pulsations, *Planet. Space Sci.*, 15, 347-355, 1967.
- Parks, G. K., Spatial characteristics of auroral-zone X-ray microbursts, *J. Geophys. Res.*, 72(1), 215-226, 1967.
- Parsons, N. R. and K. B. Fenton, Observations of the aurora australis, Macquarie Island, May 1950-April 1951, ANARE Interim Report No. 5, pp. 327, 1953.
- Paul, J. M. W., L. S. Holmes, M. J. Parkinson and J. Sheffield, Experimental observations on the structure of collisionless shock waves in a magnetized plasma, *Nature*, 208, 133-135, 1965.
- Photographic Atlas of Auroral Forms, The International Geodetic and Geophysical Union, Oslo, 1930.
- Piddington, J. H., The magnetosphere and its environs, *Planet. Space Sci.*, 13, 363-376, 1965.

- Piddington, J. H., A theory of auroras and the ring current, J. Atmosph. Terrest. Phys., 29, 87-105, 1967.
- Rees, M. H., Note on the penetration of energetic electrons into the earth's atmosphere, Planet. Space Sci., 12, 722-725, 1964.
- Rosenberg, T. J., J. Bjordal and G. J. Kvifte, On the coherency of X-ray and optical pulsations in auroras, J. Geophys. Res., 72 (13), 3504-3506, 1967.
- Spitzer, Lyman Jr., Physics of fully ionized gases, Wiley, New York, Second edition, 1962.
- Störmer, C., Remarkable aurora-forms from southern Norway, Geofysiske Publikasjoner, 13, No. 7, 3-82, 1942.
- Störmer, C., "The Polar Aurora", Clarendon Press, Oxford, 1955.
- Vestine, E. H., Remarkable auroral forms, Meanook observatory, Polar Year, 1932-33. Terr. Mag. 48, 233-236, 1943.
- Wentworth, R. C., W. M. MacDonald and S. F. Singer, Lifetimes of trapped radiation belt particles determined by Coulomb scattering, Phys. Fluid, 2, 499-509, 1959.